Ab Initio Organic Chemistry. A survey of ground- and excited states and aromaticity

Ab initio organische chemie. Een onderzoek naar grond- en aangeslagen toestanden en aromaticiteit

(met een samenvatting in het Nederlands)

Proefschrift

Ter verkrijging van de graad van doctor aan de Universiteit Utrecht, op gezag van de Rector Magnificus, Prof. Dr. H.O. Voorma, ingevolge het besluit van het College voor Promoties in het openbaar te verdedigen op dinsdag 28 november 2000 des ochtends te 10.30 uur

door

Remco Walter Alexander Havenith

geboren op 24 juni 1971, te Apeldoorn.

promotor: Prof. Dr. L.W. Jenneskens

co-promotor: Dr. J.H. van Lenthe

beiden verbonden aan het Debye Instituut van de Universiteit Utrecht.

ISBN 90-393-2499-9

This work was partially sponsored by NCF, Cray Research Inc (NCF grant CRG 96.18) and the Stichting Nationale Computerfaciliteiten (NCF) (use of supercomputer facilities), with financial support from the Nederlandse Organisatie voor Wetenschappelijk Onderzoek (NWO).

I want to believe in the madness that calls now

I want to believe that a light is shining through somehow

(David Bowie, The Cygnet Committee, 1969)

Aan mijn ouders

Contents

Chapter 1

General introduction

1. General introduction

At the time that alchemy was evolving into modern chemistry, unexplainable differences existed between substances derived from living sources (organic substances) and those from minerals (inorganic substances). The term organic chemistry came to mean the chemistry of living organisms. After the discovery that organic substances could be turned into inorganic ones and *vice versa*, the term organic chemistry is used to denote the study of compounds built up mainly from carbon [1]. These organic materials have a wide spread use, *e.g.* as medicines, dyes, plastics, fuels and opto-electric materials. A major challenge in organic chemistry is the understanding of the relation between the physical properties of a compound and its structure. This knowledge can assist in the development of new materials with pre-defined properties. The properties of a molecule can be studied using either experimental or theoretical techniques. A variety of analytical and spectroscopic tools are nowadays available for the experimental study of structures and properties [2]. For organic synthesis, the knowledge of reaction mechanisms assists in steering reactions and rationalising the formation of side products. Reaction mechanisms can be studied for example by measuring reaction kinetics or by using isotope labelling techniques [3].

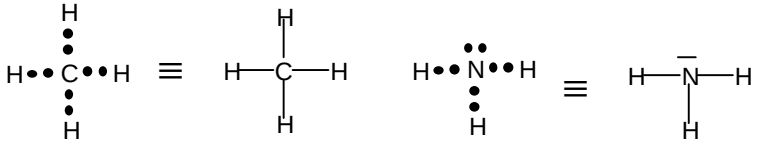

Scheme 1 The Lewis and Kekulé structures of methane (CH_4) and ammonia (NH_3).

The theoretical study of organic molecules started with the first description of the chemical bond in molecules, which was given by Lewis [4]. He considered only the outer electrons (the valence electrons) to be important in the formation of chemical bonds. A covalent chemical bond is formed between atoms by sharing electrons. This is done because atoms aim at a noble gas electron configuration (octet rule). Carbon, having four

valence electrons, is thus able to share four electrons and can thus form four bonds. Dots (Lewis structures) or lines (Kekulé structures) in a graphical representation of a molecule denote the electron pairs as is shown in Scheme 1.

The development of quantum chemistry led to a better understanding of the formation of chemical bonds. In 1927, Heitler and London formulated a wave function for the hydrogen molecule [5]. The chemical bond between the two hydrogen atoms (H_A and H_B) is formed by coupling the spins from one electron in the 1s atomic orbital positioned on H_A and one electron in the 1s atomic orbital positioned on H_B into a singlet. The corresponding wave function is called the Valence Bond (VB) wave function. The chemical bond (a line in a Kekulé structure) is described by a singlet coupled electron pair.

Another view at chemical bonding is provided by the molecular orbital (MO) theory, developed by Hund [6], Mulliken [7] and many others. According to MO theory, the atomic orbitals are combined into molecular orbitals (LCAO-MO expansion), and all molecular orbitals can be doubly occupied.

2. The application of quantum chemical calculations in organic chemistry

The simplest MO theory is the Hückel theory [8,9]. Despite its numerous approximations (only nearest neighbour interactions and neglect of explicit electron-electron repulsion), it is successfully employed for the qualitative description of unsaturated hydrocarbons. The Hückel rule for cyclic annulenes possessing [4n+2] and [4n] π electrons and the frontier orbital theory [10-12] have been derived using Hückel MO theory. The frontier orbital theory, in which the symmetries of the HOMO and LUMO are considered as the controlling factor in chemical reactions, has successfully been used for explaining the stereochemistry of pericyclic and Diels-Alder reactions [3].

Further development of MO methods led to the current wealth of methods for calculating the electronic structure of molecules. Equilibrium geometries and molecular (response) properties, like dipole moments, infrared and nuclear magnetic resonance spectra, can be computed. Quantitative results can be obtained by the use of large (read

huge) basis sets and accurate methods. These methods should include electron correlation effects and, for heavier elements, relativistic effects.

In organic chemistry, quantum chemistry is most often used for the determination of equilibrium geometries and reaction pathways, *i.e.* reaction and activation energies. The calculation of the different accessible reaction routes for a molecule is helpful in rationalising the product formation of chemical reactions. Reactive intermediates (short-lived molecules) that are experimentally not or hard to access can be studied in computro. *Ab initio* techniques can be used for predicting properties of yet unknown compounds. Nowadays, calculations on molecules are frequently used in many areas of organic chemistry. Only a few examples are given of the application of quantum chemistry in organic chemistry. The examples are chosen to illustrate the strengths of this theoretical tool and its application in experimental chemistry. The abbreviations and quantum chemical concepts can be found in chapter 2 ("A glance at electronic structure theory") and in quantum chemistry textbooks [13,14].

2.1. The structure of the 2-norbornyl cation

The structure of the 2-norbornyl cation (**1**, see Scheme 2) has been a widely debated issue in organic chemistry [15-18]. The question was whether **1** is a non-classical carbocation or that a rapid equilibrium exists between the classical carbocations **2a** and **2b**.

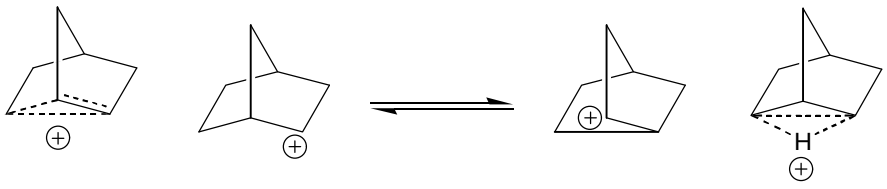

(**1**) (**2a**) (**2b**) (**3**)

Scheme 2 The possible structures of the 2-norbornyl cation.

Ab initio calculations at different levels of theory were performed to elucidate the nature of the 2-norbornyl cation [19]. At the RHF level, the symmetric (C_s) structure **1** corresponds to a transition state when basis sets with no polarisation functions are used. Thus, at the RHF/4-21G and 4-31G level of theory, the structures **2a** and **2b** are minima. However, structure **1** becomes a minimum when polarisation functions are added to the basis set, while the geometries of **2a** and **2b** cannot be located! The inclusion of electron correlation at the MP2/6-31G* level of theory did not alter the conclusions: **1** is a minimum, while **2a** and **2b** are no stationary points. The edge-protonated structure **3** corresponds to a saddle point.

The experimental ^{13}C NMR chemical shifts are in good agreement with those calculated for the non-classical structure [20]. The conclusion must thus be that the 2-norbornyl cation (**1**) is a non-classical carbocation.

2.2. A body-diagonal bond in 1,4-dehydrocubane?

In 1990, Michl and co-workers tried to synthesise a cubane derivative with a body-diagonal bond (**1** in Scheme 3) [21]. Infrared studies in an argon matrix at 12 K showed that in all attempts only one single species was formed. The observation that oligomers are formed upon treatment of 1,4-dihalocubanes with organolithium compounds, suggests a biradical species as an intermediate [22]. Quantum chemical calculations were used to study whether **2** is a possible candidate for the structure of this species [21,23].

Singlet **2** was identified as a minimum on the potential energy surface, positioned 10.5 kcal/mol (GVB/6-31G*) below the triplet state. The distance between the carbon atoms over the diagonal is 2.63 Å. The structure with the anti-bonding combination of the orbitals centred at the indicated carbon atoms in Scheme 3 (**2**) is 91.0 kcal/mol lower in energy than that with the bonding combination (**1**). Thus the strain imposed on the other C-C bonds is larger than the energy gain by forming a body-diagonal bond!

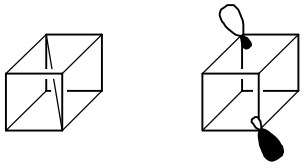

(**1**) 91.0 (**2**) 0.0

Scheme 3 The studied cubanes. Indicated is their relative energy in kcal/mol, calculated at the GVB/6-31G* level of theory [23].

The unknown species in the argon matrix at 12 K is thus presumably indeed 1,4-dehydrocubane (**2**), with no body-diagonal bond. The agreement of the calculated IR spectrum with the experimental one further supports this assignment [21].

2.3. The rotational barrier in formamide

The amide moiety represents an important functionality in for example peptides, *i.e.* in the polymerisation of amino acids. The origin of the high rotational barrier and planarity of the simplest molecule possessing an amide group, *viz.* formamide, is still an issue that attracts considerable attention. It was always assumed that a delocalised π system as a consequence of the resonance between the two structures, depicted in Scheme 4, led to the planar form and relatively high (calculated 15.3 kcal/mol [24]; experimental 18-19 kcal/mol [25-27]) rotational barrier of formamide. As a result of this resonance, the C-N bond is shorter and the C=O bond is longer than a normal C-N and C=O bond, respectively. However, the C=O bond length of formamide (1.219 Å) is almost equal to that of formaldehyde (1.206 Å) [28]. Upon rotation, the resonance stabilisation will be lost, and therefore a relatively high rotational barrier is expected.

This view was challenged by Wiberg *et al.* [24,29] in 1987 on the ground of theoretical calculations. They studied the rotational barrier of formamide at the RHF/6-31G*, MP3/6-31G*//RHF/6-31G* [24] and MP2/6-31G* [29] levels of theories. Two

transition states were located for the rotation, positioned 16.7 kcal/mol and 18.6 kcal/mol, respectively, above formamide.

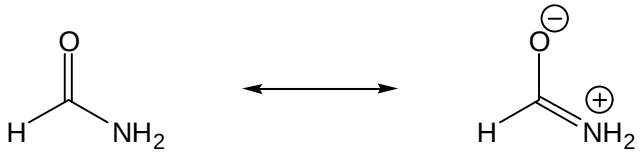

Scheme 4 The two resonance structures of formamide.

In the transition state, the C-N bond is substantially elongated by 0.08 Å, but the C=O bond is unaffected (decrease of only 0.01 Å). The calculated electron population on nitrogen decreases upon rotation (0.25 electron) and that on the carbonyl oxygen atom decreases only slightly (0.05 electron). These observations militate against the resonance model. Wiberg *et al.* [29] expected a more equal change in bond lengths for the C-N and C=O bond, if the resonance model is correct. The electron population on nitrogen for the planar form should be lower than for the transition state, while the electron population on oxygen should be higher in the planar form. Further evidence that the resonance picture is not correct comes from an analysis of the force constants. The carbonyl stretching force constant (planar: 15.80 mdyn/Å; TS: 16.95 mdyn/Å) does not change much upon rotation of the NH_2 group. The major changes were found in the C=N (planar: 8.22 mdyn/Å; TS: 6.15 mdyn/Å) and C=O/C-N interaction force constants (planar: 1.59 mdyn/Å; TS: 1.01 mdyn/Å). Thus it was concluded that the C=O bond is unaffected upon rotation. A further analysis using the atoms-in-molecules theory [30] led to the same conclusions: the role of the oxygen atom is to polarise the carbonyl group and make the carbon atom able to interact with the nitrogen.

Wiberg *et al.* [29] rationalise the change in the C-N bond length by hybridisation arguments: in the planar form, the nitrogen atom is sp^2 hybridised, and is thus more electronegative (thus leading to the shortening of the C-N bond) than in the transition state, where the nitrogen atom is sp^3 hybridised. The rotation barrier is explained by the fact that the amino group is destabilised as a consequence of the loss of electron

population, while the carbonyl carbon gains electron population. However, the amino group is destabilised more than the carbonyl carbon is stabilised. Their main conclusion is that the C=O bond is only a spectator. The resonance picture does not give an adequate description of the system.

It should be mentioned, however, that their calculated bond orders for the C=O and C-N bonds indicate that the resonance picture is correct. Upon rotation, the π bond order of the C=O bond increases from 0.458 to 0.571, while that of the C-N bond decreases from 0.229 to 0.046. In contrast, the σ C=O bond order is only moderately affected (planar: 0.668; TS: 0.677) while that of the C-N bond increases (planar: 0.655; TS 0.844) [29]. The total covalent C=O bond order is only 1.127, indicating a high degree of ionic character of the bond.

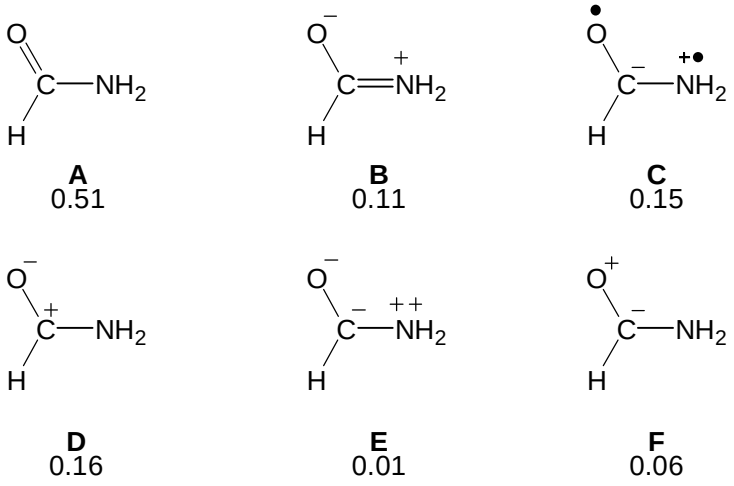

Scheme 5 **The weights of the six most important resonance structures of formamide (VB/6-31G).**

Furthermore, Wiberg *et al.* claim that their conclusions are in accord with valence bond calculations previously performed on formaldehyde [31]. A more recent VB/6-31G calculation (performed at RHF/6-31G geometry, using TURTLE [32]; the orbitals were fully optimised) is in line with the earlier VB calculations using STO-5G

and STO-6G basis sets. The weights of the different structures (depicted in Scheme 5) indicate that structure **A** is the most important one. The C=O bond has, in agreement with the calculated bond orders, a high ionic character, as structure **D** is important. Indeed, the weight of structure **B** is small, though structure **C** cannot be ignored. Upon rotation, the structures **B** and **C** do not contribute anymore to the wave function [31], while structures **A** and **D** do. Thus, according to the VB results, the resonances between the structures **A**↔**B** and **A**↔**C** contribute to the rotational barrier (see also [33]).

Later, in 1997, Glendening *et al.* [34] provided evidence that reaffirmed the traditional view. They analysed the wave function using the natural bond orbital methods [35,36]. Atomic charges were derived using a natural population analysis (NPA) [37] and the results were also analysed in light of the natural resonance theory [38,39] (NRT). They found that upon rotation the electron population on the nitrogen atom increases, while that on oxygen decreases! The electron population on carbon was essentially unaffected. These results are in line with the resonance model as is shown in Scheme 4.

According to natural resonance theory (NRT), formamide should be described by the two resonance structures depicted in Scheme 4 in the ratio 2:1. Glendening *et al.* concluded that the torsional behaviour of formamide is consistent with the conventional amide resonance model, in contrast to the conclusion of Wiberg *et al*.

This example shows that a careful analysis is necessary. Wiberg *et al.* considered only the change in bond length and atomic charges. Atomic charges cannot be uniquely defined, thus neither the AIM charges nor the NPA charges can be considered to be correct [34]. The changes in bond order were almost ignored by Wiberg *et al*. The changes in π bond order calculated by Wiberg *et al.* actually support the traditional view. The high ionic character of the C=O bond could explain the small change in its bond length upon rotation, as the bond length is less influenced by covalent bond orders. The VB calculations suggest that resonance is a contributing factor. Thus the resonance model (or equivalently the delocalised π system) does rationalise at least in part the high rotational barrier and the planar geometry of the amide group.

2.4. The study of through-bond interactions

The mechanism of electron transfer mediated *via* saturated hydrocarbon bridges is also an important subject of study. It is of particular relevance for the development of opto-electric materials and, thus, for an upcoming field of research, *viz.* molecular electronics [40]. In this context, the diethynyl[n]staffanes (**1**), polynorbornyl-dienes (**2**) and divinyl alkanes (**3**) (the structural formulas of **1**-**3** are shown in Scheme 6) have been studied [41,42]. It is expected that their π bonds are degenerate as both groups are separated from each other by a large distance. Thus both π bonds do not have a direct interaction (through-space interaction). However, calculations on **1**-**3** show that the ionisation potentials of the π bonds differ significantly [41,42]. These results were verified by photo-electron spectroscopy experiments [43]. This observation led to the question how these bonds interact with each other. It should be noted that the strict notations σ and π are not valid, as these molecules are not linear and even not planar. In this case, as a consequence of the symmetry, the π bonds of these molecules can interact with the σ bonds. The π bonds can thus interact with each other *via* the intervening σ bonds, which is a through-bond mechanism [44].

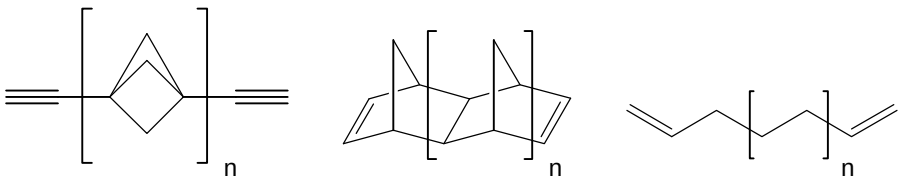

(**1**) (**2**) (**3**)

Scheme 6 Diethynyl[n]staffanes (1), polynorbornyl dienes (2) and divinyl alkanes (3).

It has been proposed that through-bond interactions enhance the rate of electron or hole transfer processes [44-49]. Thus an understanding of the requirements for through-

bond coupling and how these interactions are established as well as its length dependency are important criteria for the design of opto-electric materials.

A model for the description of through-bond coupling was outlined by McConnell [50]. Accordingly, the molecule can be represented as composed of two chromophores [C] that interact with each other *via* a bridge consisting of *N* units [B]. A graphical representation of the McConnell model is given in Scheme 7. The chromophores interact with their nearest bridge site (interaction *T*) and the bridge sites interact only with their nearest neighbours (interaction *t*).

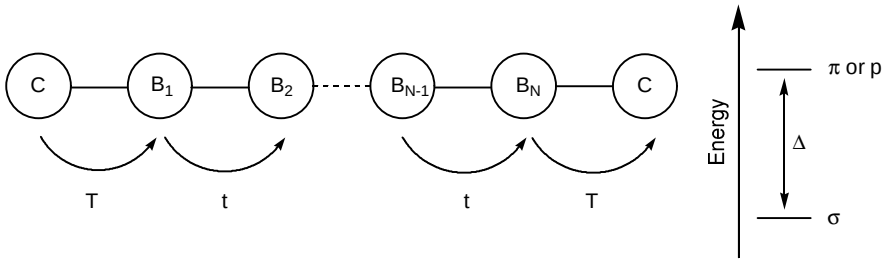

Scheme 7 **A graphical representation of the McConnell model for the description of through-bond orbital coupling. The chromohpores (C) interact with each other *via* the *N* bridges B.**

The splitting ΔE of the energy levels of the orbitals on the chromophores is then expressed as a product of a term describing the interaction between the chromophore and the bridge, and a term describing the propagation of the interaction along the bridge (*1*). Both terms are inversely proportional to the difference in energy of the orbital on the chromophore and the orbital on the bridge site (*D*).

$$\Delta E = -2\frac{T^2}{\Delta}\left(\frac{t}{\Delta}\right)^{N-1} \qquad (1)$$

The McConnell model does not give an accurate description of through-bond coupling in real molecules, as only the interactions between nearest neighbouring bridges are taken into account. The splitting of the energies of the orbitals on the chromophore depends also on the interaction between non-nearest neighbouring bridges. Since it is too complicated to include the other interactions into the McConnell model and one is only interested in qualitative answers, the formula has been simplified. The McConnell model predicts an exponential decrease with the chain length for the orbital energy splitting if t/D is smaller than 1. Therefore, an exponential decay for the orbital splitting as a function of the number of intervening σ bonds was proposed [51-54].

$$\Delta E = Ae^{-b\frac{N}{2}} \qquad (2)$$

In this equation, β is the attenuation coefficient (units: per bond) for hole and electron transfer, respectively. The smaller the β value, the better electron (hole) transfer can occur over large distances [51-54].

Table 1 **The splitting in energy between the π bonds (RHF/3-21G) and the β(i,i+1) values (per bond) determined from the splittings for adjacent members of 1, 2 [41] and 3 [42].**[1]

	ΔE			β(i,i+1)		
n	**1**	**2**	**3**	**1**	**2**	**3**
1	0.68	1.06	0.58	0.59	1.03	0.69
2	0.28	0.38	0.29	0.51	0.80	0.59
3	0.13	0.17	0.16	0.43	0.69	0.54
4	0.07	0.09	0.09	0.39	0.68	0.53
5	0.04	0.04	0.06			0.53
6			0.03			0.53
7			0.02			

[1] The β(i,i+1) values in Table 1 are two times larger than those cited in the references [41] and [42]. The division by 2 in equation (*2*) was later added [54].

The β values for **1**, **2** and **3** have been calculated from the ionisation potentials of the consecutive pairs in the series. The energy splittings of **1** (n=1-5), **2** (n=1-5) and **3** (n=1-7) were obtained using Koopmans [55] ionisation potentials at the RHF/3-21G level of theory and are presented in Table 1. The small β values indicate that the σ skeleton is able to mediate orbital interactions over a large distance [41]. **1** has the smallest β(i,i+1) values, suggesting that **1** is the most efficient bridge.

The bonds of the σ skeleton which are involved in the through-bond interactions can be identified by analysing the wave function in terms of for example natural bond orbitals (NBO's) [36,56].

This idea of measuring the splittings in orbital energies as an indicator of through-bond orbital interactions is also applied in Chapter 6 of this thesis. For tetrahydro-*4H*-thiopyran end-capped oligo(cyclohexylidenes), β values between 0.06 and 0.12 are found, indicating that the oligo(cyclohexylidene) bridge is more efficient in mediating through-bond interactions than **1**, **2** or **3**.

2.5. The concept of aromaticity

Benzene was originally described as an aromatic compound because of its particular fragrance [57]. The initial studies revealed that benzene has a molecular formula of $(CH)_6$, and thus is an unsaturated compound. However, benzene has a markedly different reactivity compared to other alkenes. Kekulé suggested that benzene consists of two conformers, which in fact are rapidly equilibrating 1,3,5-cyclohexatrienes [58] (Scheme 8).

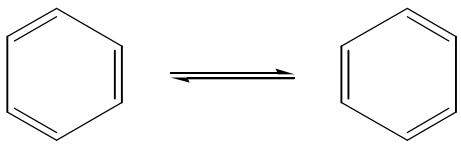

Scheme 8 **The equilibrium between the two isomers of 'benzene', according to Kekulé [58].**

Further experimental results showed that benzene indeed possesses different properties. The heat of hydrogenation of benzene is *ca*. 34 kcal/mol less than what would be expected for a molecule possessing three double bonds [3]. This means that benzene is more stable than a hypothetical reference molecule with three double bonds. Benzene possesses D_{6h} symmetry thus all bond lengths are equal (1.399 Å [59]). In contrast to alkenes, benzene undergoes electrophilic substitution rather than addition reactions [3], *i.e*. the three double bonds are retained after the reaction. The observations of the anomalous chemical reactivity and the bond length equalisation led to the chemical reactivity and the geometric criteria of aromaticity.

The quantum mechanical description of benzene using Hückel MO theory [8,9], suggests that benzene possesses a delocalised π system. The π bonds are not localised between two neighbouring atoms, but are delocalised over the entire molecule. An extra amount of energy is gained (delocalisation energy), due to this delocalisation of the π electrons.

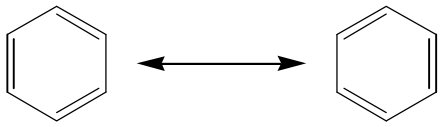

Scheme 9 The Kekulé resonance structures of benzene.

The VB wave function of benzene is a superposition of both Kekulé resonance structures depicted in Scheme 9. Note that the geometry of the benzene skeleton is not changed in the structures in Scheme 9, in contrast to those in Scheme 8; *only the position of the double bonds is changed*. The interaction between these structures lowers the total energy of the molecule compared to that of one structure. This energy difference is the resonance energy, according to Pauling [60,61]. The descriptions of benzene in terms of either resonating Kekulé structures or with a delocalised π electron system are equivalent and so are delocalisation and resonance. Both models are able to explain the chemical reactivity of benzene.

The resonance or delocalisation energy of an aromatic hydrocarbon, which serves as the energetic criterion of aromaticity, can be calculated in various ways. With MO techniques as well as with experiment, the extra stabilisation of an aromatic compound must be calculated with respect to suitable chosen reference molecules, for example polyene references [62]. The stabilisation of benzene can be calculated using the following homodesmotic reaction [63]:

3 *trans*-butadiene $\rightarrow$ benzene + 3 ethene ΔH=-35.2 kcal/mol.

This reaction enthalpy indicates that the delocalised π system of benzene is more stable than three isolated π bonds, and this ΔH is associated with the resonance or delocalisation energy of benzene. Other attempts have been undertaken to calculate the resonance energy of benzene by replacing the benzene π bonds by localised (non-interacting) ethene π bonds [64].

Using VB theory, the resonance energy can directly be calculated as the energy difference between the total VB energy and the energy of the most stable structure [60,61]. The electronic structure of benzene has been addressed using VB calculations [65]. The resonance energy of benzene was calculated using the VB methodology and ranges from 28.5 [66] to 74.3 [67] kcal/mol, depending on the number of structures included in the calculation.

Both the superposition of more than one Kekulé resonance structure and the delocalised π orbitals lead to specific magnetic properties characteristic for aromatic molecules. Aromaticity is now associated with cyclic electron delocalisation [63]. Due to the presence of the highly mobile π electrons, ring currents can be induced when applying an external magnetic field. A consequence of this ring current is a highly anisotropic magnetic susceptibility. In addition, the hydrogen atoms are more deshielded than those attached to normal alkenes, resulting in a downfield shift of their ^{1}H NMR resonances [68,69]. The magnetic properties of unsaturated cyclic systems are nowadays frequently used for the assessment of their aromatic properties [63].

The situation was recently further complicated by the papers of Shaik, Hiberty and co-workers [70-72]. Whereas it was always assumed that the π electrons determine the symmetric geometry of benzene, their calculations indicate that the σ electrons favour the symmetric hexagonal structure, while the π electrons favour alternating single and double bonds. Their view on benzene led to a debate in the literature about the influence of the σ and π electrons on the structure of benzene [73-76]. Recent VB results suggest that a subtle interplay of the forces of the σ skeleton (favours D_{6h} symmetry), resonance (favours D_{6h} symmetry) and the π bonds (favours D_{3h} symmetry) determine the geometry of benzene [77]. This subject is outlined in Chapter 7 in more detail.

2.6. Pyramidal tetracoordinated carbon atoms

In 1874 Le Bel and Van 't Hoff proposed the tetrahedral geometry of tetracoordinated carbon [78,79]. Since then, organic chemists started the quest for finding examples of molecules in which a tetracoordinated carbon atom has a planar geometry or has all four bonds on its same side, to find out whether the tetrahedral geometry of tetracoordinated carbon is a hard and fast rule. A molecule that has been the subject of various recent theoretical studies is pyramidane (see Scheme 10) [80-82].

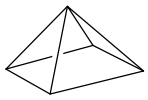

pyramidane

Scheme 10

MP2/6-31G* calculations show that pyramidane is a real minimum on the C_5H_4 potential energy surface and possesses C_{4v} symmetry [82,83]. The carbon-carbon distances towards the apical carbon atom are rather long, *viz.* 1.64 Å. The lowest located barrier for the rearrangement of pyramidane is that for the reaction of pyramidane to

tricyclo[2.1.0.0^{2,5}]pent-3-ylidene (see Scheme 11). The barrier height is 23.0 kcal/mol, thus pyramidane is a fairly stable molecule.

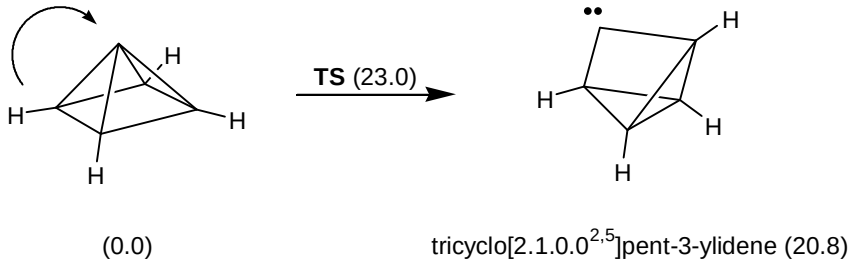

(0.0) tricyclo[2.1.0.0^{2,5}]pent-3-ylidene (20.8)

Scheme 11 The rearrangement reaction of pyramidane to tricyclo[2.1.0.0^{2,5}]pent-3-ylidene. The reaction and activation energies are shown between parentheses (in kcal/mol).

The electronic structure of pyramidane was analysed by calculating the Löwdin bond orders [84,85] and performing an NBO analysis [36,56]. The bond order between the apical carbon atom with one of the four carbon atoms forming the square is only 0.79, suggesting very weak bonds from the apical carbon to the base carbon atoms. The NBO analysis shows that pyramidane possesses a lone pair at the apical carbon atom. Thus pyramidane is proposed to consist of a C^{2-} unit bonded to a cyclobutadiene dication. However, a calculation of the magnetic properties of pyramidane shows that the base square does not possess aromatic properties, as is expected for the cyclobutadiene dication [83].

Other structures possessing a pyramidal carbon atom, also have this electronic structure [86], suggesting that these molecules are strong bases. The calculated proton affinities indeed suggest this (proton affinities in the range 268-282 kcal/mol). These proton affinities are larger than that of the superbase 1,8-bis(dimethylamino)naphthalene, which is 246 kcal/mol [87]. The proton affinity of pyramidane itself is 233 kcal/mol [83]).

All these examples show that *ab initio* theory is a very useful tool for both the interpretation of experimental phenomena and for the study of the fundamentals in organic chemistry.

3. Subjects covered in this thesis

In this thesis, *ab initio* methods will be used to study ground- and excited state properties and the concept of aromaticity. It starts off with the photo-electric properties of oligo(cyclohexylidenes) [Chapters 3-6]. Oligo(cyclohexylidenes) have been put forward as a novel class of molecular rods [88-90]. They are composed of cyclohexyl moieties, connected *via* olefinic bonds [see Scheme 12 for the general structure of oligo(cyclohexylidenes)]. The π bonds in oligo(cyclohexylidenes) do not form a conjugated system, as they are separated from each other by three σ bonds. The symmetry of these oligomers is such that the π bonds can interact with the σ bonds. The π bonds interact thus with each other *via* the σ bonds. This suggests that functional groups positioned at the α and ω termini can interact with each other *via* a through-bond orbital coupling mechanism, which is indeed the case [91]. It is shown that this hydrocarbon skeleton is a very efficient mediator in through-bond coupling. The application of the McConnell model reveals that the rate of electron transfer *via* tetrahydro-*4H*-thiopyran end-capped oligo(cyclohexylidenes) has a very weak distance dependence. These properties of the oligo(cyclohexylidenes) make them candidates for their application as active spacers in opto-electric compounds [92].

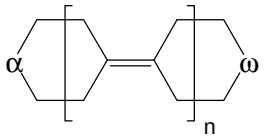

α and/or ω: CH_2; C=O; C=NOH; S; C=CH-$(CH_2)_n$-CH_3 etc.

Scheme 12 General formula of α,ω end-functionalised oligo(cyclohexylidenes).

The photo-physical properties of oligo(cyclohexylidenes) and of tetrahydro-*4H*-thiopyran end-capped oligo(cyclohexylidenes) are explored in the chapters 3-6. Various computational techniques are used to set up a framework for calculating the UV spectra of this class of compounds. The UV spectra are calculated as a function of the length and the conformation of the oligo(cyclohexylidenes).

The central theme in chapters 7 and 8 is related to the concept of aromaticity, which has been studied using the VB methodology. It is shown that it is not straightforward to extend this concept to (non)-alternant polycyclic aromatic hydrocarbons (PAH), possessing extended π systems and multiple rings. The different aromaticity criteria outlined in section 2.5 ("The concept of aromaticity") may lead to different conclusions concerning the aromatic character of the different rings. First the concept of aromaticity is explored by studying the resonance energy of benzene and its elusive reference molecule 1,3,5-cyclohexatriene. Next, it is extended towards larger systems.

Finally, another aspect of benzene is considered, *i.e.* the valence isomerisation of Dewar benzene into benzene (Chapter 9). It was always assumed within the context of the Woodward and Hoffmann rules [93] that this reaction proceeds *via* the thermally forbidden [93] *dis-rotatory* transition state. Otherwise, *via* the *con-rotatory* pathway, the highly strained isomer *cis, cis, trans*-1,3,5-cyclohexatriene (*trans*-benzene) would be formed. Recently, tentative computational evidence was reported that a *con-rotatory* pathway is accessible. However, this issue has never been scrutinised in detail.

References

[1] For example: J. McMurry, Organic chemistry, (Brooks/Cole, California, 1988).

[2] For example: H.H. Willard, L.L. Merritt Jr., J.A. Dean and F.A. Settle Jr., Instrumental methods of analysis, (Wadsworth publishing company, Belmont, California, 1988).

[3] For example: J. March, Advanced organic chemistry. Reactions, mechanisms, and structure, (John Wiley & Sons, New York, 1992).

[4] G.N. Lewis, *J. Am. Chem. Soc.*, **38** (1916) 762.

[5] W. Heitler and F. London, *Z. Physik*, **44** (1927) 455.

[6] F. Hund, *Z. Physik*, **73** (1931) 1.

[7] R.S. Mulliken, *Phys. Rev.*, **41** (1932) 49.

[8] E. Hückel, *Z. Physik*, **70** (1931) 204.

[9] E. Hückel, *Z. Physik*, **76** (1932) 628.

[10] K. Fukui, *Acc. Chem. Res.*, (1971) 57.

[11] K.N. Houk, *Acc. Chem. Res.*, **8** (1975) 361.

[12] K. Fukui, *Angew. Chem. Int. Ed. Engl.*, **21** (1982) 801.

[13] W.J. Hehre, L. Radom, P. von R. Schleyer and J.A. Pople, Ab initio molecular orbital theory, (John Wiley and Sons, New York, 1986).

[14] A. Szabo and N.S. Ostlund, Modern quantum chemistry. Introduction to advanced electronic structure theory, (McGraw-Hill Inc., New York, 1989).

[15] C.A. Grob, *Acc. Chem. Res.*, **16** (1983) 426.

[16] H.C. Brown, *Acc. Chem. Res.*, **16** (1983) 432.

[17] G.A. Olah, G.K.S. Prakash and M. Saunders, *Acc. Chem. Res.*, **16** (1983) 440.

[18] C. Walling, *Acc. Chem. Res.*, (1983) 448.

[19] W. Kock and B. Liu, *J. Am. Chem. Soc.*, **111** (1989) 1527.

[20] P. von R. Schleyer and S. Sieber, *Angew. Chem. Int. Ed.*, **32** (1993) 1606.

[21] K. Hassenrück, J.G. Radziszewski, V. Balaji, G.S. Murthy, A.J. McKinley, D.E. David, V.M. Lynch, H.-D. Martin and J. Michl, *J. Am. Chem. Soc.*, **112** (1990) 873.

[22] P.E. Eaton and J. Tsanaktsidis, *J. Am. Chem. Soc.*, **112** (1990) 876.

[23] D.A. Hrovat and W.T. Borden, *J. Am. Chem. Soc.*, **112** (1990) 875.

[24] K.B. Wiberg and K.E. Laidig, *J. Am. Chem. Soc.*, **109** (1987) 5935.

[25] B. Sunner, L.H. Piette and W.G. Schneider, *Can. J. Chem.*, **38** (1960) 681.

[26] H. Kamei, *Bull. Chem. Soc. Jpn.*, **41** (1968) 2269.

[27] T. Drakenberg and S. Forsen, *J. Phys. Chem.*, **74** (1970) 1.

[28] M.D. Harmony, V.W. Laurie, R.L. Kuczkowski, R.H. Schwendeman, D.A. Ramsay, F.J. Lovas, W.J. Lafferty and A.G. Maki, *J. Phys. Chem. Ref. Data*, **8** (1979) 619.

[29] K.B. Wiberg and C.M. Breneman, *J. Am. Chem. Soc.*, **114** (1992) 831.

[30] R.F.W. Bader, Atoms in molecules: a quantum theory, (Oxford University Press, Oxford, 1990).

[31] R.H. Flegg and R.D. Harcourt, *J. Mol. Struct. (Theochem)*, **164** (1988) 67.

[32] J. Verbeek, J.H. Langenberg, C.P. Byrman, F. Dijkstra and J.H. van Lenthe, *TURTLE, an ab initio VB/VBSCF program*, 1988-2000.

[33] D. Lauvergnat and P.C. Hiberty, *J. Am. Chem. Soc.*, **119** (1997) 9478.

[34] E.D. Glendening and J.A. Hrabal II, *J. Am. Chem. Soc.*, **119** (1997) 12940.

[35] J.P. Foster and F. Weinhold, *J. Am. Chem. Soc.*, **102** (1980) 7211.

[36] A.E. Reed, L.A. Curtiss and F. Weinhold, *Chem. Rev.*, **88** (1988) 899.

[37] A.E. Reed, R.B. Weinstock and F. Weinhold, *J. Chem. Phys.*, **83** (1985) 735.

[38] E.D. Glendening and F. Weinhold, *J. Comput. Chem.*, **19** (1998) 593.

[39] E.D. Glendening and F. Weinhold, *J. Comput. Chem.*, **19** (1998) 610.

[40] M.N. Paddon-Row and J.W. Verhoeven, *New J. Chem.*, **15** (1991) 107.

[41] M.N. Paddon-Row and K.D. Jordan, *J. Am. Chem. Soc.*, **115** (1993) 2952.

[42] M.J. Shephard, M.N. Paddon-Row and K.D. Jordan, *J. Am. Chem. Soc.*, **116** (1994) 5328.

[43] R. Gleiter, K.-H. Pfeifer, G. Szeimies and U. Bunz, *Angew. Chem. Int. Ed. Engl.*, **29** (1990) 413.

[44] R. Hoffmann, A. Imamura and W.J. Hehre, *J. Am. Chem. Soc.*, **90** (1968) 1499.

[45] R. Hoffmann, *Acc. Chem. Res.*, **4** (1971) 1.

[46] R. Gleiter, *Angew. Chem. Int. Ed. Engl.*, **13** (1974) 696.

[47] M.N. Paddon-Row, *Acc. Chem. Res.*, **15** (1982) 245.

[48] M.N. Paddon-Row, M.J. Shephard and K.D. Jordan, *J. Phys. Chem.*, **97** (1993) 1743.

[49] S.H. Pullen, M.D. Edington, S.L. Studer-Martinez and J.D. Simon, *J. Phys. Chem. A*, **103** (1999) 2740.

[50] H.M. McConnell, *J. Chem. Phys.*, **35** (1961) 508.

[51] M.N. Paddon-Row and S.S. Wong, *Chem. Phys. Lett.*, **167** (1990) 432.

[52] K.D. Jordan and M.N. Paddon-Row, *J. Phys. Chem.*, **96** (1992) 1188.

[53] S. Broo and S. Larsson, *Chem. Phys.*, **148** (1990) 103.

[54] M.J. Shephard and M.N. Paddon-Row, *Chem. Phys. Lett.*, **301** (1999) 281.

[55] T.A. Koopmans, *Physica*, **1** (1933) 104.

[56] A.E. Reed and F. Weinhold, *J. Chem. Phys.*, **83** (1985) 1736.

[57] M. Faraday, *Phil. Trans.*, (1825) 440.

[58] A. Kekulé, *Liebigs Ann.*, **162** (1872) 77.

[59] J.H. Callomon, E. Hirota, K. Kuchitsu, W.J. Lafferty, A.G. Maki, C.S. Pote, I. Buck and B. Starck, Vol. 7, *Structure data of free polyatomic molecules* in Landolt-Börnstein, numerical data and functional relationships in science and technology (Springer-Verlag, Berlin, 1976).

[60] L. Pauling and G.W. Wheland, *J. Chem. Phys.*, **1** (1933) 362.

[61] L. Pauling, The nature of the chemical bond and the structure of molecules and crystals: An introduction to modern structural chemistry, third ed. (Cornell University Press, Ithaca, New York, 1960).

[62] M.J.S. Dewar and C. de Llano, *J. Am. Chem. Soc.*, **91** (1969) 789.

[63] P. von R. Schleyer and H. Jiao, *Pure & Appl. Chem.*, **68** (1996) 209.

[64] H. Kollmar, *J. Am. Chem. Soc.*, **101** (1979) 4832.

[65] D.L. Cooper, J. Gerratt and M. Raimondi, *Nature*, **323** (1986) 699.

[66] G.F. Tantardini, M. Raimondi and M. Simonetta, *J. Am. Chem. Soc.*, **99** (1977) 2913.

[67] Y. Mo, W. Wu and Q. Zhang, *J. Phys. Chem.*, **98** (1994) 10048.

[68] L. Pauling, *J. Chem. Phys.*, **4** (1936) 673.

[69] U. Fleischer, W. Kutzelnigg, P. Lazzeretti and V. Mühlenkamp, *J. Am. Chem. Soc.*, **116** (1994) 5298.

[70] P.C. Hiberty, S.S. Shaik, J.M. Lefour and G. Ohanessian, *J. Org. Chem.*, **50** (1985) 4657.

[71] S.S. Shaik, P.C. Hiberty, J.M. Lefour and G. Ohanessian, *J. Am. Chem. Soc.*, **109** (1987) 363.

[72] S.S. Shaik, A. Shurki, D. Danovich and P. Hiberty, *J. Mol. Struct. (Theochem)*, **398-399** (1997) 155.

[73] K. Jug and A.M. Köster, *J. Am. Chem. Soc.*, **112** (1990) 6772.

[74] E.D. Glendening, R. Faust, A. Streitwieser, K.P.C. Vollhardt and F. Weinhold, *J. Am. Chem. Soc.*, **115** (1993) 10952.

[75] L.W. Jenneskens, E.N. van Eenige and E.J. Vlietstra, *New. J. Chem.*, **18** (1994) 553.

[76] A. Moyano and J.C. Paniagua, *J. Mol. Struct. (Theochem)*, **369** (1996) 39.

[77] F. Dijkstra, Valence Bond theory. Implementation and use of analytical gradients, Ph.D. Thesis, Utrecht University, Utrecht, The Netherlands (2000).

[78] J.A. le Bel, *Bull. Soc. Chim. Fr. II*, **22** (1874) 337.

[79] J.H. van 't Hoff, *Bull. Soc. Chim. Fr. II*, **23** (1875) 295.

[80] V.I. Minkin, R.M. Minyaev and G.V. Orlova, *J. Mol. Struct. (Theochem)*, **110** (1984) 241.

[81] V. Balaji and J. Michl, *Pure & Appl. Chem.*, **60** (1988) 189.

[82] E. Lewars, *J. Mol. Struct. (Theochem)*, **423** (1998) 173.

[83] E. Lewars, *J. Mol. Struct. (Theochem)*, **507** (2000) 165.

[84] M.A. Natiello and J.A. Medrano, *Chem. Phys. Lett.*, **105** (1984) 180.

[85] M.A. Natiello and J.A. Medrano, *Chem. Phys. Lett.*, **110** (1984) 445.

[86] D. Rasmussen and L. Radom, *Chem. Eur. J.*, **6** (2000) 2470.

[87] E.P.L. Hunter and S.G. Lias, *J. Phys. Chem. Ref. Data*, **27** (1998) 413.

[88] F.J. Hoogesteger, R.W.A. Havenith, J.W. Zwikker, L.W. Jenneskens, H. Kooijman, N. Veldman and A.L. Spek, *J. Org. Chem.*, **60** (1995) 4375.

[89] A.W. Marsman, Functionalized oligo(cyclohexylidenes). Semi-rigid molecular rods for crystal engineering, through-bond orbital interactions and self-assembly, Ph.D. Thesis, Utrecht University, Utrecht, The Netherlands (1999).

[90] F.J. Hoogesteger, Oligo(cyclohexylidenes). Development of novel functional and organized materials, Ph.D. Thesis, Utrecht University, Utrecht, The Netherlands (1996).

[91] A.W. Marsman, R.W.A. Havenith, S. Bethke, L.W. Jenneskens, R. Gleiter and J.H. van Lenthe, *Eur. J. Org. Chem.*, (2000) 2629.

[92] E.P.A.M. Bakkers, A.W. Marsman, L.W. Jenneskens and D. Vanmaekelbergh, *Angew. Chem. Int. Ed.*, **39** (2000) 2297.

[93] R.B. Woodward and R. Hoffmann, The conservation of orbital symmetry, (Verlag Chemie GmbH, Academic Press Inc., New York USA, 1971).

Chapter 2

A glance at electronic structure theory

1. The Schrödinger equation

All calculations performed in this thesis start by solving the time-independent non-relativistic Schrödinger equation [1].

$$\hat{H}\Psi = E\Psi \qquad (1)$$

where $\hat{H}$ is the Hamilton operator, which describes the system, E is its eigenvalue, *i.e.* the total energy of the system, and Ψ is the wave function. The total energy in the absence of an external field (like electric or magnetic field) depends on the kinetic energy of the nuclei and electrons, the coulomb attraction between the nuclei and electrons, the repulsion between the electrons and the repulsion between the nuclei, respectively. Hence, the motions of electrons and nuclei are coupled.

The Born-Oppenheimer approximation [2] was introduced to separate the nuclear and the electronic motion. Within this approximation, the wave function is separated into an electronic and a nuclear part. It is assumed that the electronic wave function does not change much for a small displacement of the nuclear coordinates. The electronic energy depends, after applying the Born-Oppenheimer approximation, parametrically on the nuclear coordinates.

The Schrödinger equation can only be solved analytically for one-electron systems within the Born-Oppenheimer approximation. If the Hamiltonian could be written as a sum of one-electron operators, a solution would be the product of one-electron functions (orbitals) (Hartree product) and the problem is separated into a set of one-electron problems. This product function is not anti-symmetric with respect to the exchange of two electrons. In order to anti-symmetrise this product function, the electrons are permuted among all orbitals, and the wave function is written as a linear combination of all these Hartree products. This anti-symmetric wave function can be written as a determinant and is designated as a Slater determinant [3]. This function is still an eigenfunction of the above-mentioned Hamilton operator.

The electron-electron repulsion term in the Hamiltonian makes that it cannot be written as a sum of one-electron operators. Thus a Slater determinant is only a first approximation to the solution of the Schrödinger equation. Therefore, various approximate schemes have been developed for solving the Schrödinger equation for *n*-electron systems.

2. SCF procedure

A first approximation to solve the Schrödinger equation (*1*) for *n*-electron systems, is treating the electron-electron repulsion that one electron experiences from the other electrons, as a mean field repulsion (Hartree-Fock procedure). The wave function is taken as a single determinant, composed of one-electron functions (molecular orbitals [MO's]). The problem is then finding the best MO's *i.e.* those that minimise the total energy.

At this point, an expression for the MO's is needed. For a one-electron atom, the solutions of the Schrödinger equation are the hydrogenic atomic orbitals (AO's). A natural way to guess the MO's (y) is by expanding them into a linear combination of atomic orbitals (f):

$$y = \sum_i c_i f_i \qquad (2)$$

The choice of the AO's (f) in which the MO's (y) are expanded is called the basis set. In principle, an infinite set of AO's should be used, although in practice this can never be accomplished. Hence, depending on the required accuracy for a calculation, a basis set is chosen.

The coefficients in (*2*) are varied to minimise the energy of the wave function. In Hartree-Fock theory, the MO's are constrained to remain orthonormal. When doing so, the Hartree-Fock integro-differential equation is obtained. This differential equation can be written as an eigenvalue equation.

$$f\psi = \varepsilon\psi \qquad (3)$$

in which f is the Fock operator.

The Fock operator depends on the kinetic and potential energy of the electron and a mean field repulsion that the electron experiences from the other electrons in the molecule. This mean electron repulsion is dependent on the orbitals (ψ). Thus the operator is dependent on its solutions. Therefore, the Hartree-Fock equations should be solved iteratively.

The eigenfunctions of the Fock operator are the canonical MO's, *i.e.* they diagonalise the Fock matrix. The energies of the canonical Hartree-Fock orbitals can be interpreted as the ionisation potential for the removal of an electron from that orbital (Koopmans' theorem [4]). The expectation values derived from a single determinantal wave function are invariant under unitary transformations of the molecular orbitals. This means that the occupied molecular orbitals may be mixed among themselves, without changing for example either the electron density or the total energy [3,5]. Thus the significance of a single MO should not be overrated.

For most organic molecules the Hartree-Fock approximation gives an acceptable description of the ground state of the system. As the Born-Oppenheimer approximation [2] is applied, the energy can be calculated for a particular nuclear configuration and the nuclear coordinates can be varied, until a minimum in energy is found. The corresponding structure represents the equilibrium geometry of a molecule, although the nuclei in a real molecule do not have a fixed position, due to the zero-point vibration. The geometries obtained using a Hartree-Fock wave function are generally close to the experimental ones. The resulting bond lengths are usually shorter than the experimental ones [6].

3. Electron correlation

As the Hartree-Fock procedure is only an approximation to the electronic problem, we have to find ways in which we can improve this solution. The difference between the exact total energy and the Hartree-Fock total energy is called the correlation

energy. Several ways exist to obtain estimates of the correlation energy. The inclusion of electron correlation is at least necessary for obtaining reliable estimates of the energies of excited and transition states.

3.1. Configuration Interaction

If the wave function is expanded in a complete set of N-electron wave functions, the exact energy is obtained. The Hartree-Fock wave function is an N-electron wave function formed from molecular orbitals, thus a complete basis of N-electron wave functions within a given one-electron basis set can be generated by placing the N-electrons in the K molecular orbitals in all possible ways. This procedure is called Full-CI [3]. The Full-CI procedure gives the exact energy within a given basis set. A disadvantage, however, is that the number of determinants grows extremely fast both with an increasing number of electrons and with an increasing number of molecular orbitals. This is exemplified in Table 1, where the total number of determinants is tabulated as a function of the number of electrons and MO's. Consequently, Full-CI calculations can only be performed in practice with a small number of electrons in fairly small basis sets. This limits its use. If a set of good orbitals (obtained by *e.g.* a Hartree-Fock calculation) is used, it is sufficient to include only the single and double excitations from the ground state Hartree-Fock configuration in the CI expansion. This procedure is called single double configuration interaction (SDCI) [7,8].

Table 1 **The number of determinants in a Full-CI calculations for systems containing *K* MO's and *N* electrons.**

	number of MO's (*K*)		
number of electrons (*N*)	25	50	75
10	$1.0 \cdot 10^{10}$	$1.7 \cdot 10^{13}$	$1.2 \cdot 10^{16}$
20	$4.7 \cdot 10^{13}$	$5.4 \cdot 10^{21}$	$3.6 \cdot 10^{25}$
30	$4.7 \cdot 10^{13}$	$2.9 \cdot 10^{26}$	$3.2 \cdot 10^{32}$

To improve the SDCI method, one can generate all single and double excitations from carefully chosen reference functions and not only from the Hartree-Fock wave function. This is the multi-reference SDCI [MR-SDCI] method. For large molecules, the inclusion of all single and double excitations in the CI expansion can still be too excessive. Since not all single and double excitations are equally important in the description of a particular state, methods have been developed to estimate the energy contribution of a configuration [9-12]. If this contribution is smaller than a preset energy threshold (δ, typically in the range 10^{-3} - 10^{-5} Hartree), the configuration is not considered further in the calculation. This method is often denoted as the MRDCI method, which is used in the chapters 2-5 in this thesis for the calculation of excited state properties and transition energies. The MRDCI method was first developed by Buenker and Peyerimhoff [12], and later modified by Engels *et al.* [13].

The disadvantage of the (MR)-CI methods is that all truncated CI methods are not size-consistent. This means that the energy of two non-interacting molecules treated in a (MR)-SDCI calculation is not equal to twice the energy of one molecule. The Davidson correction can be used for approximately correcting this size-consistency error [14].

Other schemes for calculating the correlation energy, which are size-consistent, have been developed. Examples are CEPA [15] and CCSD [16-18]. The CCSD method is now frequently used, and the effects of triple excited states are often estimated from perturbational calculations (CCSD(T) [18,19]).

3.2. Møller-Plesset perturbation theory

Another method to estimate the correlation energy is the use of many-body perturbation theory [6,20,21]. Perturbation theory can also be used for the derivation of molecular properties (as can CI), like magnetic properties (*vide infra*).

The Hamiltonian is partitioned in the zeroth order Hamiltonian (H^0) (unperturbed Hamiltonian) and the perturbation. For estimating the correlation energy, H^0 is the sum of the one-electron Fock operators. One can then derive that the Hartree-Fock energy is equal to the sum of E_0 and $E^{(1)}$, and thus that the first correction to E_{HF} becomes $E^{(2)}$ [3].

Perturbation theory works only for the estimation of the correlation energy if the Hartree-Fock wave function gives already a good description of the molecule, *viz.* in the case of a small perturbation. In the case of near-degeneracies (degenerate HOMO and LUMO), perturbation theory fails and blows up. In these cases, it is necessary to use (multi-reference) CI methods.

It has been shown that the energy obtained by using perturbation theory is size-extensive, like *e.g.* the CCSD(T) method, in every order [22,23]. Another advantage of perturbation theory over CI based methods is that it is computationally less expensive to get estimates of the correlation energy, if it is used in low order. However, the convergence of the series is not guaranteed [24-27].

4. The MCSCF and CASSCF methods

In the case that degeneracies or near-degeneracies occur between different electronic configurations, for example for molecules that possess diradical character (near degenerate HOMO and LUMO), a one-determinantal approach is sometimes insufficient [28]. In this case, the wave function should be written as a linear combination of several determinants (a small CI). The molecular orbitals and the CI coefficients are optimised during the self-consistent field calculation. This approach is called the multi-configuration self-consistent field (MCSCF) approach [29]. If all possible excitations are included within a given space, this approach is called the complete active space self-consistent field approach (CASSCF) [30].

5. Magnetic properties

The effect of a magnetic field on the wave function of a molecule can be estimated by using perturbation theory [31]. The magnetic susceptibility (χ) of a molecule and the absolute chemical shielding of a distinct nucleus (σ) can be written as second derivatives of the total energy [32] with respect to the external magnetic field and to the nuclear magnetic fields. The magnetic field enters the equations as a vector potential,

leading to a gauge dependency in the calculation [33]. Gauge dependency means that the magnitude of the different components (in this case the paramagnetic and diamagnetic part) is dependent on the chosen origin, and one has always a free choice for the place of the origin of the vector potential. The total shielding (sum of the diamagnetic and paramagnetic part), however, is not gauge dependent.

The main problem for the calculation of the magnetic properties lies in the choice of these gauges. To avoid numerical problems, the gauges should be chosen in such a way that the paramagnetic and diamagnetic parts are as small as possible. Several methods to solve these problems have been developed like the Individual Gauges for Localised molecular Orbitals (IGLO) [34-36], Gauge Invariant (including) Atomic Orbitals (GIAO) [37-39] and Continuous Transformation of Origin of Current Density (CTOCTD) approaches [40]. The IGLO method is implemented in *e.g.* Turbomole [41] and Molpro [42]. The GIAO method is implemented in Texas [43] and the Gaussian suite of programs [44]. The accuracy of the GIAO and IGLO methods is comparable.

The calculation of NMR chemical shifts, using the IGLO formalism [34,35], requires three steps. First, the wave function is calculated at the RHF or CASSCF [45] level of theory, then the molecular orbitals are localised, and the last step consists of solving the IGLO equations in an iterative manner. The gauge origins are chosen as the charge centroids of the localised molecular orbitals. For most organic molecules the ^{1}H and ^{13}C NMR chemical shifts can be accurately calculated using a HF wave function, provided that sufficiently large basis sets are used. In contrast, the spin-spin couplings calculated using a HF wave function, are useless [33].

6. Valence Bond theory

In Valence Bond (VB) theory [46-49], the wave function is written as a linear combination of Kekulé (line-bond) structures. These structures are built from a number of determinants, which are composed of doubly and singly occupied orbitals. A structure defines the spin-coupling pattern of the singly occupied orbitals (a line in a Kekulé structure represents a spin singlet coupled electron pair). This method allows an

interpretation of the wave function in terms of single and double bonds. The disadvantage of this method is the large computational demand, due to the non-orthogonality of the orbitals and the multi-determinantal nature of the wave function.

Several VB methods have been developed. The most general one is the valence bond self-consistent field method (VBSCF) [50,51] in which the coefficients of the structures are optimised with respect to the total energy. From the coefficients of the structures, weights of the structures can be evaluated, which indicate the importance of a particular structure in the wave function. The orbitals, which are used in the description of the structures, can be optimised simultaneously. However, the optimal orbitals of an ionic structure differ from those of a covalent structure. In the breathing orbital method, the orbitals of each structure are optimised separately and simultaneously [52-54].

In the spin coupled VB method [55-57], all spin-couplings for the singly occupied orbitals are considered and the orbitals are completely optimised. A method has been devised to transform CASSCF wave functions to spin-coupled wave functions (CASVB) [58-60].

7. Density functional theory

The calculations described in this thesis were performed using wave function methods. Since the popularity of methods based on density functional theory (DFT) [61,62] has increased in the last decade, some general remarks are made. The idea in DFT is that once the electron density is known, the position of the nuclei and their charges is known, and hence the energy is known [63]. The derivation of the Kohn-Sham equations showed that the orbitals [64] have the property that they give the exact electron density, if the exact exchange-correlation functional $E_{xc}[r]$ has been determined. Unfortunately, no expressions exist for the exact exchange-correlation functional, thus $E_{xc}[r]$ should be approximated, making DFT a semi-empirical method. Numerous approximations have been developed, and the B3LYP [65] functional is nowadays very popular.

8. Programs used for the calculations described in this thesis

The calculations described in this thesis have been performed using different programs on different computers. The general calculations (geometry optimisations and Hessian calculations) were performed using the GAMESS-UK program [66].

For performing MRDCI calculations, three programs were available. The MRDCI program of Buenker and Peyerimhoff [67] and the semi Direct MRDCI program of Engels [68], which are both implemented in GAMESS-UK. The newly developed C++ DIESEL-CI program of Hanrath and Engels [13] is linked to GAMESS-UK. The semi Direct MRDCI program was kindly provided by Bernd Engels, and the DIESEL-CI program was kindly provided by Michael Hanrath and Bernd Engels.

Non-selected MRCI calculations were performed with the Direct-CI program [69], which is a part of the ATMOL program package [70], or with the Direct-CI version as implemented in GAMESS-UK.

For the calculations of NMR chemical shieldings, the Direct IGLO program [71] as implemented in Turbomol [41] was used. Ulrich Fleischer is gratefully acknowledged for providing the DSCF and DIGLO programs.

Valence bond calculations were performed with TURTLE [72]. TURTLE is a VBSCF program for optimising the structure coefficients and orbitals of the structures. The recently implemented analytical gradients for VBSCF wave functions [73] make it possible to perform geometry optimisations.

Most of the calculations were run on Silicon Graphics machines, equipped with R8K (90 MHz, 360 Mflop/s), R10K (195 MHz, 390 Mflop/s) and R12K (300MHz, 600 Mflop/s) CPU's. The CRAY YMP (240 MHz, 960 Mflop/s) which is located at SARA at Amsterdam, was used for the very large and memory consuming calculations.

References

[1] E. Schrödinger, *Ann. Physik*, **79** (1926) 361.

[2] M. Born and R. Oppenheimer, *Ann. Physik*, **84** (1927) 457.

[3] A. Szabo and N.S. Ostlund, Modern quantum chemistry. Introduction to advanced electronic structure theory, (McGraw-Hill Inc., New York, 1989).

[4] T.A. Koopmans, *Physica*, **1** (1933) 104.

[5] J. Almlöf, *Notes on Hartree-Fock theory and related topics* in: Lecture notes in quantum chemistry II. European summer school in quantum chemistry, Vol. 64, ed. B.O. Roos (Springer-Verlag, Berlin, 1994).

[6] W.J. Hehre, L. Radom, P. von R. Schleyer and J.A. Pople, Ab initio molecular orbital theory, (John Wiley and Sons, New York, 1986).

[7] I. Shavitt, *The method of configuration interaction* in: Methods of electronic structure theory, ed. H. F. Schaeffer III (Plenum Press, New York, 1977).

[8] P.E.M. Siegbahn, *The configuration interaction method* in: Lecture notes in quantum chemistry. European summer school in quantum chemistry, Vol. 58, ed. B.O. Roos (Springer-Verlag, Berlin, 1992).

[9] J.L. Whitten and M. Hackmeyer, *J. Chem. Phys.*, **51** (1969) 5584.

[10] M. Hackmeyer and J.L. Whitten, *J. Chem. Phys.*, **54** (1971) 3739.

[11] S.D. Peyerimhoff and R.J. Buenker, *Chem. Phys. Lett.*, **16** (1972) 235.

[12] R.J. Buenker and S.D. Peyerimhoff, *Theor. Chim. Acta*, **35** (1974) 33.

[13] M. Hanrath and B. Engels, *Chem. Phys.*, **225** (1997) 197.

[14] S.R. Langhoff and E.R. Davidson, *Int. J. Quant. Chem.*, **8** (1974) 61.

[15] W. Meyer, *J. Chem. Phys.*, **58** (1973) 1017.

[16] J. ¤i¢ek, *Adv. Chem. Phys.*, **14** (1969) 35.

[17] J. ¤i¢ek and J. Paldus, *Physica Scripta*, **21** (1980) 251.

[18] P.R. Taylor, *Coupled-cluster methods in quantum chemistry* in: Lecture notes in quantum chemistry II. European summer school in quantum chemistry, Vol. 64, ed. B.O. Roos (Springer-Verlag, Berlin, 1994).

[19] K. Raghavachari, G.W. Trucks, J.A. Pople and M. Head-Gordon, *Chem. Phys. Lett.*, **157** (1989) 479.

[20] C. Møller and M.S. Plesset, *Phys. Rev.*, **46** (1934) 618.

[21] R.J. Bartlett, *Ann. Rev. Phys. Chem.*, **32** (1981) 359.

[22] J. Goldstone, *Proc. Roy. Soc.*, **A239** (1957) 267.

[23] B.H. Brandow, *Rev. Mod. Phys.*, **39** (1967) 771.

[24] N.C. Handy, P.J. Knowles and K. Somasundram, *Theor. Chim. Acta*, **68** (1985) 87.

[25] J. Olsen, O. Christiansen and P. Jørgensen, *J. Chem. Phys.*, **105** (1996) 5082.

[26] O. Christiansen, J. Olsen, P. Jørgenson, H. Koch and P.-Å. Malmqvist, *Chem. Phys. Lett.*, **261** (1996) 369.

[27] J. Olsen, P. Jørgensen, T. Helgaker and O. Christiansen, *J. Chem. Phys.*, **112** (2000) 9736.

[28] B.O. Roos, *The multiconfigurational (MC) self-consistent field (SCF) theory* in: Lecture notes in quantum chemistry. European summer school in quantum chemistry, Vol. 58, ed. B.O. Roos (Springer-Verlag, Berlin, 1992).

[29] R. Shepard, *Adv. Chem. Phys.*, **69** (1987) 63.

[30] B.O. Roos, *Adv. Chem. Phys.*, **69** (1987) 399.

[31] R. McWeeny, Methods of molecular quantum mechanics, (Academic Press, New York, 1992).

[32] C. van Wüllen and W. Kutzelnigg, *The IGLO method. Ab-initio calculation of magnetic susceptibilities and NMR shielding tensors (chemical shifts)* in: Methods and techniques in computational chemistry: Metecc-95, eds. E. Clementi and G. Corungiu Strasbourg, 1995).

[33] T. Helgaker, M. Jaszunski and K. Ruud, *Chem. Rev.*, **99** (1999) 293.

[34] W. Kutzelnigg, *Israel J. Chem.*, **19** (1980) 193.

[35] M. Schindler and W. Kutzelnigg, *J. Chem. Phys.*, **76** (1982) 1919.

[36] U. Fleischer, W. Kutzelnigg, P. Lazzeretti and V. Mühlenkamp, *J. Am. Chem. Soc.*, **116** (1994) 5298.

[37] F. London, *J. Phys. Rad.*, **8** (1937) 397.

[38] R. Ditchfield, *J. Chem. Phys.*, **56** (1972) 5688.

[39] K. Wolinski, J.F. Hinton and P. Pulay, *J. Am. Chem. Soc.*, **112** (1990) 8251.

[40] R. Zanasi, P. Lazzeretti, M. Malagoli and F. Piccinini, *J. Chem. Phys.*, **102** (1995) 7150.

[41] *TURBOMOLE has been designed by the Quantum Chemistry Group, University of Karlsruhe, Germany*, 1988. With contributions from R. Ahlrichs, M. Bär, H.-P. Baron, R. Bauernschmitt, S. Böcker, M. Ehrig, K. Eichkorn, S. Elliott, F. Furche, F. Haase, M.

Häser, H. Horn, C. Huber, U. Huniar, C. Kölmel, M. Kollwitz, C. Ochsenfeld, H. Öhm, A. Schäfer, U. Schneider, O. Treutler, M. von Arnim, F. Weigend, P. Weis and H. Weiss.

[42] H.-J. Werner and P.J. Knowles, *MOLPRO is a package of ab initio programs*, With contributions from R.D. Amos, A. Bernhardsson, A. Berning, P. Celani, D.L. Cooper, M.J.O. Deegan, A.J. Dobbyn, F. Eckert, C. Hampel, G. Hetzer, T. Korona, R. Lindh, A.W. Lloyd, S.J. McNicholas, F.R. Manby, W. Meyer, M.E. Mura, A. Nicklass, P. Palmieri, R. Pitzer, G. Rauhut, M. Schütz, H. Stoll, A. J. Stone, R. Tarroni, and T. Thorsteinsson.

[43] K. Wolinski, J.F. Hinton and P. Pulay, *J. Am. Chem. Soc.*, **112** (1990) 8251.

[44] M.J. Frisch, G.W. Trucks, H.B. Schlegel, G.E. Scuseri, M.A. Robb, J.R. Cheeseman, V.G. Zakrzewski, J. J. A. Montgomery, R.E. Stratmann, J.C. Burant, S. Dapprich, J.M. Millam, A.D. Daniels, K.N. Kudin, M.C. Strain, O. Farkas, J. Tomasi, V. Barone, M. Cossi, R. Cammi, B. Mennucci, C. Pomelli, C. Adamo, S. Clifford, J. Ochterski, G.A. Petersson, P.Y. Ayala, Q. Cui, K. Morokuma, D.K. Malick, A.D. Rabuck, K. Raghavachari, J.B. Foresman, J. Cioslowski, J.V. Ortiz, B.B. Stefanov, G. Liu, A. Liashenko, P. Piskorz, I. Komaromi, R. Gomperts, R.L. Martin, D.J. Fox, T. Keith, M.A. Al-Laham, C.Y. Peng, A. Nanayakkara, C. Gonzalez, M. Challacombe, P.M.W. Gill, B. Johnson, W. Chen, M.W. Wong, J.L. Andres, C. Gonzalez, M. Head-Gordon, E.S. Replogle and J.A. Pople, *Gaussian 98*, 1998 .

[45] C. van Wüllen and W. Kutzelnigg, *Chem. Phys. Lett.*, **205** (1993) 563.

[46] W. Heitler and F. London, *Z. Physik*, **44** (1927) 455.

[47] R. McWeeny, *Valence bond theory. A re-examination of concepts and methodology* in: Modern modelling of the chemical bond. Theoretical and computational chemistry, Vol. 6, eds. Z. B. Maksic and W. J. Orville-Thomas (Elsevier Science B.V., Amsterdam, The Netherlands, 1999).

[48] G.A. Gallup, R.L. Vance, J.R. Collins and J.M. Norbeck, *Adv. Quantum Chem.*, **16** (1982) 229.

[49] M. Raimondi, M. Simonetta and G.F. Tantardini, *Comput. Phys. Rep.*, **2** (1985) 171.

[50] J.H. van Lenthe and G.G. Balint-Kurti, *Chem. Phys. Lett.*, **76** (1980) 138.

[51] J.H. van Lenthe and G.G. Balint-Kurti, *J. Chem. Phys.*, **78** (1983) 5699.

[52] P.C. Hiberty, J.P. Flament and E. Noizet, *Chem. Phys. Lett.*, **189** (1992) 259.

[53] P.C. Hiberty, S. Humbel, C.P. Byrman and J.H. van Lenthe, *J. Chem. Phys.*, **101** (1994) 5969.

[54] P.C. Hiberty, *J. Mol. Struct. (Theochem)*, **398-399** (1997) 35.

[55] D.L. Cooper, J. Gerratt and M. Raimondi, *Adv. Chem. Phys.*, **69** (1987) 319.

[56] D.L. Cooper, J. Gerratt and M. Raimondi, *Chem. Rev.*, **91** (1991) 929.

[57] D.L. Cooper, J. Gerratt, M. Raimondi and M. Sironi, *Theor. Chim. Acta*, **85** (1993) 261.

[58] T. Thorsteinsson, D.L. Cooper, J. Gerratt, P.B. Karadakov and M. Raimondi, *Theor. Chim. Acta*, **93** (1996) 343.

[59] T. Thorsteinsson and D.L. Cooper, *Theor. Chim. Acta*, **94** (1996) 233.

[60] T. Thorsteinsson, D.L. Cooper and J. Gerratt, *Theor. Chim. Acta*, **95** (1997) 131.

[61] A.D. Becke, *Exchange-correlation approximations in density-functional theory* in: Modern electronic structure theory, part II, Vol. 2, ed. D. R. Yarkony (World Scientific, Singapore, 1995).

[62] W. Kohn, *Rev. Mod. Phys.*, **71** (1999) 1253.

[63] N.C. Handy, *Density functional theory* in: Lecture notes in quantum chemistry II. European summer school in quantum chemistry, Vol. 64, ed. B.O. Roos (Springer-Verlag, Berlin, 1994).

[64] W. Kohn and L.J. Sham, *Phys. Rev.*, **A140** (1965) 1133.

[65] A.D. Becke, *J. Chem. Phys.*, **98** (1993) 5648.

[66] M.F. Guest, J.H. van Lenthe, J. Kendrick, K. Schöffel, P. Sherwood and R.J. Harrison, *GAMESS-UK, a package of ab initio programs*, 2000.
With contributions from R.D. Amos, R.J. Buenker, M. Dupuis, N.C. Handy, I.H. Hillier, P.J. Knowles, V. Bonacic-Koutecky, W. von Niessen, V.R. Saunders and A.J. Stone.
It is derived from the original GAMESS code due to M. Dupuis, D. Spangler and J. Wendolowski, *NRCC Software Catalog*, Vol. 1, Program No. QG01 (GAMESS) 1980.

[67] R.J. Buenker, *Stud. Phys. Theor. Chem.*, **21** (1982) 17.

[68] B. Engels, V. Pleß and H.-U. Suter, *Direct MRD-CI, University of Bonn*, Bonn, Germany, 1993. See also reference [13].

[69] V.R. Saunders and J.H. van Lenthe, *Mol. Phys.*, **48** (1983) 923.

[70] V.R. Saunders and M.F. Guest, *Atmol program package, SERC Daresbury Laboratorium,* Daresbury, Great Britain.

[71] U. Meier, C. van Wüllen and M. Schindler, *J. Comp. Chem.*, **13** (1992) 551.

[72] J. Verbeek, J.H. Langenberg, C.P. Byrman, F. Dijkstra and J.H. van Lenthe, *TURTLE, an ab initio VB/VBSCF program,* 1988-2000.

[73] F. Dijkstra and J.H. van Lenthe, *J. Chem. Phys.*, **113** (2000) 2100.

Chapter 3

The lowest valence transitions of 1,1'-bicyclohexylidene and 1,1':4',1"-tercyclohexylidene.[†]

[†] R.W.A. Havenith, J.H. van Lenthe, L.W. Jenneskens and F.J. Hoogesteger, *Chem. Phys.*, **225** (1997) 139-152

Abstract: *Ab initio* MRDCI calculations were performed on the oligo(cyclohexylidenes) 1,1'-bicyclohexylidene (**1**) and 1,1':4',1"-tercyclohexylidene (**2**) using RHF/6-31G geometries and molecular orbitals for the assignment of their lowest valence transitions taking into account the four lowest states of each symmetry. The calculations unequivocally show that the valence transitions of **1** and **2** correspond to $\pi\rightarrow\pi^*$ and $\pi\rightarrow\sigma^*$ transitions. In the case of **1**, the MRDCI results were verified by Direct-CI calculations. Mulliken population analyses suggest that the $\pi\rightarrow\sigma^*$ transitions possess charge transfer character; upon excitation electron density shifts from the olefinic carbon atoms towards hydrogen atoms positioned in the cyclohexylidene rings. The transition energies and oscillator strengths of the $\pi\rightarrow\pi^*$ and $\pi\rightarrow\sigma^*$ transitions of **1** and **2** differ from those of the reference compounds tetramethylethene (**3**) and 1,4-diisopropylidene-cyclohexane (**4**), respectively. In going from **3** to **1** both the $\pi\rightarrow\pi^*$ and the first $\sigma\rightarrow\pi^*$ transitions of **1** are bathochromically shifted by *ca.* 0.24 eV. The first $\pi\rightarrow\sigma^*$ transition of **1** is hypsochromically shifted (0.79 eV) with respect to that of **3**. In the case of **2** both the $\pi\rightarrow\pi^*$ and $\pi\rightarrow\sigma^*$ transitions are *ca.* 0.9 eV bathochromically shifted with respect to those of **4**.

1. Introduction

End-functionalised oligo(cyclohexylidenes) composed of cyclohexyl rings connected *via* carbon-carbon double bonds were recently proposed as novel molecular building blocks for supramolecular and functional systems [1-4]. Derivatives bearing an oxime functionality at an end position were shown to be suitable amphiphiles for Langmuir film formation at the air/water interface, which could be transferred onto hydrophilic silicon substrates [1]. Furthermore, derivatives containing at the α, ω-positions an electron-donating and electron-accepting moiety, respectively ([DσA]), were shown to possess opto-electric properties. Upon excitation of [DσA] to either a local [D^{*}σA] or [DσA^{*}] state, rapid intramolecular electron transfer occurs leading to the population of a dipolar, charge separated state [$D^{+\bullet}$σ$A^{-\bullet}$]* [5]. Hence, the intervening oligo(cyclohexylidene) bridge can be envisaged as a semi-rigid redox-active moiety. To deepen our insight in the factors contributing to the photoinduced charge separation [6] process we were prompted to study the photo-physical properties of the oligo(cyclohexylidenes). It is noteworthy that the simplest representative of the oligo(cyclohexylidene) series, *viz.* 1,1'-bicyclohexylidene (**1**), has already received considerable attention due to its peculiar UV spectrum both in the solid-state and solution in comparison with that of a related reference compound, *viz.* tetramethylethene (**3**).

Both in the vapour phase and in solution (solvent: *n*-pentane) the UV absorption spectrum of 1,1'-bicyclohexylidene (**1**) contains two distinct bands centred at 5.95 eV and 6.82 eV, and, at 6.01 eV and 6.85 eV, respectively [7], whereas for **3** only one band at 7.0 eV attributed to a $\pi \rightarrow \pi^{*}$ valence transition was found [8]. Unequivocal evidence that the two UV absorption bands of **1** are due to valence transitions was obtained from the solid-state UV spectrum of a single crystal of **1**; two bands at 5.95 eV and 6.32 eV were found which both were shown to be polarised along the carbon-carbon double bond C(1)-C(2) [9]. Similar results were found for a solid-solution of **1** in stretched polyethylene films [10]. Since Rydberg transitions possess vanishingly low intensities both in the solid-state and in solution, they have to be attributed to valence transitions [11,12]. The 5.95 eV (6.01 eV) band of **1** was assigned to a $\pi \rightarrow \pi^{*}$ valence transition. However, the assignment

of the 6.82 eV (6.85 eV) band was less straightforward. It was tentatively concluded to correspond with a charge transfer '$\pi(CH_2)'\rightarrow\pi^*$ valence transition in which electron density is shifted from the cyclohexyl rings into the carbon-carbon double bond [7].

To explain the difference in absorption spectra of **1** and **3** and to obtain a reliable assignment of their valence transitions *ab initio* MRDCI calculations using RHF/6-31G geometries and molecular orbitals (MO's) taking into account the two lowest excited states of each symmetry were recently performed by some of the present authors [13]. The 6-31G basis set, which does not contain polarisation functions, was used to circumvent the inclusion of Rydberg character into the transitions. The results showed that the first valence transition of **1** is indeed a $\pi\rightarrow\pi^*$ transition. However, in contrast with the previous proposal [7], the second transition had to be unequivocally assigned to a $\pi\rightarrow\sigma^*$ transition. In line with the solid-state [9] and solid solution [10] UV data both transitions were polarised along the carbon-carbon double bond C(1)-C(2). Moreover, Mulliken population analysis [14] revealed that the $\pi\rightarrow\sigma^*$ transition possesses charge transfer character, *viz.* electron density is shifted from the carbon-carbon double bond towards the *equatorial* hydrogen atoms of the cyclohexylring moieties.

The objective of this chapter is three-fold: *1)* In our initial *ab initio* MRDCI [15,16] study two states per symmetry of **1** were calculated using *ca.* 5000 configuration state functions (CSF's) per symmetry for the assignment of the lowest valence transitions. To probe the convergence of the MRDCI results, the calculations were repeated taking into account *ca.* 60000 CSF's and four states per symmetry. The latter extension is a prerequisite for the calculation of the lowest valence transitions of the next higher homologue of **1**, *viz.* 1,1':4',1"-tercyclohexylidene (**2**). For **2** it is anticipated that through-bond interactions [17] between the carbon-carbon double bonds will be operational. Hence, MRDCI calculations using only two states per symmetry will not be sufficient to give estimates of the $\pi\rightarrow\sigma^*$ transitions. *2)* Furthermore, the reliability of the *ab initio* MRDCI approach, *viz.* the influence of the frozen core approximation and the configuration selection procedure for **1** was evaluated by doing Direct-CI [18] calculations on the ground state ($1A_g$) and several excited states ($1B_u$, $2B_u$ and $1B_g$). *3)* Since the results reveal that the MRDCI approximations are appropriate, the lowest

valence transitions of 1,1':4',1"-tercyclohexylidene (**2**) were calculated taking into account four states per symmetry. To assist the interpretation of the MRDCI results obtained for **2** the reference compound 1,4-diisopropylidene-cyclohexane (**4**) was also studied.

2. Computational details

All calculations were run on a Silicon Graphics Power Challenge computer using the quantum chemical program system GAMESS-UK [19] and its MRDCI package [20]. All geometries were optimised at the RHF/6-31G level (**1**, **2**, **4** and **5**; C_{2h} symmetry and **3**; D_2 symmetry) and were characterised as local minima by means of a Hessian calculation.

MRDCI [15,16] calculations were performed using the RHF/6-31G geometry and molecular orbitals (MO's); transition energies and oscillator strengths *(f)* were calculated for the four lowest states of each symmetry. The active CI space of **1** and **2** consisted of 10 occupied MO's (20 electrons) and 88 virtual MO's. Configuration selection [21] for **1** resulted in the inclusion of 56740 CSF's of A_g, 62452 CSF's of A_u, 69783 CSF's of B_u and 66311 CSF's of B_g symmetry. In the case of **2**, 62154 CSF's of A_g, 63549 CSF's of A_u, 49207 CSF's of B_u, and of 43734 CSF's of B_g symmetry were included. The active CI space of **3** consisted of 13 occupied MO's (26 electrons) and 54 virtual MOs. The configuration selection procedure gave 83295 CSF's of A_1, 88043 CSF's of B_1, 88427 CSF's of B_2, and 86363 CSF's of B_3 symmetry. The active CI space of **4** consisted of 15 occupied MO's (30 electrons) and 68 virtual MO's furnishing 84986 CSF's of A_g, 63521 CSF's of A_u, 67089 CSF's of B_u, and 66907 CSF's of B_g symmetry.

Direct-CI [18] calculations were performed for **1** on the $1A_g$ ground state, and the $1B_u$, $2B_u$ and $1B_g$ excited states with the ATMOL [22] program package to test the influence of the frozen core and the configuration selection procedure in the MRDCI calculations. In the Direct-CI calculations only the twelve 1s orbitals on carbon of **1** were frozen.

Both MRDCI and Direct-CI energies were corrected for size-consistency errors by the Davidson correction [23], generalised for multi-reference CI expansions. This is done in the MRDCI calculations by taking for c_0^2, the sum of the squares of the coefficients of all the reference configurations [16], while in the Direct-CI calculations c_0 is a projection of the reference function on the CI function [24].

Ground state and excited state electron distributions were calculated by Mulliken population analyses [14].

3. Results and discussion

*3.1. Ground state properties of compounds **1-5***

In Figure 1, the RHF/6-31G geometry of 1,1'-bicyclohexylidene (**1**) is shown. As discussed in a preliminary account [13], the RHF/6-31G results (bond lengths, valence angles and dihedral angles) are in satisfactory agreement with those found by single crystal X-ray analysis [25]. It is noteworthy that in the solid-state **1** only possesses 'approximate' C_{2h} symmetry. Besides a crystallographic inversion centre, a non-crystallographic mirror-plane perpendicular to the carbon-carbon double bond C(1)-C(2) bisecting the carbon atoms C(11) and C(12) is found.

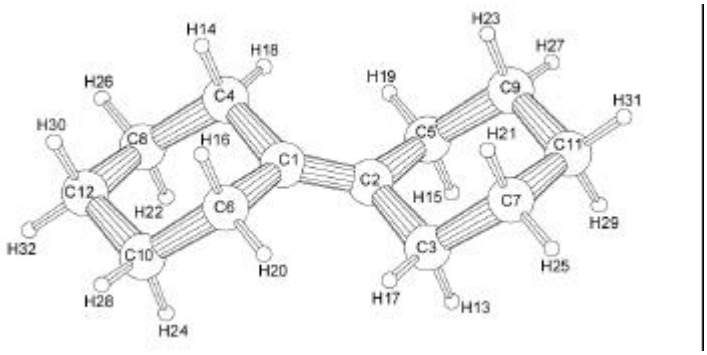

Figure 1 RHF/6-31G geometry of 1,1'-bicyclohexylidene (1).

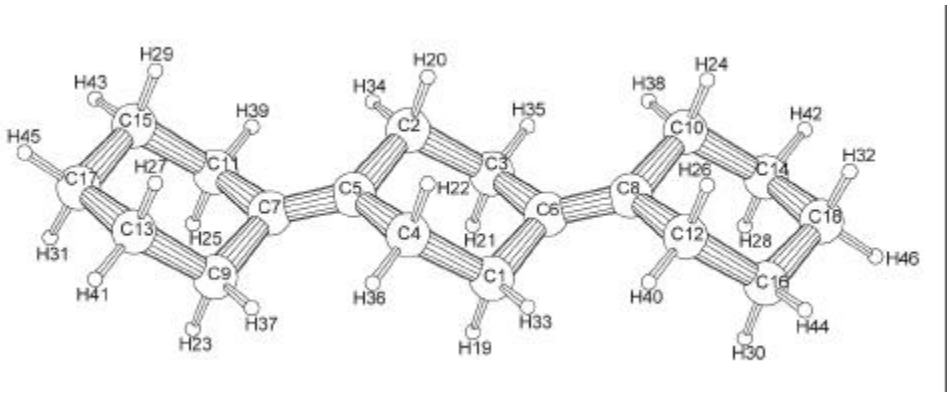

Figure 2 **RHF/6-31G geometry of 1,1':4',1"-tercyclohexylidene (2).**

Table 1 **Calculated bond lengths (Å), valence angles (°) and dihedral angles (°) of 2. Between parentheses the single crystal X-ray data for *trans*-4,4"-diheptyl-1,1':4',4"-tercyclohexylidene (6) is presented.[a]**

Bond length (Å)		Valence angles (°)		Dihedral angles (°)	
C(1)-C(4)	1.55	C(1)-C(4)-C(5)	111.7	C(1)-C(6)-C(8)-C(10)	179.6
	(1.52)		(112.3)		
C(1)-C(6)	1.52	C(1)-C(6)-C(3)	110.2	C(1)-C(6)-C(8)-C(12)	0.9
	(1.50)		(110.1)		
C(5)-C(7)	1.34	C(4)-C(5)-C(7)	124.9		
	(1.34)		(125.7)		
C(7)-C(9)	1.52	C(5)-C(7)-C(9)	124.9		
	(1.52)		(124.1)		
C(9)-C(13)	1.54	C(7)-C(9)-C(13)	111.3		
	(1.53)		(112.3)		
C(13)-C(17)	1.53	C(9)-C(13)-C(17)	111.5		
	(1.52)		(112.2)		
		C(13)-C(17)-C(15)	111.0		
			(109.3)		

[a]For single crystal X-ray data of **6** see reference [26].

The RHF/6-31-G geometries of **2** and its reference compounds **4** as well as 1,4-dimethylidene-cyclohexane (**5**) are shown in Figures 2 and 3, respectively. Unfortunately,

no single crystal X-ray structure is available for **2**. However, a comparison of its RHF/6-31G structure with the single crystal X-ray structure of an 1',1"-*bis*-alkyl substituted derivative, *viz. trans*-4,4"-diheptyl-1,1':4',1"-tercyclohexylidene (**6**) [26], shows that the structural features of the tercyclohexylidene bridge are satisfactorily reproduced at the RHF/6-31G level (Table 1).

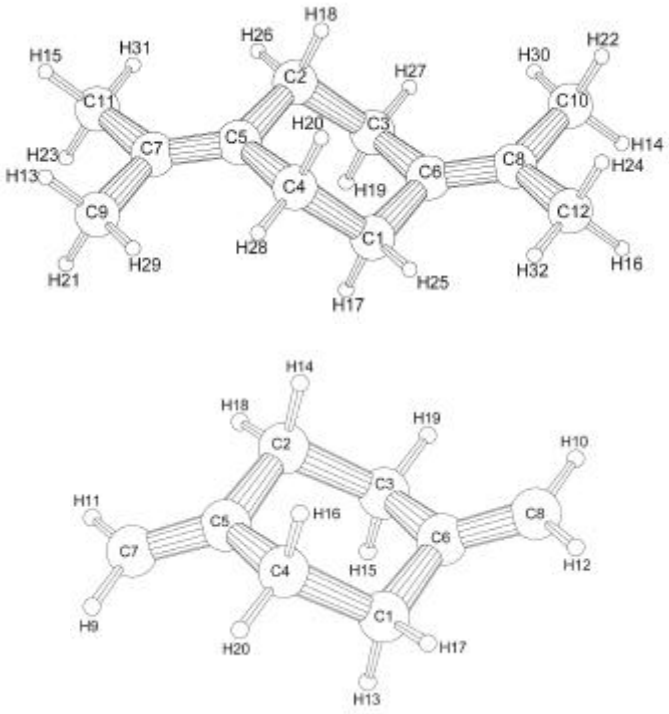

Figure 3 RHF/6-31G geometries of 1,4-diisopropylidene-cyclohexane (4) and 1,4-dimethylidene-cyclohexane (5).[a]

[a]Selected RHF/6-31G structural data of **4** and **5**: **4** C(1)-C(4) 1.546 Å, C(1)-C(6) 1.517 Å, C(6)-C(8) 1.337 Å, C(8)-C(10) 1.515 Å, C(5)-C(6) 2.976 Å, C(4)-C(1)-C(6) 111.67°, C(1)-C(6)-C(8) 124.86°, C(6)-C(8)-C(10) 124.66° and **5** C(1)-C(4) 1.545 Å, C(1)-C(6) 1.512 Å, C(6)-C(8) 1.326 Å, C(5)-C(6) 2.908 Å, C(4)-C(1)-C(6) 111.06°, C(1)-C(6)-C(8) 122.99°.

As expected, the highest occupied MO's of compounds **1-5** are π-like. The RHF/6-31G π MO energies of **1-5** together with the π MO energies of two ethene

molecules possessing the same relative geometry as found in **1**, **2**, **4** and **5**, respectively, are given in Table 2.

The lowest RHF/6-31G Koopmans [27] ionisation potential (IP) of **1** (IP_1 8.48 eV) is well separated from the next ionisation potential IP_2 (10.89 eV); both values are in reasonable agreement with available photo-electron spectroscopy data (**1**: IP_1 8.16 eV, IP_2 9.8 eV) [7,28]. In the case of **2**, **4** and **5**, a splitting of *ca.* 0.6 eV between the HOMO and HOMO-1 is found, while for the ethene analogue both π MO energies remain nearly degenerate. This near-degeneracy for the π MO energies of both ethene molecules in the geometry of **2** is also observed, if ghost-centres, with the appropriate basis functions, are placed on the positions of the missing atoms. Hence, this splitting can be attributed to through-bond interactions [17] involving interactions with MO's centred on the cyclohexyl moieties. Unfortunately, no photo-electron spectroscopy data are available for **4**. However, for **2** and 1,4-dimethylidene-cyclohexane (**5**), another reference compound, the experimental ionisation potentials have been determined using PES (**2**: IP_1 7.9 eV, IP_2 8.3 eV [29]; **5**: IP_1 9.0 eV, IP_2 9.5 eV [30]). These experimental IP values are satisfactorily reproduced at the RHF/6-31G level of theory (Koopmans values; **2**: IP_1 -8.23 eV and IP_2 -8.85 eV; **5**: IP_1 9.07 eV and IP_2 9.76 eV, Table 2).

Table 2 **π MO Energies of compounds 1, 2, 3, 4 and 5.**

Compound	π MO energy (eV)	π MO energy[a]
1	-8.48	-10.19
2	-8.85	-10.09
	-8.23	-10.09
3	-8.62	-10.19
4	-8.94	-10.09
	-8.30	-10.09
5	-9.76	-10.16
	-9.07	-10.15

[a]Energy of the π MO's of two ethene molecules positioned in the same geometry (see text and Figures 1-3). For **2-5**, the two ethene π MO energies are nearly degenerate.

*3.2. The lowest valence transitions of 1,1'-bicyclohexylidene (**1**) and tetramethylethene (**3**)*

For the assignment of the lowest valence transitions of compounds **1**-**4** the MRDCI method was used (see computational detail section). In the case of **1** and **3**, the four lowest states of each symmetry were calculated. In Table 3, the results are reported for **1** and compared with those of our earlier *ab initio* MRDCI calculations [13]. On the basis of the calculated C_{2h} symmetry of **1**, only the A_u and B_u excited states will have non-zero oscillator strengths (*f*). Since the transition energies of the A_u excited states are larger than 12 eV, while those of the B_u excited states are in the range 9.40-12.39 eV, the latter were analysed in detail with respect to the assignment of experimentally observable valence transitions. For the lowest two B_u excited states the results of the calculations, in which, instead of *ca.* 5000 CSF's per symmetry, *ca.* 60000 CSF's were used, confirm the conclusions reached in our preliminary account [13]. The lowest symmetry allowed transition (9.47 eV, $1B_u$, *f* 0.9401, HOMO→LUMO) is assigned to a $\pi\rightarrow\pi^*$ transition, whereas the second lowest symmetry allowed transition (10.65 eV, $2B_u$, *f* 0.1459, HOMO→LUMO+1) corresponds to a $\pi\rightarrow\sigma^*$ transition. In line with experiment [9,10], both transitions are polarised along the carbon-carbon double bond C(1)-C(2) (Table 3).

The changes in electron population (Mulliken population analysis [14]) upon excitation from the $1A_g$ ground state to the $1B_u$ and $2B_u$ excited state, respectively, suggest that the $2B_u$ excited state possesses charge transfer character. Electron density shifts from the carbon-carbon double bond C(1)-C(2) towards the *equatorial* hydrogen atoms of the cyclohexylidene rings (Table 4).

The first symmetry forbidden $\sigma\rightarrow\pi^*$ transition is the $1A_g\rightarrow1B_g$ transition (10.45 eV, *f* 0.0000, HOMO-1→LUMO) and it possesses a lower excitation energy than the first $\pi\rightarrow\sigma^*$ transition (10.65 eV, $1A_g\rightarrow2B_u$, *f* 0.1459, HOMO→LUMO+1). The electron redistribution upon excitation to the $1B_g$ excited state indicates that electron density shifts from the cyclohexylidene ring moieties, *viz.* the allylic carbon atoms C(3) to C(6), towards the olefinic carbon atoms C(1) and C(2) (Figure 1 and Table 4).

Table 3 **The lowest state energies of each symmetry of 1, transition energies, oscillator strengths and polarisation.[a,b]**

State symmetry	Energy (Hartree)	Transition energy (eV)	Oscillator strength (*f*)	Polarisation[a]
$1A_g$	-466.011680			
	(-465.938378)			
$2A_g$	-465.581054	11.72	0.0000	
	(-465.410614)	(14.36)	(0.0000)	
$3A_g$	-465.573313	11.93	0.0000	
$4A_g$	-465.571246	11.99	0.0000	
$1A_u$	-465.568916	12.05	0.1139	⊥
	(-465.500749)	(11.91)	(0.1126)	
$2A_u$	-465.552975	12.48	0.0140	⊥
	(-465.488344)	(12.25)	(0.0086)	
$3A_u$	-465.512080	13.60	0.0401	⊥
$4A_u$	-465.510265	13.64	0.0005	⊥
$1B_u$	-465.663816	9.47	0.9401	‖
	(-465.597163)	(9.28)	(0.8494)	
$2B_u$	-465.620345	10.65	0.1459	‖
	(-465.552797)	(10.49)	(0.1282)	
$3B_u$	-465.583480	11.65	0.1361	⊥⊥
$4B_u$	-465.556349	12.39	0.0513	‖
$1B_g$	-465.627530	10.45	0.0000	
	(-465.560505)	(10.28)	(0.0000)	
$2B_g$	-465.584964	11.61	0.0000	
	(-465.518276)	(11.43)	(0.0000)	

[a]Notation; ‖: polarised parallel to the double bond; ⊥: polarised perpendicular to the double bond in plane with the carbon atoms C(3) to C(6); ⊥⊥: polarised perpendicular to the double bond and perpendicular to the plane occupied by the carbon atoms C(3) to C(6) (see Figure 1). [b]Numbers between parentheses are taken from the preliminary account [13].

To assess the effect of the presence of the cyclohexane-like moieties on the MRDCI results in the case of **1**, transition energies as well as oscillator strengths for the four lowest valence transitions of each symmetry were calculated for the reference compound tetramethylethene (**3**) using a similar approach (Table 5). The first excited state

of **3** has to be assigned to a $\pi \rightarrow \pi^*$ excitation (9.71 eV, $1B_2$, *f* 1.0870, HOMO→LUMO; experimental 7.0 eV [8]). The second excited state is a $\pi \rightarrow \sigma^*$ excitation (9.86 eV, $1B_1$, *f* 0.0337, HOMO→LUMO+1), whereas the third excited state corresponds to a $\sigma \rightarrow \pi^*$ excitation (10.68 eV, $2B_2$, *f* 0.0042, HOMO-1→LUMO). Again these assignments are in line with our earlier MRDCI results in which, instead of *ca.* 88000 CSF's per symmetry, only *ca.* 8500 CSF's were used [13].

Table 4 **Mulliken population analysis [14] of the ground state and Mulliken population differences for the excited states of 1,1'-bicyclohexylidene (1).**

Atom	State							
	$1A_g$	$1A_u$[a]	$2A_u$[a]	$1B_u$[a]	$2B_u$[a]	$3B_u$[a]	$4B_u$[a]	$1B_g$[a]
C(1),C(2)	5.993	-0.249	0.139	-0.062	-0.208	-0.218	-0.208	0.170
C(3)-C(6)	6.337	0.051	-0.030	-0.004	-0.021	-0.005	0.007	-0.073
C(7)-C(10)	6.293	-0.089	-0.040	-0.024	-0.023	-0.027	-0.031	-0.005
C(11),C(12)	6.301	0.048	-0.086	-0.019	0.014	-0.010	-0.068	-0.031
H(13)-H(16)	0.843	0.025	0.041	0.024	-0.018	0.090	-0.026	0.029
H(17)-H(20)	0.835	-0.004	-0.019	0.007	0.147	-0.005	0.035	-0.016
H(21)-H(24)	0.848	0.063	0.000	0.008	0.014	0.060	0.031	-0.004
H(25)-H(28)	0.847	0.066	0.003	0.023	-0.009	-0.011	0.016	-0.005
H(29),H(30)	0.854	-0.008	0.028	0.017	-0.004	0.024	0.095	0.011
H(31),H(32)	0.847	-0.015	0.005	-0.005	0.019	0.000	0.107	-0.002

[a]For the excited states a positive number indicates an increase in electron population, while a negative number corresponds to a decrease in electron population.

A comparison of the calculated valence transitions of **1** and **3** shows that the second (HOMO→LUMO+1) and third (HOMO-1→LUMO) transitions of **3** are interchanged with the second (HOMO-1→LUMO) and third (HOMO→LUMO+1) transitions of **1**. Presumably, this is a consequence of the lower second ionisation potential (IP_2) of **1**. Whereas for **3** IP_1 and IP_2 equal 8.62 eV and 12.07 eV, in the case of **1** the corresponding values are 8.48 eV and 10.89 eV, respectively. Hence, IP_2 of **1** is lowered by 1.18 eV, and, therefore, the second and third valence transitions of **1** are interchanged compared to those of **3**.

Table 5 **The lowest state energies of each symmetry of 3, transition energies, oscillator strengths and polarisation.[a,b]**

State symmetry	Energy (Hartree)	Transition energy (eV)	oscillator strength (*f*)	Polarisation[a]
$1A_1$	-234.455310			
	(-234.086330)			
$2A_1$	-234.002146	12.33	0.0000	
	(-233.701057)	(14.68)		
$3A_1$	-233.979363	12.95	0.0000	
$4A_1$	-233.935493	14.15	0.0000	
$1B_1$	-234.092957	9.86	0.0337	⊥⊥
	(-233.867100)	(10.16)		
$2B_1$	-234.046092	11.14	0.0447	⊥⊥
	(-233.818473)	(11.48)		
$3B_1$	-233.986440	12.76	0.0002	⊥⊥
$4B_1$	-233.939905	14.03	0.0030	⊥⊥
$1B_2$	-234.098550	9.71	1.0870	‖
	(-233.882086)	(9.75)		
$2B_2$	-234.063002	10.68	0.0042	‖
	(-233.838799)	(10.93)		
$3B_2$	-234.038101	11.35	0.0000	‖
$4B_2$	-233.972970	13.13	0.0102	‖
$1B_3$	-234.060525	10.74	0.0011	⊥
	(-233.833501)	(11.07)		
$2B_3$	-234.010001	12.12	0.0002	⊥
	(-233.787136)	(12.34)		

[a]Notation; ‖: polarised parallel to the double bond; ⊥: polarised perpendicular to the double bond in plane with the carbon atoms C(3) to C(6); ⊥⊥: polarised perpendicular to the double bond and perpendicular to the plane occupied by the carbon atoms C(3) to C(6). [b]Numbers between parentheses are taken from the preliminary account [13].

*3.3. Direct-CI calculations on the lowest valence excited states of 1,1'-bicyclohexylidene (**1**)*

To assess the reliability of the MRDCI approach for the calculation of the valence transitions of **1**, *i.e.* in particular the applied frozen core approximation as well as the configuration selection procedure [15,16,21], Direct-CI [18] calculations were performed on the $1A_g$ ground state (6015806 states), the $1B_u$ ($\pi\rightarrow\pi^*$, HOMO→LUMO) (18135443 states), $2B_u$ ($\pi\rightarrow\sigma^*$, HOMO→LUMO+1) (18135443 states) and $1B_g$ ($\sigma\rightarrow\pi^*$, HOMO-1→LUMO) (21633690 states) excited states (Table 6). In these calculations only the MO's corresponding to the carbon 1s atomic orbitals were frozen. In general, the MRDCI excitation energies of the lowest transitions deviate *ca.* 1.2 eV from the Direct-CI values. The error of 2.3 eV for the lowest $\pi\rightarrow\pi^*$ transition energy calculated by the Direct-CI method (8.29 eV), compared to experiment ($\pi\rightarrow\pi^*$ 6.01 eV [7]), is attributed to the use of the relatively small 6-31G basis set.

Table 6 **A comparison of excitation energies of 1 calculated by the Direct-CI method and the MRDCI method.**

State symmetry	Energy (Direct-CI in Hartree)	Transition energy (Direct-CI in eV)	Transition energy (MRDCI in eV)
$1A_g$	-466.949201[a]		
$1B_u$	-466.644486	8.29	9.47
$2B_u$	-466.598399	9.55	10.65
$1B_g$	-466.613303	9.14	10.45

[a]MRDCI ground state energy : -466.01168043 Hartree

In spite of the difference in transition energy of more than 1 eV, the most important configurations in the CI vector calculated by both the MRDCI and the Direct-CI method for each state are essentially identical (Table 7). Thus, the MRDCI frozen core approximation and configuration selection procedure can be applied for the study of the optical properties of the oligo(cyclohexylidenes). These results provide additional support for the reliability of the assignment of the lowest valence excited states of **1**.

Table 7 **Comparison of c^2 in the CI vector calculated by the MRDCI method and the Direct-CI method for compound 1. Only $c^2 > 0.0002$ are tabulated.**

$1A_g$ state

		MO									
MRDCI	**DIRECT**	**42**	**43**	**44**	**45**	**46**	**47**	**48**	**52**	**54**	**Y**
0.93004	0.77845	2	2	2	2	2	-	-	-	-	
0.00646	0.00616	2	2	2	2	-	2	-	-	-	
0.00257	0.00053	2	2	2	2	-	1	1	-	-	
	0.00035	2	2	2	2	-	1	-	-	1	
	0.00025	2	2	2	2	-	1	-	-	-	1[a]

Y is an unoccupied MO: [a]Y = 72.

$1B_u$ state

		MO									
MRDCI	**DIRECT**	**36**	**44**	**45**	**46**	**47**	**48**	**49**	**51**	**52**	**54**
0.92397	0.77631	2	2	2	1	1	-	-	-	-	-
0.00008	0.00179	2	2	2	1	-	1	-	-	-	-
	0.00061	2	1	2	2	-	-	1	-	-	-
	0.00070	2	2	1	2	-	-	-	1	-	-
0.00512		2	2	2	1	-	-	-	-	-	1

$2B_u$ state

		MO														
MRDCI	**DIRECT**	**X**	**40**	**41**	**42**	**43**	**44**	**45**	**46**	**47**	**48**	**49**	**51**	**52**	**54**	**Y**
0.00077	0.00170		2	2	2	2	2	2	1	1	-	-	-	-	-	
0.87488	0.77401		2	2	2	2	2	2	1	-	1	-	-	-	-	
	0.00120		2	2	2	2	1	2	2	-	-	1	-	-	-	
	0.00036		2	2	2	2	2	1	2	-	-	-	1	-	-	
	0.00024	1[a]	2	2	2	2	2	2	1	1	1	-	-	-	-	
0.03162	0.00025		2	2	2	2	2	2	1	-	-	-	-	-	1	
	0.00026	1[b]	2	2	2	2	2	2	1	-	1	-	-	-	-	1[c]
0.01414			2	2	2	2	2	2	1	-	-	-	-	1	-	

X is an occupied MO and Y is an unoccupied MO: [a]X = 31, [b]X = 33 and [c]Y = 72.

Table 7 ***Continued***

$1B_g$ state

			MO													
MRDCI	**DIRECT**	**X**	**36**	**37**	**40**	**43**	**45**	**46**	**47**	**48**	**49**	**51**	**52**	**54**	**57**	**Y**
0.84382	0.73092		2	2	2	2	1	2	1	-	-	-	-	-	-	
0.04809	0.03760		2	2	2	2	1	2	-	1	-	-	-	-	-	
	0.00697		2	2	2	1	2	2	-	-	1	-	-	-	-	
	0.00091		2	2	2	1	2	2	-	-	-	-	-	-	-	1[a]
	0.00027	1[b]	2	2	2	2	2	2	1	-	-	-	-	-	-	
	0.00039		1	2	2	2	2	2	1	-	-	-	-	-	-	
0.00546	0.00020		2	1	2	2	2	2	1	-	-	-	-	-	-	
0.00925	0.00025		2	2	1	2	2	2	1	-	-	-	-	-	-	
	0.00023	1[c]	2	2	2	2	2	1	2	-	-	-	-	-	-	
0.00410	0.00039		2	2	2	1	2	1	2	-	-	-	-	-	-	
0.00949	0.00040		2	2	2	2	1	2	-	-	-	-	-	1	-	
0.00212	0.00020		2	2	2	2	1	2	-	-	-	-	-	-	-	1[d]
0.00047			2	2	2	2	2	1	-	-	-	1	-	-	-	
0.00033			2	2	2	2	2	1	-	-	-	-	-	-	1	
0.00180			2	2	2	2	2	1	-	-	-	-	-	-	-	1[e]

X is an occupied MO and Y is an unoccupied MO: [a]Y = 59, [b]X = 21, [c]X = 33, [d]Y = 76 and [e]Y = 60.

*3.4. The lowest valence transitions of 1,1':4',1"-tercyclohexylidene (**2**) and 1,4-diisopropylidene-cyclohexane (**4**)*

The MRDCI transition energies, oscillator strengths (*f*) and polarisation of the four lowest states of each symmetry for **2** are reported in Table 8. A survey of the data reveals that the $1B_u$ and $2B_u$ states correspond to the two $\pi\rightarrow\pi^*$ (HOMO→LUMO and HOMO-1→LUMO+1) transitions, which are both polarised along the double bonds C(5)-C(7) and C(6)-C(8). As expected, Mulliken population analysis [14] shows that for these excited states no significant electron redistribution occurs (Table 9). The excitation to the $3B_u$ state (10.87 eV, *f* 0.13040) corresponds to a $\pi\rightarrow\sigma^*$ transition, which despite its multi-reference character possesses mainly HOMO→LUMO+2 character (c^2 HOMO→LUMO+2: 0.65; HOMO-1→LUMO+3: 0.12). In analogy with the $2B_u$ excited

state of **1**, it is polarised along the carbon-carbon double bonds C(5)-C(7) and C(6)-C(8). Among the A_u states, only the $4A_u$ excitation does not have a vanishingly low oscillator strength. The other A_u excited states ($1A_u$, $2A_u$ and $3A_u$) will not be analysed further. The $4A_u$ (12.18 eV, *f* 0.1832, HOMO-1→LUMO+8) excited state resembles the $1A_u$ state of **1** and is assigned to a $\pi \rightarrow \sigma^*$ transition, which is polarised perpendicular to the carbon-carbon double bonds C(5)-C(7) and C(6)-C(8), and, in plane of the carbon atoms C(1), C(3) and C(10).

Table 8 **The four lowest state energies of each symmetry of 2, transition energies, oscillator strengths and polarisation.**[a]

State symmetry	Energy (Hartree)	Transition energy (eV)	Oscillator strength (*f*)	Polarisation[a]
$1A_g$	-697.739594			
$2A_g$	-697.394330	9.40	0.0000	
$3A_g$	-697.378812	9.82	0.0000	
$4A_g$	-697.350313	10.59	0.0000	
$1A_u$	-697.363365	10.24	0.0004	⊥
$2A_u$	-697.318984	11.45	<0.0001	⊥
$3A_u$	-697.294821	12.10	0.0067	⊥
$4A_u$	-697.292093	12.18	0.1832	⊥
$1B_u$	-697.400453	9.23	1.8993	∥ (18° ⊥⊥)
$2B_u$	-697.369086	10.08	0.1956	∥ (24° ⊥⊥)
$3B_u$	-697.340076	10.87	0.1340	∥ (14° ⊥⊥)
$4B_u$	-697.314832	11.56	0.1895	⊥⊥ (7° ∥)
$1B_g$	-697.353366	10.51	0.0000	
$2B_g$	-697.303811	11.86	0.0000	
$3B_g$	-697.292895	12.16	0.0000	
$4B_g$	-697.283680	12.41	0.0000	

[a]Notation; ∥: polarised parallel to the double bond; ⊥: polarised perpendicular to the double bond in plane with the carbon atoms C(1), C(3), C(10) and C(11), C(2), C(4), C(9), C(12); ⊥⊥: polarised perpendicular to the double bond and perpendicular to the planes occupied by the carbon atoms C(1), C(3), C(10), C(11) and C(2), C(4), C(9), C(12), respectively (see Figure 2). Between parentheses the angle (°) with the specified polarisation direction is denoted.

The $4B_u$ excited state (11.56 eV, *f* 0.1895, HOMO→LUMO+9) of **2** and the $3B_u$ excited state of **1** are both $\pi\rightarrow\sigma^*$ transitions, polarised perpendicular to both the carbon-carbon double bonds (C(5)-C(7) and C(6)-C(8)) as well as perpendicular to the plane of carbon atoms (C(1), C(3) and C(10)).

Table 9 **Mulliken population analysis [14] of the ground state and Mulliken population differences of the excited states of 2.**

Atom	**State**							
	$1A_g$	$4A_u$[a]	$1B_u$[a]	$2B_u$[a]	$3B_u$[a]	$4B_u$[a]	$1A_u$[a]	$1B_g$[a]
C(1)-C(4)	6.329	0.000	0.001	-0.019	-0.015	-0.024	-0.037	-0.044
C(5),C(6)	6.001	-0.124	-0.013	-0.083	-0.078	-0.147	0.083	0.079
C(7),C(8)	5.999	-0.137	-0.016	-0.064	-0.135	-0.119	0.098	0.084
C(9)-C(12)	6.336	-0.005	-0.002	-0.010	-0.024	0.000	-0.038	-0.040
C(13)-C(16)	6.293	-0.032	-0.005	-0.008	-0.021	-0.005	-0.006	-0.010
C(17),C(18)	6.305	0.014	-0.010	-0.009	-0.011	-0.004	-0.019	-0.021
H(19)-H(22)	0.836	0.004	-0.005	0.038	-0.005	0.174	0.008	0.020
H(23)-H(26)	0.843	0.032	0.008	0.011	0.014	0.004	0.013	0.017
H(27)-H(30)	0.847	0.039	0.002	0.005	0.026	0.001	-0.001	0.000
H(31),H(32)	0.854	-0.003	0.008	0.006	0.019	-0.001	0.005	0.006
H(33)-H(36)	0.834	0.032	0.004	0.030	0.020	-0.004	-0.014	-0.005
H(37)-H(40)	0.834	0.035	0.001	0.018	0.073	-0.005	-0.008	-0.008
H(41)-H(44)	0.847	0.022	0.011	0.007	0.018	-0.006	-0.002	-0.004
H(45),H(46)	0.845	-0.005	-0.002	0.002	0.032	-0.002	-0.001	-0.001

[a]For the excited states a positive number indicates an increase in electron population, while a negative number corresponds to a decrease in electron population.

As shown by Mulliken population analyses [14], the $\pi\rightarrow\sigma^*$ transitions again possess charge transfer character; electron density shifts from the carbon-carbon double bonds towards the cyclohexylidene rings. Upon excitation to the $3B_u$ state, the electron population on C(7) and C(8) decreases, while that on the *equatorial* hydrogen atoms H(37) to H(40) present in the outermost cyclohexylidene rings increases. For the $4A_u$ excited state, the electron population of the olefinic carbon atoms C(5) to C(8) decreases, whereas concomitantly that on the *equatorial* hydrogen atoms H(37) to H(40) and *axial*

hydrogen atoms H(23) to H(30) of the outermost cyclohexylidene rings as well as the *equatorial* hydrogen atoms H(33) to H(36) of the central cyclohexylidene ring increases. In the $4B_u$ excited state, the electron population on the olefinic carbon atoms C(5) to C(8) decreases while the electron population of the *axial* hydrogen atoms H(19) to H(22) of the central cyclohexylidene ring increases.

The $2A_g$ and $3A_g$ excited states correspond to the symmetry forbidden $\pi\rightarrow\pi^*$ transitions HOMO→LUMO+1 and HOMO-1→LUMO, respectively. The $1A_g\rightarrow1A_u$ ($\sigma\rightarrow\pi^*$, 10.24 eV, *f* 0.0004, HOMO-2→LUMO) transition, which possesses only a small oscillator strength, is polarised perpendicular to the double bonds (C(5)-C(7) and C(6)-C(8)), but in plane of the carbon atoms (C(1), C(3) and C(10)). The excitation to the $1B_g$ state (10.51 eV, *f* 0.0000, HOMO-2→LUMO+1), which is symmetry forbidden, of **2** corresponds to a $\sigma\rightarrow\pi^*$ transition. Upon excitation to either the $1A_u$ or $1B_g$ excited states of **2** the electron population on C(1) to C(4) and C(9) to C(12) decreases, while that on the olefinic carbon atoms increases (Table 9).

Compared to **1** the lowest lying active $\sigma\rightarrow\pi^*$ excitation is lowered in energy (**1**; $1A_u$; 12.05 eV and **2**; $1A_u$; 10.24 eV), but the oscillator strength (*f*) also decreases (**1**; *f* 0.1139 and **2**; *f* 0.0004).

To further corroborate the assignment of the lowest valence transitions of **2** and the effect of the outermost cyclohexane-like rings on the calculated valence transitions, the reference compound 1,4-diisopropylidene-cyclohexane (**4**) was also studied using the *ab initio* MRDCI method (Table 10). Again the excitations to the $1B_u$ and $2B_u$ states have to be assigned to $\pi\rightarrow\pi^*$ transitions (9.83 eV and 11.09 eV; *f* 1.6150 and 0.7306; HOMO→LUMO and HOMO-1→LUMO+1, respectively). The charge redistribution upon excitation to the A_u and B_u states is presented in Table 11. It is noteworthy that the transition energies for **4** are all hypsochromically shifted by *ca.* 0.7 eV with respect to those of **2**, presumably due to the higher ionisation potentials of **4**. The RHF/6-31G Koopmans [27] ionisation potentials of the π MO's of **2** are 8.23 eV and 8.86 eV, whereas for **4** the corresponding values are 8.30 eV and 8.94 eV, respectively, which are in satisfactory agreement. The next two lower ionisation potentials of **2** are 10.75 eV and 11.33 eV, respectively, while for **4** they are 11.15 eV and 12.19 eV.

All oscillator strengths, with the exception of those for the $2B_u$ and $2A_u$ state, increase in going from **4** to **2**. This hypochromic effect can be rationalised by considering the increase in size of **2**. The excitation to the $3B_u$ state is assigned to a $\pi \rightarrow \sigma^*$ excitation (12.10 eV; *f* 0.0855; HOMO-1→LUMO+2), which has the largest coefficient in the CI vector (c^2: HOMO-1→LUMO+2: 0.47; HOMO→LUMO+3: 0.38). The electron redistribution upon excitation to the $3B_u$ excited state indicates that the electron population on the carbon-carbon double bonds decreases while that on the hydrogen atoms H(13) to H(16) and H(21) to H(24) increases (Figure 3, Table 11).

Table 10 The four lowest state energies of each symmetry of 4, transition energies, oscillator strengths and polarisation.[a]

State symmetry	Energy (Hartree)	Transition energy (eV)	Oscillator strength (*f*)	Polarisation[a]
$1A_g$	-466.073989			
$2A_g$	-465.709065	9.93	0.0000	
$3A_g$	-465.676952	10.80	0.0000	
$4A_g$	-465.627426	12.15	0.0000	
$1A_u$	-465.644143	11.70	0.0002	⊥
$2A_u$	-465.617664	12.42	0.0590	⊥
$3A_u$	-465.577974	13.50	0.0005	⊥
$4A_u$	-465.522690	15.00	0.0239	⊥
$1B_u$	-465.712667	9.83	1.6150	‖
$2B_u$	-465.666572	11.09	0.7306	‖
$3B_u$	-465.629417	12.10	0.0855	‖ (42° ⊥⊥)
$4B_u$	-465.588186	13.22	0.0397	‖ (9° ⊥⊥)
$1B_g$	-465.640139	11.81	0.0000	
$2B_g$	-465.581173	13.41	0.0000	
$3B_g$	-465.559887	13.99	0.0000	
$4B_g$	-465.532518	14.73	0.0000	

[a]Notation; ‖: polarised parallel to the double bond; ⊥: polarised perpendicular to the double bond in plane with the carbon atoms C(1), C(3), C(10) and C(11), C(2), C(4), C(9), C(12); ⊥⊥: polarised perpendicular to the double bond and perpendicular to the planes occupied by the carbon atoms C(1), C(3), C(10), C(11) and C(2), C(4), C(9), C(12), respectively (see Figure 3). Between parentheses the angle (°) with the specified polarisation direction is denoted.

For **4**, excitation to the $4B_u$ state ($\pi\rightarrow\sigma^*$; 13.22 eV; *f* 0.0397) leads to an increase of the electron population on the outermost methyl groups, while it concomitantly decreases on the olefinic carbon atoms (C(5) to C(8)). This transition also possesses multi-reference character (c^2: HOMO→LUMO+3: 0.45; HOMO-1→LUMO+2: 0.38). The $1A_u$ excited state is assigned to a $\sigma\rightarrow\pi^*$ transition (11.70 eV; *f* 0.0002; HOMO-2→LUMO). The $2A_u$ state is assigned to a $\pi\rightarrow\sigma^*$ transition (12.42 eV; *f* 0.0590; HOMO→LUMO+5); upon excitation the electron population at the olefinic carbon atoms decreases, and that at the *equatorial* hydrogen atoms H(25) to H(28) of the cyclohexane ring increases.

Thus from a comparison of the results obtained for **2** and **4**, it can be concluded, that the outermost cyclohexylidene rings in **2** do have an influence on the lowest lying $\pi\rightarrow\sigma^*$ transitions; oscillator strengths in the case of **2** increase compared to that of **4** ($1A_g\rightarrow1B_u$; **2**: *f* 1.8993 and **4**: *f* 1.6150).

Table 11 Mulliken population analysis [14] of the ground state and Mulliken population differences of the excited states of 4.

Atom	State						
	$1A_g$	$1A_u$[a]	$2A_u$[a]	$1B_u$[a]	$2B_u$[a]	$3B_u$[a]	$4B_u$[a]
C(1),C(2),C(3),C(4)	6.330	-0.039	-0.056	0.002	-0.027	-0.003	-0.014
C(5),C(6)	5.977	0.069	-0.073	-0.001	-0.055	-0.050	-0.065
C(7),C(8)	6.018	0.096	-0.121	-0.007	-0.045	-0.100	-0.126
C(9),C(10),C(11),C(12)	6.474	-0.039	-0.011	-0.004	-0.011	-0.045	-0.046
H(13),H(14),H(15),H(16)	0.842	0.015	0.004	0.013	-0.009	0.071	0.053
H(17),H(18),H(19),H(20)	0.836	-0.001	0.036	-0.013	0.043	-0.017	-0.015
H(21),H(22),H(23),H(24)	0.842	0.007	-0.013	-0.003	0.019	0.044	0.047
H(25),H(26),H(27),H(28)	0.838	-0.025	0.099	0.005	0.026	-0.007	0.025
H(29),H(30),H(31),H(32)	0.840	0.000	0.039	0.003	0.009	0.037	0.045

[a]For the excited states a positive number indicates an increase in electron population, while a negative number corresponds to a decrease in electron population.

In summary, the $1B_u$ and $2B_u$ state of **2** and **4** are $\pi\rightarrow\pi^*$ transitions. However, the excitation energies for **4** are larger (**2**: 9.23 eV, 10.08 eV and **4**: 9.83 eV, 11.09 eV). The $3B_u$ state of **2** ($\pi\rightarrow\sigma^*$ transition) corresponds to the $3B_u$ state of **4**, but it possesses

considerably less multi-reference character. Moreover, the excitation energy to the $3B_u$ state of **2** is lower than that for **4** (**2**: 10.87 eV and **4**: 12.10 eV). Notwithstanding, the electron redistribution upon excitation to the $3B_u$ state has the same characteristics, *i.e.* a decrease in electron population on the olefinic carbon atoms concomitant with an increase in electron population on the hydrogen atoms is found. In the case of **2** and **4**, hydrogen atoms positioned in the outermost cyclohexylidene rings and the methyl groups, respectively, are involved.

4. Conclusions

The lowest valence transitions for the oligo(cyclohexylidenes), 1,1'-bicyclohexylidene (**1**) and 1,1':4',1"-tercyclohexylidene (**2**) were assigned using *ab initio* MRDCI calculations. In the case of **1**, the MRDCI results were verified using Direct-CI calculations; the most important configurations in the CI vector were identical for each state.

For **1** three valence transitions were found possessing $\pi\rightarrow\pi^*$ ($1B_u$; 9.47 eV, *f* 0.9401), $\sigma\rightarrow\pi^*$ ($1B_g$; 10.45 eV, *f* 0.0000) and $\pi\rightarrow\sigma^*$ ($2B_u$; 10.65 eV, *f* 0.1459) character, respectively. In line with experiment, the $\pi\rightarrow\pi^*$ and $\pi\rightarrow\sigma^*$ transitions are polarised along the carbon-carbon double bond C(1)-C(2). A comparison with the results calculated for tetramethylethene (**3**; $\pi\rightarrow\pi^*$ ($1B_2$; 9.71 eV, *f* 1.0870), $\pi\rightarrow\sigma^*$ ($1B_1$; 9.86 eV, *f* 0.0337) and $\sigma\rightarrow\pi^*$ ($2B_2$; 10.68 eV, *f* 0.0042), respectively) shows that for **1** the second transition has to be assigned to a $\sigma\rightarrow\pi^*$ transition, whereas for **3** the second transition corresponds to a $\pi\rightarrow\sigma^*$ transition. This is a consequence of the lower second ionisation potential of **1** (IP_2 10.89 eV) with respect to that of **3** (IP_2 12.07 eV).

In the case of **2**, two active $\pi\rightarrow\pi^*$ transitions ($1B_u$; 9.23 eV, *f* 1.8993 and $2B_u$; 10.08 eV, *f*: 0.1956) and three active $\pi\rightarrow\sigma^*$ transitions ($3B_u$; 10.87 eV, *f* 0.1340, $4B_u$; 11.56 eV, *f* 0.1895 and $4A_u$; 12.18 eV, *f* 0.1832) were found. In addition, a $\pi\rightarrow\sigma^*$ ($2A_u$; 11.45 eV, *f* <0.0001) and two $\sigma\rightarrow\pi^*$ ($1A_u$; 10.24 eV, *f* 0.0004 and $3A_u$; 12.10 eV, *f* 0.0067) transitions are found which possesses very low oscillator strengths. For 1,4-

diisopropylidene-cyclohexane (**4**) the corresponding transitions are hypsochromically shifted.

According to Mulliken population analyses the $\pi \rightarrow \sigma^*$ transitions of oligo(cyclohexylidenes) **1-2** possess charge transfer character; upon excitation electron density shifts from the olefinic carbon atoms towards *equatorial* hydrogen atoms of the cyclohexylidene rings.

Acknowledgement

Financial support from NCF and Cray Research Inc for R.W.A. Havenith (NCF grant CRG 96.18) is gratefully acknowledged.

References

[1] F.J. Hoogesteger, J.M. Kroon, L.W. Jenneskens, E.J.R. Südholter, T.J.M. de Bruin, J.W. Zwikker, E. ten Grotenhuis, C.H.M. Marée, N. Veldman and A.L. Spek, *Langmuir*, **12** (1996) 4760.

[2] F.J. Hoogesteger, L.W. Jenneskens, H. Kooijman, N. Veldman and A.L. Spek, *Tetrahedron*, **52** (1996) 1773.

[3] F.J. Hoogesteger, Oligo(cyclohexylidenes). Development of novel functional and organized materials, Ph.D. Thesis, Utrecht University, Utrecht, The Netherlands (1996).

[4] A.W. Marsman, Functionalized oligo(cyclohexylidenes). Semi-rigid molecular rods for crystal engineering, through-bond orbital interactions and self-assembly, Ph.D. Thesis, Utrecht University, Utrecht, The Netherlands (1999).

[5] F.J. Hoogesteger, C.A. van Walree, L.W. Jenneskens, M.R. Roest, J.W. Verhoeven, W. Schuddeboom, J.J. Piet and J.M. Warman, *Chem. Eur. J.*, **6** (2000) 2948.

[6] M.N. Paddon Row, *Acc. Chem. Res.*, **27** (1994) 18.

[7] M. Allan, P.A. Snyder and M.B. Robin, *J. Phys. Chem.*, **89** (1985) 4900.

[8] M.B. Robin, R.R. Hart and N.A. Kuebler, *J. Chem. Phys.*, **44** (1966) 1803.

[9] P.A. Snyder and L.B. Clark, *J. Chem. Phys.*, **52** (1970) 998.

[10] A. Yogev, J. Sagiv and Y. Mazur, *J. Am. Chem. Soc.*, **94** (1972) 5122.

[11] M.B. Robin, Higher excited states of polyatomic molecules, Vol. III (Academic Press, New York, 1985).

[12] M.B. Robin, in: Chemical spectroscopy and photochemistry in the vacuum-ultraviolet, eds. C. Sandorfy, P.J. Ausloos and M.B. Robin (Reidel, Dordrecht, 1974).

[13] F.J. Hoogesteger, J.H. van Lenthe and L.W. Jenneskens, *Chem. Phys. Lett.*, **259** (1996) 178.

[14] R.S. Mulliken, *J. Chem. Phys.*, **23** (1955) 1833.

[15] R.J. Buenker, S.D. Peyerimhoff and W. Butscher, *Mol. Phys.*, **35** (1978) 771.

[16] R.J. Buenker, S.-K. Shih and S.D. Peyerimhoff, *Chem. Phys.*, **36** (1979) 97.

[17] R. Hoffmann, A. Imamura and W. Hehre, *J. Am. Chem. Soc.*, **90** (1968) 1499.

[18] V.R. Saunders and J.H. van Lenthe, *Mol. Phys.*, **48** (1983) 923.

[19] M.F. Guest, J.H. van Lenthe, J. Kendrick, K. Schöffel, P. Sherwood and R.J. Harrison, *GAMESS-UK, a package of ab initio programs*, 1998.
With contributions from R.D. Amos, R.J. Buenker, M. Dupuis, N.C. Handy, I.H. Hillier, P.J. Knowles, V. Bonacic-Koutecky, W. von Niessen, V.R. Saunders and A.J. Stone.
It is derived from the original GAMESS code due to M. Dupuis, D. Spangler and J. Wendolowski, *NRCC Software Catalog*, Vol. 1, Program No. QG01 (GAMESS) 1980.

[20] R.J. Buenker, *Stud. Phys. Theor. Chem.*, **21** (1982) 17.

[21] R.J. Buenker and S.D. Peyerimhoff, *Theor. Chim. Acta*, **35** (1974) 33.

[22] V.R. Saunders and M.F. Guest, *Atmol Program Package, SERC Daresbury Laboratorium*, Daresbury, Great Britain.

[23] S.R. Langhoff and E.R. Davidson, *Int. J. Quant. Chem.*, **8** (1974) 61.

[24] J. Verbeek, J.H. van Lenthe, P.J.J.A. Timmermans, A. Mackor and P.H.M. Budzelaar, *J. Org. Chem.*, **52** (1987) 2955.

[25] N. Veldman, A.L. Spek, F.J. Hoogesteger, J.W. Zwikker and L.W. Jenneskens, *Acta Crystallogr. C*, **50** (1994) 742.

[26] F.J. Hoogesteger, R.W.A. Havenith, J.W. Zwikker, L.W. Jenneskens, H. Kooijman, N. Veldman and A.L. Spek, *J. Org. Chem.*, **60** (1995) 4375.

[27] T.A. Koopmans, *Physica*, **1** (1933) 104.

[28] R.S. Brown, J.M. Buschek, K.R. Kopecky and A.J. Miller, *J. Org. Chem.*, **48** (1983) 3692.

[29] A.W. Marsman, R.W.A. Havenith, S. Bethke, L.W. Jenneskens, R. Gleiter, J.H. van Lenthe, M. Lutz and A.L. Spek, *J. Org. Chem.*, **65** (2000) 4584.

[30] G. Bieri, F. Burger, E. Heilbronner and J.P. Maier, *Helv. Chim. Acta*, **60** (1977) 2213.

Chapter 4

The excitation energies of 1,1'-bicyclohexylidene and 1,1':4',1"-tercyclohexylidene. A comparison of multi-reference configuration interaction and perturbation theory approaches.[†]

[†] R.W.A. Havenith, H.J.J. van Dam, J.H. van Lenthe and L.W. Jenneskens, *Chem. Phys.*, **246** (1999) 49-56

Abstract: The lowest valence transition energies of the first two homologues of the oligo(cyclohexylidene) series, *viz.* 1,1'-bicyclohexylidene (**1**) and 1,1':4',1"-tercyclohexylidene (**2**), are computed using Multi-Reference Perturbation Theory at second (MR-MP2) and third order (MR-MP3). The results are compared to the previously reported results using a non-selected Multi-Reference single-double CI (Direct-CI) and a Selected Multi-Reference single-double CI (MRDCI) approach in order to obtain insight in the applicability of the MRDCI approach for the prediction of absorption spectra of large organic molecules.

The calculations on the lowest valence excited states of 1,1'-bicyclohexylidene (**1**) show that MR-MP3 gives energies comparable to those of Direct-CI; for the transition energies, MR-MP2 and MR-MP3 perform equally well. The calculations on the excited states of 1,1':4',1"-tercyclohexylidene (**2**) reveal that the MR-MP2 methodology is not reliable for the prediction of its transition energies, if the multi-reference character of the excited states increases.

Although remarkable differences in the absolute transition energies are found, the assignments of the lowest valence transitions of 1,1'-bicyclohexylidene (**1**) and 1,1':4',1"-tercyclohexylidene (**2**) are similar at all levels of theory.

1. Introduction

The UV absorption spectrum of the simplest representative in the oligo(cyclohexylidene) series, *viz.* 1,1'-bicyclohexylidene (**1**, Scheme 1) has been studied in detail [1-4]. In contrast to its analogue tetramethylethene, which possesses only one band at 7.0 eV, that corresponds to the $\pi \rightarrow \pi^*$ transition [5], for **1** in the vapour phase (electron energy loss spectroscopy) as well as in solution (*n*-pentane), two bands were observed at 5.95 eV and 6.82 eV [1], and at 6.01 eV and 6.85 eV [2], respectively. In the solid-state polarised UV spectrum of a single crystal the two bands were also discernible at 5.95 eV and 6.32 eV [3]. This suggests that both bands of **1** are valence transitions, since the intensity of Rydberg states will be diminished in solid-state and solution UV-spectra. Similar results were obtained for a solid solution of **1** in stretched polyethylene films [4]. Although the band at 5.95 eV was assigned to a $\pi \rightarrow \pi^*$ transition, the assignment of the second band was less straightforward. It was proposed to correspond to a $\sigma(CH_2) \rightarrow \sigma^*$ excitation [1].

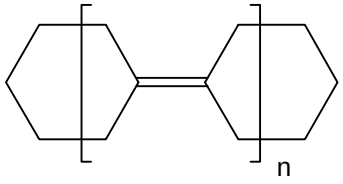

n=1: 1,1'-bicyclohexylidene (**1**)
n=2: 1,1':4',1"-tercyclohexylidene (**2**)

Scheme 1

To obtain an unambiguous assignment for the valence transitions of **1**, configuration selected Multi-Reference single-double CI (MRDCI) [6-9] calculations, were performed [10,11]. In order to exclude undesired mixing in of Rydberg states, the 6-31G basis set was chosen.

The first excited state had to be assigned to a $\pi \rightarrow \pi^*$ excitation (calc.: 9.47 eV), while the second transition corresponds to a $\pi \rightarrow \sigma^*$ transition (calc.: 10.65 eV). In line with experiment [3,4], both transitions are calculated to be polarised parallel to the carbon-carbon double bond. The inclusion of polarisation functions, using a 6-31G* basis set, did not alter the results. Hence, the 6-31G basis set gave a qualitative correct description of the lowest lying valence excited states of **1** [11].

However, the MRDCI program version currently in GAMESS-UK possesses three drawbacks, especially upon extension of this methodology for the calculation of the excited state energies and properties of larger molecules. Firstly, the number of electrons that can be correlated is restricted to thirty, which can cause a serious error in the transition energies. Secondly for larger molecules only limited CI expansions are possible in a reasonable amount of time and disk space, thus, severely restricting the amount of correlation allowed for. And lastly, all truncated CI approaches are not size-consistent. This can influence the transition energies of the excited states of large molecules and this error will increase concomitant with the increasing size of the system.

To test the influence of the configuration selection procedure and the effect of neglect of electron correlation on the valence transition energies of **1**, non-selected Multi-Reference single-double CI (Direct-CI) [12] calculations were performed [10]. It was shown that, upon correlating all valence electrons and with the inclusion of all generated single and double excitations in the CI expansion, the transition energies were decreased from 9.47 eV to 8.29 eV for the $1A_g \rightarrow 1B_u$ transition and from 10.65 eV to 9.55 eV for the $1A_g \rightarrow 2B_u$ transition, respectively. At both levels of theory, the CI vectors were similar, indicating that a qualitative assignment of the lowest valence transitions can be made using the above mentioned MRDCI approach.

To set up a framework for future calculations, in which the excited states of large organic molecules, *viz.* in particular functionalised higher homologues of **1**, will be the subject of study, a comparison of the applicability of several methods is necessary. For large systems Direct-CI calculations are not feasible, and alternatives like MRDCI or MR-MP approaches may be used. In this study, we compare the MR-MP2 and MR-MP3 methods with previously reported MRDCI and Direct-CI results as well as available

experimental data. The objective is to gain insight, which method gives results that are accurate enough to explain the experimental results and still are computationally feasible for our intended future work taking into account the recent developments of Direct MRDCI methods [13-15]. Hence, we have chosen to verify our previously reported MRDCI results for 1,1'-bicyclohexylidene (**1**) and 1,1':4',1"-tercyclohexylidene (**2**) [10] with MR-MP calculations.

It should be emphasised that Direct-CI calculations on the next higher homologue of **1**, *viz.* 1,1':4',1"-tercyclohexylidene (**2**), cannot be done in a reasonable amount of CPU time. The MRDCI calculations on **2** can be validated using the Multi-Reference MP2 (MR-MP2) and Multi-Reference MP3 (MR-MP3) method [16-18]. A special variant of the MR-MP2 method is the frequently used CASPT2 approach [19-21]. The advantage of the MR-MP methodology is that it is size-consistent [16,22]. Moreover, the MR-MP method allows us to choose the same reference configurations as in the MRDCI and Direct-CI calculations for a consistent comparison of the results.

In this chapter, we first give a short description of the methods used, and then the results of the calculations on the excited state energies of **1** and **2** are presented.

2. Theory

In the MRDCI calculations, all single and double excitations are generated from a set of reference functions. For every configuration, the effect on the total energy is predicted and if it is larger than a preset threshold, the configuration is included in the CI expansion [6-9]. In the Direct-CI procedure, no configuration selection takes place, so all generated single and double excitations are included in the CI expansion [12].

Our Multi-Reference (MR) MP2/MP3 program is based on the early work of Wolinsky and Pulay [17,18] and implemented in our Direct-CI program [12]. It employs all single and double excitations generated from an internally contracted reference wave function. Since it does not employ the density matrix techniques developed by Roos *et al.* [20,21], it may be less efficient for a CASSCF reference function in CASPT2. It does,

however, allow arbitrarily chosen reference wave functions and enables MR-MP3 calculations in a straightforward fashion.

The Hamiltonian is partitioned in the usual way into

$$H = H_0 + V \tag{1}$$

The Fock operator employed to construct the zeroth-order Hamiltonian H_0 is

$$\hat{F} = \sum_{rs} f_{rs} \hat{E}_{rs} \tag{2}$$

with

$$f_{rs} = h_{rs} + \sum_{ij} \langle \Psi_0 | \hat{E}_{ij} | \Psi_0 \rangle \left[(rs \mid ij) - \frac{1}{2} (ri \mid js) \right] \tag{3}$$

where the $\hat{E}_{xy}$ are the unitary group generators. The zeroth-order Hamiltonian is defined as

$$H_0 = P_0 \hat{F} P_0 + \sum_{i,j=0}^{1} P_{(i,j)S} \hat{F} P_{(i,j)S} + \sum_{i,j=0}^{2} P_{(i,j)D} \hat{F} P_{(i,j)D} \tag{4}$$

where P_0 is the projection operator onto the ground state, $P_{(i,j)S}$ is the projector onto the singly excited states with *i* electrons excited out of the doubly occupied orbitals and *j* electrons excited into the virtual orbitals, $P_{(i,j)D}$ is similar to $P_{(i,j)S}$ but projects onto the doubly excited states. This choice for the zeroth-order Hamiltonian ensures the size extensivity of our results [22,23].

The MR-MP CI vectors are back transformed to the configuration state basis and renormalised to unity. This ensures that the characterisation of the states calculated using the MR-MP approach is consistent with the CI calculations.

3. Computational details

For all calculations, the 6-31G basis set was used. All CI and MR-MP calculations were performed at the RHF/6-31G geometry [10] and molecular orbitals (MO's). The MRDCI calculations were performed with the GAMESS-UK [24] package, using the MRDCI approach of Buenker and Peyerimhoff [8,9]. The highest 10 occupied MO's and lowest 88 virtual MO's were correlated in the MRDCI calculations, further denoted as 'MRD Space'. The Direct-CI calculations were performed with the ATMOL [25] program package. In these calculations, only the 1s orbitals of the carbon atoms were frozen, resulting in 34 occupied and 102 virtual MO's. The MR-MP calculations were performed with the ATMOL [25] program package. Two sets of calculations were performed. The first set of calculations were performed in which the same orbitals were correlated as in the MRDCI calculations (MRD Space), and an additional set of MR-MP calculations were performed in which the same orbitals were correlated as in the Direct-CI calculations.

Table 1 **The chosen reference functions in the MR-MP calculations. Only the configurations with $c^2 \geq 0.01$ in the MRDCI wave function of the lowest state of each symmetry are listed. For the A_u state of 2, the contributions of the reference functions for the $4A_u$ state are listed. Single excitations from the Hartree-Fock (HF) determinant are denoted by (s) and double excitations by (d).**

State sym.	1,1'-bicyclohexylidene (1)	c^2	1,1':4',1"-tercyclohexylidene (2)	c^2
A_g	HF	0.93	HF	0.93
	(d) HOMO (b_u)→LUMO (a_g)	0.01		
B_u	(s) HOMO (b_u)→LUMO (a_g)	0.95	(s) HOMO (a_g)→LUMO (b_u)	0.83
			(s) HOMO-1 (b_u)→LUMO+1 (a_g)	0.09
A_u			(s) HOMO (a_g)→LUMO+6 (a_u)	0.10
			(s) HOMO-1 (b_u)→LUMO+8 (b_g)	0.63

Both the Direct-CI and the MRDCI results were corrected for size-consistency errors by the Davidson method [26,27]. Note that the MRDCI results were not obtained by energy extrapolation [28]. In the Direct-CI and MR-MP calculations, the same reference configuration state functions were chosen. The reference set consisted of singly and doubly excited configurations in the space of the five highest occupied and nine lowest unoccupied MO's. In Table 1, the most important reference configurations are shown.

Whereas in the MRDCI calculations on **1**, 56 740 configuration state functions (CSF's) of A_g and 69 783 CSF's of B_u symmetry were selected, in the Direct-CI calculations, 6 015 806 CSF's of A_g and 18 135 443 CSF's of B_u symmetry were considered. These numbers of CSF's result in 1 741 540 of A_g and 1 930 392 contracted states of B_u symmetry which were treated in the MR-MP calculations.

In the MRDCI calculations on **2** *ca.* 55 000 CSF's were selected, and in the MR-MP calculations 8 349 394 contracted states of A_g symmetry, 7 766 858 contracted states of B_u symmetry and 8 434 604 contracted states of A_u symmetry were considered. In Direct-CI calculations, using the same reference configurations, 108 001 918 CSF's of A_g, 67 949 272 CSF's of B_u and 69 107 646 CSF's of A_u symmetry have to be included in the CI expansion, indicating that these calculations are currently computationally not attractive.

To indicate the duration of these kind of calculations, typical timings for the largest calculation on **1** and **2** are summarised in Table 2.

Table 2 **Timings (in hours) for the largest calculations on 1,1'-bicyclohexylidene (1) and 1,1':4',1"-tercyclohexylidene (2) performed on the CRAY C90 supercomputer.**

Method	**1,1'-bicyclohexylidene (1)**	**1,1':4',1"-tercyclohexylidene (2)**
	$1B_u$ state	**$1A_g$ state**
MRDCI	0.6	0.7
Direct-CI	7.8	--[a]
MR-MP2	0.5	2.6
MR-MP3	2.2	12.8

[a]Not currently feasible.

4. Results

*4.1. The valence excited state energies of 1,1'-bicyclohexylidene (**1**)*

In our previous MRDCI study [10], it was shown that only the $1B_u$ and $2B_u$ excited states are of interest, since they correspond to the experimentally observed transitions. In Table 3, the excitation energies are summarised, which were obtained using the MRDCI, Direct-CI, MR-MP2 and MR-MP3 methodologies.

Table 3 **The excitation energies towards the $1B_u$ and $2B_u$ states (in eV) of 1,1'-bicyclohexylidene (1).**[a]

State symmetry	MRDCI	Oscillator strength (*f*)[b]	Direct-CI[c]	MR-MP2[d]	MR-MP3[d]	Exp. [1]
$1B_u$	9.47	0.9401	8.29 {8.56}	7.14	8.01	5.95
MRD Space				(8.53)	(8.65)	
$2B_u$	10.65	0.1459	9.55 {9.89}	8.19	9.10	6.82
MRD Space				(10.58)	(10.21)	

[a]Ground state total energies: MRDCI: -466.01168043 a.u.; Direct-CI: -466.94920140 a.u.; MR-MP2: -466.96005147 a.u.; MR-MP3: -467.04625575 a.u. [b]Oscillator strengths (*f*) were calculated using the MRDCI wave functions. [c]Size-consistency uncorrected Direct-CI results are between braces. [d]The excitation energies calculated using the MRD Space are between parentheses.

A comparison of the transition energies calculated at the MRDCI and those at the MR-MP3 level of theory using the MRD Space reveals that for the $1B_u$ state the transition energy decreases by *ca.* 0.8 eV upon going to the MR-MP3 level of theory, while for the $2B_u$ state, the transition energy decreases only by *ca.* 0.4 eV (Table 3). Since the same number of electrons is correlated, this difference is mainly due to the fact that the MR-MP3 methodology employs no configuration selection. Upon correlating all valence electrons, the MR-MP3 excitation energy towards the $1B_u$ state further decreases by *ca.* 0.6 eV, whereas for the $2B_u$ state the excitation energy decreases by *ca.* 1.1 eV. In going from the MRDCI to the MR-MP calculations the transition energies for both excitations decrease by *ca.* 1.5 eV (Table 3). These results indicate that for a proper description of the

$2B_u$ state, the lower lying MO's should be correlated. The configuration selection procedure produces only a small error. However, for the $1B_u$ state, electron correlation of the lower lying MO's is less important. This leads to the conclusion that for a proper description of the valence transitions, in which σ MO's are involved, the restricted number of electrons correlated can cause a large error in the transition energies.

The for size-consistency uncorrected excitation energies calculated at the Direct-CI level of theory, are *ca.* 0.7 eV higher than the size-consistent MR-MP3 values. By applying the Davidson correction, the Direct-CI results are still approximately 0.4 eV higher than the excitation energies calculated at the MR-MP3 level of theory (Table 3). However, an inspection of the size-consistency corrected as well as the uncorrected Direct-CI results reveals that the size-consistency errors are practically constant, and small (0.3 eV) compared to the deviation of the calculated transition energies with the experimental values.

Whereas the transition energies calculated at the MR-MP2 level of theory are considerably lower than those at the other levels of theory, the excitation energies obtained at the MR-MP3 level are close to the Direct-CI results. This is in agreement with Werner's study, which shows that the MR-MP3 methodology is effective in approximating the Direct-CI results [29].

The assignment of the excitations is not influenced by the shifts in transition energies. The $1B_u$ state corresponds to the HOMO→LUMO excitation ($\pi\rightarrow\pi^*$) according to the CI vectors at all levels of theory in which this configuration has the largest contribution in the CI vector ($c^2_{\text{MRDCI}} = 0.92; c^2_{\text{MR-SDCI}} = 0.78; c^2_{\text{MR-MP}} = 0.66$). The CI vector of the $2B_u$ state is at all three levels of theory dominated by the HOMO→LUMO+1 ($\pi\rightarrow\sigma^*$) excitation ($c^2_{\text{MRDCI}} = 0.87; c^2_{\text{MR-SDCI}} = 0.77; c^2_{\text{MR-MP}} = 0.64$).

The total energy of the ground state decreases more than the total energies of both excited states upon going from the MR-MP2 to the MR-MP3 level of theory, leading to a concomitant increase of the excitation energies (Table 3). Notwithstanding, the difference between the first and second B_u excited states (exp. 0.87 eV) is for all methods in the same range, *viz.* 1.18 (MRDCI), 1.26 (Direct-CI), 1.05 (MR-MP2) and 1.09 eV (MR-MP3). This indicates that, although the absolute transition energies differ, at all

levels of theory the lowest valence excited states of **1** are described in an equivalent manner relative to each other using the 6-31G basis set.

*4.2. The valence excited state energies of 1,1':4',1"-tercyclohexylidene (**2**)*

According to symmetry, for **2** only the B_u and A_u excited states have a non-zero oscillator strength. In the earlier MRDCI study [10], it was concluded that the lowest valence transitions of **2** are of B_u symmetry. Therefore, these states were studied using the MR-MP methodology (Table 4).

The transition energies for the $1B_u$ and $2B_u$ excited states decrease by *ca.* 0.7 eV in going from the MRDCI level to the MR-MP3 level of theory using the MRD Space (Table 4). The excitation energy of the $1A_g \rightarrow 3B_u$ transition is nearly equal at both levels of theory. These results, together with the results obtained for **1**, confirm that for the description of the valence excitations in which σ MO's are involved, the low lying σ MO's should be correlated.

The $1B_u$ and $2B_u$ states were both assigned at the MRDCI level of theory [10] to $\pi \rightarrow \pi^*$ transitions, *viz.* the HOMO→LUMO and the HOMO-1→LUMO+1 transitions, respectively. The $3B_u$ state was assigned to a $\pi \rightarrow \sigma^*$ transition (HOMO→LUMO+2) and the $4B_u$ state to a HOMO→LUMO+9 excitation. At the MR-MP level of theory, the assignments of the two lowest ($1B_u$; HOMO→LUMO [$c^2_{\text{MRDCI}} = 0.83; c^2_{\text{MR-MP}} = 0.45$] and $2B_u$; HOMO-1→LUMO+1 [$c^2_{\text{MRDCI}} = 0.75; c^2_{\text{MR-MP}} = 0.37$]) transitions are similar. However, the higher excited B_u states have more multi-reference character at the MR-MP level of theory. In the MRDCI calculations for the $3B_u$ state, c^2 for the HOMO→LUMO+2 excitation equals 0.66, while at the MR-MP level the c^2 for this configuration is only 0.28. In the CI vector of the $4B_u$ excited state, the main configuration is the HOMO→LUMO+9 excitation with $c^2_{\text{MRDCI}} = 0.82$ and $c^2_{\text{MR-MP}} = 0.31$.

The increase of multi-reference character, *i.e.* the decrease of c^2 in the excited state CI vectors at the MR-MP level, is a consequence of the increase in the number of states considered in the MR-MP calculations. Since the CI vectors at the MRDCI and MR-MP level are similar, the trend in the oscillator strengths calculated at the MRDCI

level has to be correct. Therefore, since the transition to the $4A_u$ excited state is the only one of the A_u states which has a non-zero oscillator strength, this transition energy was also recalculated using the MR-MP methodologies. The assignment (HOMO-1→LUMO+8 $c^2_{MRDCI} = 0.63$ and $c^2_{MR\text{-}MP} = 0.38$) of the $4A_u$ state is at the MR-MP level in line with the previous assignment at the MRDCI level of theory [10].

Table 4 The excitation energies for the B_u and $4A_u$ states (in eV) of 1,1':4',1"-tercyclohexylidene (2).[a]

Excited State symmetry	**MRDCI**	**Oscillator strength (*f*)**[b]	**MR-MP2**[c]	**MR-MP3**[c]	**Exp.**[d] [30]
$1B_u$	9.23	1.8993	6.77	7.83	6.02
MRD Space			(8.44)	(8.60)	
$2B_u$	10.08	0.1956	7.05	8.52	6.78
MRD Space			(9.22)	(9.39)	
$3B_u$	10.87	0.1340	8.74	9.69	
MRD Space			(10.65)	(10.67)	
$4B_u$	11.56	0.1895	9.00	9.77	
MRD Space			(10.81)	(10.70)	
$4A_u$	12.18	0.1832	9.73	10.42	
MRD Space			(11.86)	(11.42)	

[a]Ground state total energies: MRDCI: -697.73959400 a.u.; MR-MP2: -699.26482217 a.u.; MR-MP3: -699.38604538 a.u. [b]Oscillator strengths (*f*) were calculated using the MRDCI wave functions. [c]The excitation energies calculated using the MRD Space are between parentheses. [d]Solution UV-spectral data (solvent: *n*-pentane).

The UV spectrum of **2** in solution (solvent *n*-pentane) consists of two broad absorption bands, centred at 6.02 and 6.78 eV [30]. The calculated transition energies at the MR-MP level are 6.77 eV (MR-MP2) and 7.83 eV (MR-MP3), for the $1B_u$ state and 7.05 eV (MR-MP2) and 8.52 eV (MR-MP3) for the $2B_u$ state, respectively. These transition energies are considerably lower than the MRDCI (9.23 eV and 10.08 eV) results (Table 4). The MR-MP2 excitation energies for the first and second excited states are close to the experimental values. However, at the MR-MP3 level of theory, all excitation energies are again higher in energy than the corresponding MR-MP2 values.

The MR-MP2 ground state energy decreases by 0.12 a.u. upon going to the MR-MP3 level of theory (Table 4), while the total energies of the $1B_u$ and $2B_u$ states decrease by 0.08 and 0.07 a.u., respectively. This leads to an increase of the transition energies to the lowest excited B_u states. The trends found for **1**, *viz.* the MR-MP2 excitation energies are lower than the MR-MP3 excitation energies, and consequently, closer to the experimental values (Table 3), are also observed for **2**.

The energy difference between the first and second transition is experimentally 0.76 eV. The total state energy difference between the $1B_u$ and $2B_u$ excited states at the MRDCI (0.85 eV) and MR-MP3 (0.69 eV) levels are in line with the experimental value. However, the difference in state energy of the $1B_u$ and $2B_u$ excited states at the MR-MP2 level of theory is much lower (0.28 eV) than the experimental value of 0.76 eV. In contrast to **1**, where all methodologies gave comparable results, a considerable difference is found in the case of **2** using the MR-MP2 approach. The observation that the relative positioning of the excited state energies is qualitatively wrong at the MR-MP2 level of theory for **2** can be rationalised by the fact that the excited states of **2** possess more multi-reference character than the excited states of **1**, and consequently H_0 is worse and the perturbation is larger for **2**. In general, perturbation theory at the second order then overestimates the correlation energy, resulting in transition energies, which are too low. Perturbation theory at third order compensates for this effect, so the transition energies are increased upon going to third order perturbation theory [31].

We have shown that for large molecules, where concomitantly the multi-reference character of the excited states is increased, MR-MP2 theory gave a qualitatively wrong description of the excited state energies. Despite the deviation of the absolute transition energies with the experimental ones, the relative energy of the second excitation energy with respect to the first excited state, calculated using the MRDCI and MR-MP3 methods are in accordance with available experimental results. Moreover, as the calculated direction of polarisation of the first two lowest valence transitions of **1** are in line with the experimental data, the assignment of these two absorptions is correct.

Therefore, the MRDCI and MR-MP3 methods correctly describe the lowest valence transitions of the oligo(cyclohexylidenes) **1** and **2**, using the modest 6-31G basis set.

5. Conclusions

The lowest valence excited states of 1,1'-bicyclohexylidene (**1**) and 1,1':4',1"-tercyclohexylidene (**2**) were calculated at the MR-MP2 and MR-MP3 level of theory. The results of these calculations for **1** and **2** were compared to earlier MRDCI and in the case of **1** also to Direct-CI calculations. For **1**, all methods predict the UV absorption spectrum equivalently, *i.e.* the difference of the excited state energies are in the same range, and in line with the experimental data, although the absolute transition energies are too high. Although the MR-MP2 method gets closest to the experimental values for **1**, the difference between the first and second excited state energies for **2** is significantly lower than the experimental value. The relative excitation energies calculated with the MRDCI and MR-MP3 method are in line with the experimental data. It can therefore be concluded that the MR-MP2 method erroneously describes the lowest valence transitions at least in the oligo(cyclohexylidene) series. The application of the MRDCI method for the calculation of the excited states of **1** and **2** is justified despite the lack of electron correlation by freezing too many orbitals. This is especially promising taking into consideration the newly developed MRDCI codes [13-15], which will be more effective and which can be used for handling even larger molecules.

Acknowledgements

This work was sponsored by the Stichting Nationale Computerfaciliteiten (NCF) for the use of supercomputer facilities, with financial support from the Nederlandse Organisatie voor Wetenschappelijk Onderzoek (NWO).

References

[1] M. Allan, P.A. Snyder and M.B. Robin, *J. Phys. Chem.*, **89** (1985) 4900.

[2] F.J. Hoogesteger, R.W.A. Havenith, J.W. Zwikker, L.W. Jenneskens, H. Kooijman, N. Veldman and A.L. Spek, *J. Org. Chem.*, **60** (1995) 4375.

[3] P.A. Snyder and L.B. Clark, *J. Chem. Phys.*, **52** (1970) 998.

[4] A. Yogev, J. Sagiv and Y. Mazur, *J. Am. Chem. Soc.*, **94** (1972) 5122.

[5] M.B. Robin, R.R. Hart and N.A. Kuebler, *J. Chem. Phys.*, **44** (1966) 1803.

[6] R.J. Buenker, S.D. Peyerimhoff and W. Butscher, *Mol. Phys.*, **35** (1978) 771.

[7] R.J. Buenker, S.-K. Shih and S.D. Peyerimhoff, *Chem. Phys.*, **36** (1979) 97.

[8] R.J. Buenker and S.D. Peyerimhoff, *Theor. Chim. Acta*, **35** (1974) 33.

[9] R.J. Buenker, *Stud. Phys. Theor. Chem.*, **21** (1982) 17.

[10] R.W.A. Havenith, J.H. van Lenthe, L.W. Jenneskens and F.J. Hoogesteger, *Chem. Phys.*, **225** (1997) 139 (*cf.* Chapter 3).

[11] R.W.A. Havenith, L.W. Jenneskens and J.H. van Lenthe, *Chem. Phys. Lett.*, **282** (1998) 39 (*cf.* Chapter 5).

[12] V.R. Saunders and J.H. van Lenthe, *Mol. Phys.*, **48** (1983) 923.

[13] R.J. Buenker and R.A. Phillips, *J. Mol. Struct. (Theochem)*, **123** (1985) 291.

[14] A.B. Alekseyev, H.P. Liebermann, G. Hirsch and R.J. Buenker, *Chem. Phys.*, **225** (1997) 247.

[15] M. Hanrath and B. Engels, *Chem. Phys.*, **225** (1997) 197.

[16] J.H. van Lenthe, P. Pulay and H.J.J. van Dam, *Multi reference Møller-Plesset perturbation theory option*, Fayetteville, Arkansas/Utrecht, The Netherlands, 1989-1996.

[17] K. Wolinski, H.L. Sellers and P. Pulay, *Chem. Phys. Lett.*, **140** (1987) 225.

[18] K. Wolinski and P. Pulay, *J. Chem. Phys.*, **90** (1989) 3647.

[19] B.O. Roos and K. Andersson, *Chem. Phys. Lett.*, **245** (1995) 215.

[20] K. Andersson, P.-Å. Malmqvist, B.O. Roos, A.J. Sadlej and K. Wolinski, *J. Phys. Chem.*, **94** (1990) 5483.

[21] K. Andersson, P.-Å. Malmqvist and B.O. Roos, *J. Chem. Phys.*, **96** (1992) 1218.

[22] H.J.J. van Dam and J.H. van Lenthe, *Mol. Phys.*, **93** (1998) 431.

[23] H.J.J. van Dam, J.H. van Lenthe and P.J.A. Ruttink, *Int. J. Quant. Chem.*, **72** (1999) 549.

[24] M.F. Guest, J.H. van Lenthe, J. Kendrick, K. Schöffel, P. Sherwood and R.J. Harrison, *GAMESS-UK, a package of ab initio programs*, 1998.
With contributions from R.D. Amos, R.J. Buenker, M. Dupuis, N.C. Handy, I.H. Hillier, P.J. Knowles, V. Bonacic-Koutecky, W. von Niessen, V.R. Saunders and A.J. Stone.
It is derived from the original GAMESS code due to M. Dupuis, D. Spangler and J. Wendolowski, *NRCC Software Catalog*, Vol. 1, Program No. QG01 (GAMESS) 1980.

[25] V.R. Saunders and M.F. Guest, *Atmol Program Package, SERC Daresbury Laboratorium*, Daresbury, Great Britain.

[26] S.R. Langhoff and E.R. Davidson, *Int. J. Quant. Chem.*, **8** (1974) 61.

[27] J. Verbeek, J.H. van Lenthe, P.J.J.A. Timmermans, A. Mackor and P.H.M. Budzelaar, *J. Org. Chem.*, **52** (1987) 2955.

[28] R.J. Buenker and S.D. Peyerimhoff, *Theor. Chim. Acta*, **39** (1975) 217.

[29] H.-J. Werner, *Mol. Phys.*, **89** (1996) 645.

[30] F.J. Hoogesteger, Oligo(cyclohexylidenes). Development of novel functional and organized materials, Ph.D. Thesis, Utrecht University, Utrecht, The Netherlands (1996).

[31] H.J.J. van Dam and J.H. van Lenthe, *Mol. Phys.*, **90** (1997) 1007.

Chapter 5

The effect of syn-anti isomerism on the lowest valence transitions of 1,1'-bicyclohexylidene.[†]

[†] R.W.A. Havenith, L.W. Jenneskens and J.H. van Lenthe, *Chem. Phys. Lett.*, **282** (1998) 39-48

Abstract: Conformational effects on the ground state and excited state properties of 1,1'-bicyclohexylidene (**1**) were studied using *ab initio* methods. The total energy difference between the two conformers *anti*- (*anti*-**1a**, C_{2h} symmetry) and *syn*-1,1'-bicyclohexylidene (*syn*-**1b**, C_{2v} symmetry), was determined at the RHF/6-31G, MP2/6-31G//RHF/6-31G, RHF/6-311G**//RHF/6-31G and MP2/6-311G**//RHF/6-31G levels of theory. *Syn*-**1b** was found to be only slightly lower in energy by 0.051 kcal/mol then *anti*-**1a** at the MP2/6-311G**//RHF/6-31G level of theory.

The valence transitions of *syn*-**1b** were calculated using the MRDCI method using its 6-31G geometry and molecular orbitals. In contrast to the predicted UV data of *anti*-**1a** for which two absorptions are found at *ca.* 6.0 eV ($\pi \rightarrow \pi^*$ transition, exp. 6.01 eV) and *ca.* 7.2 eV ($\pi \rightarrow \sigma^*$ transition, exp. 6.85 eV), for *syn*-**1b** only one absorption, *viz.* a $\pi \rightarrow \pi^*$ transition at *ca.* 6.0 eV, will be discernible. The next higher transition of *syn*-**1b** with appropriate oscillator strength (*f*) is positioned at *ca.* 7.8 eV ($\pi \rightarrow \sigma^*$ transition). Inclusion of polarisation functions on the carbon atoms in the MRDCI calculations (6-31G* basis set) does not significantly affect the calculated transition energies, oscillator strengths (*f*) and CI vectors for both *anti*-**1a** and *syn*-**1b**.

1. Introduction

The UV absorption spectrum of 1,1'-bicyclohexylidene (**1**) has received considerable attention. In contrast to its simple analogue tetramethylethene (**2**), the spectrum of **1** contains two distinct absorption bands [1] instead of only one absorption band found for **2** [2]. Both bands were also observed in the single crystal UV spectrum (5.95 eV and 6.32 eV [3], respectively) and in stretched polyethylene films (5.98 eV and 6.72 eV [4], respectively), and were found to be polarised along the carbon-carbon double bond. Also in solution (*n*-pentane) the UV spectrum of **1** contains two distinct bands centred at 6.01 eV and 6.85 eV [1]. These results strongly suggest that both transitions have to be assigned to valence transitions. It should be stipulated, however, that in the solid-state **1** is only present in its *anti* conformer (*anti*-**1a**) [5], which, due to packing effects, does not possess C_{2h} symmetry but only C_i symmetry. We recently performed *ab initio* MRDCI [6,7] calculations to obtain an unambiguous assignment of the lowest valence transitions of *anti*-**1a** [8,9]. The results revealed that the first transition of *anti*-**1a** has to be assigned to a $\pi\rightarrow\pi^*$ transition (HOMO→LUMO, c^2 0.92), whereas the second transition possesses charge-transfer character ($\pi\rightarrow\sigma^*$ transition, HOMO→LUMO+1, c^2 0.87). In line with the single crystal UV spectroscopy and stretched polyethylene films data [3,4] both transitions were calculated to be polarised perfectly along the carbon-carbon double bond. Thus, the calculations give a satisfactory explanation of the experimentally observed transitions in the solid-state. However, it should be stipulated that Frank-Condon excitation is a fast process (*ca.* 10^{-16}-10^{-14} s) [10]. Hence, if in solution bicyclohexylidene (**1**) is conformationally mobile an equilibrium mixture of conformers will be present. Indeed, ^{1}H-NMR spectroscopy (solvent $CDCl_3$, 300 K) of **1** provides compelling evidence for the occurrence of conformational isomerism; no distinct resonances for the related *equatorial* and *axial* hydrogen atoms of the cyclohexyl-like rings of **1** are found, *i.e.* they are isochronous [11,12]. These observations are rationalised by invoking rapid ring interconversions between *anti*- (*anti*-**1a**; C_{2h} symmetry) and *syn*-1,1'-bicyclohexylidene (*syn*-**1b**; C_{2v} symmetry) on the NMR timescale (Scheme 1). *Syn-anti* isomerism has been unequivocally established for a derivative of **1**, *viz.* 4,4'-di-*tert*-

butyl-bicyclohexylidene. Both the *anti*- and *syn*-conformer are conformationally frozen [12] and can be isolated separately [13]. An estimate of their energy difference was obtained from equilibration experiments (conditions: benzene, I_2 and 303 K); an equilibrium mixture with an *anti/syn* ratio 0.83/0.17 ($\Delta G=-RT\ln K=0.95$ kcal/mol) was found [12]. Hence, in contrast to the solid-state UV spectrum of **1** to which only *anti*-**1a** contributes [3,4], its solution UV spectrum will be dependent on the concentration and the absorptive properties of the distinct conformers *anti*-**1a** (C_{2h} symmetry) and *syn*-**1b** (C_{2v} symmetry) present in the equilibrium mixture.

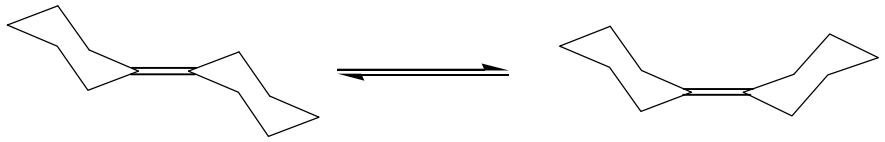

anti-**1a** *syn*-**1b**

Scheme 1 Equilibrium of *anti*- (*anti*-1a) and *syn*-1,1'-bicyclohexylidene (*syn*-1b).

In this chapter this issue is addressed. Firstly, the relative stabilities of *anti*-**1a** and *syn*-**1b** were studied at different *ab initio* levels of theory. It is shown that *anti*-**1a** and *syn*-**1b** possess nearly identical total energies. This indicates that also in solution an *anti/syn* ratio close to 0.50/0.50 will be present. Secondly, the valence transitions and oscillator strengths (*f*) of *syn*-**1b** were calculated at the MRDCI level of theory using its RHF/6-31G geometry and molecular orbitals (MO's); the results are compared with those previously calculated for *anti*-**1a** [8,9]. It is shown that the UV absorptive properties of *anti*-**1a** and *syn*-**1b** differ markedly. The effect of inclusion of polarisation functions on the carbon atoms (6-31G* basis set) on the MRDCI results was studied for both *anti*-**1a** and *syn*-**1b**.

2. Computational details

All calculations were run on a Silicon Graphics Power Challenge computer using the quantum chemical program GAMESS-UK [14,15]. The geometries of both *anti*-**1a** (C_{2h} symmetry) and *syn*-**1b** (C_{2v} symmetry) were optimised at the RHF/6-31G level and characterised as local minima by a Hessian calculation (Figures 1a and 1b). MP2 single point calculations were performed at the RHF/6-31G geometries of *anti*-**1a** and *syn*-**1b**. To assess basis set effects on the energy difference of *anti*-**1a** and *syn*-**1b**, SCF and MP2 single point calculations were done with the 6-311G** basis set.

MRDCI [6,7] calculations were performed at the RHF/6-31G geometry and MO's. The 6-31G basis set, which does not contain polarisation functions, was used to circumvent the inclusion of Rydberg character into the transitions. Transition energies and oscillator strengths (*f*) were calculated for the four lowest states of each symmetry [9]. The active CI space for *anti*-**1a** and *syn*-**1b** consists of 10 occupied MO's (20 electrons) and 88 virtual MO's. Configuration selection [16] for *syn*-**1b** resulted in the inclusion of 68135 CSF's of A_1, 65146 CSF's of B_1, 68749 CSF's of B_2, and 60905 CSF's of A_2 symmetry. MRDCI energies were corrected for size-consistency errors by the Davidson method [17], extended for multi-reference CI-expansions [7]. To assess the effect of polarisation functions on the calculated transition energies and oscillator strengths (*f*), MRDCI calculations with a 6-31G* basis set were done for the four lowest valence transitions of *anti*-**1a** (with A_g, B_u and B_g symmetry) and *syn*-**1b** (with A_1, B_1 and B_2 symmetry) at their RHF/6-31G geometries. The active CI space for *anti*-**1a** and *syn*-**1b** consists of 10 occupied MO's (20 electrons) and 138 virtual MO's. The configuration selection procedure for *anti*-**1a** resulted in the inclusion of 65323 CSF's of A_g, 76813 CSF's of B_u and 73286 CSF's of B_g symmetry. In the case of *syn*-**1b**, 77660 CSF's of A_1, 72684 CSF's of B_1 and 78350 CSF's of B_2 symmetry were selected. Ground state and excited state electron distributions were calculated by a Mulliken population analysis [18].

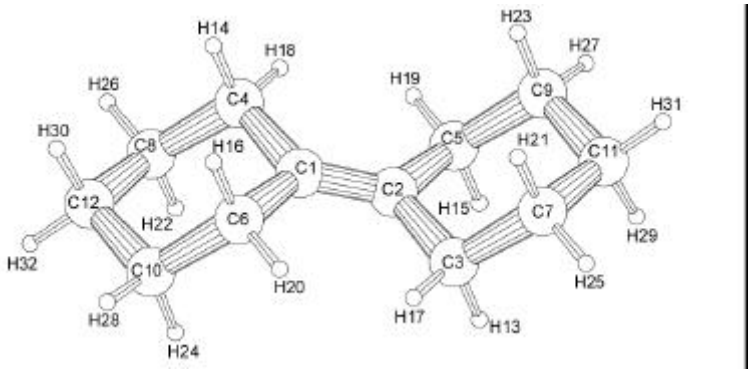

Figure 1a RHF/6-31G geometry of *anti*-1,1'-bicyclohexylidene (*anti*-1a).

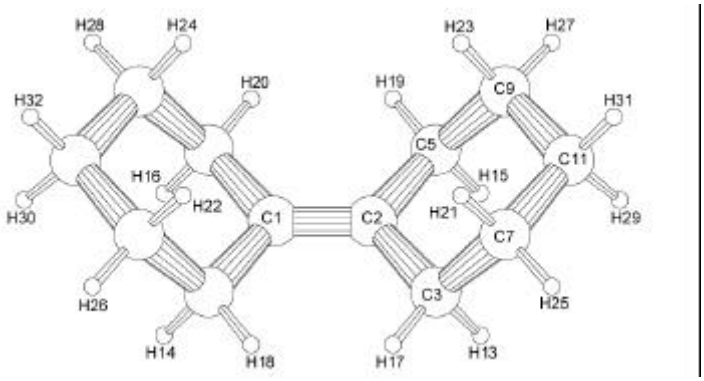

Figure 1b RHF/6-31G geometry of *syn*-1,1'-bicyclohexylidene (*syn*-1b).

3. Results

*3.1. The ground state properties of anti- (anti-**1a**) and syn-1,1'-bicyclohexylidene (syn-**1b**)*

Since **1** crystallises in its *anti*-conformer (*anti*-**1a**) [5], no single X-ray crystal data are available for *syn*-1,1'-bicyclohexylidene (*syn*-**1b**). However, the single X-ray crystal structure of *syn*-4,4'-di-*tert*-butyl-bicyclohexylidene has been reported [19]. The *tert*-butyl substituents are displaced due to packing effects leading to a symmetry reduction from C_{2v} to C_1 in the solid-state. In Table 1, selected RHF/6-31G structural

features of *syn*-**1b** are presented and compared with those of *syn*-4,4'-di-*tert*-butyl-bicyclohexylidene; satisfactory agreement is found.

To obtain an estimate of the total energy difference between *anti*-**1a** and *syn*-**1b**, *ab initio* calculations at various levels of theory were performed (Table 2). The results show that *anti*-**1a** and *syn*-**1b** possess similar total energies. As expected, the RHF/6-31G zero point energy for both conformers are nearly identical (*anti*-**1a** 201.159 kcal/mol *vs.* *syn*-**1b** 201.156 kcal/mol). Hence, the total energy difference ($\Delta E_{tot}=E_{anti} - E_{syn}$) calculated at various levels of theory, which are not corrected for zero point motion, will be reasonable estimates of the energy difference between the conformers. At the highest level of theory, *syn*-**1b** is 0.051 kcal/mol more stable than *anti*-**1a**, which suggests the presence of an equilibrium mixture consisting of 48% *anti*-**1a** and 52% *syn*-**1b** upon application of $\Delta E_{tot}(=E_{anti} - E_{syn})=\Delta G=-RT\ln K$ with T=300 K (Table 2).

Table 1 **Selected single crystal X-ray crystal structural data of *syn*-4,4'-di-*tert*-butyl-bicyclohexylidene [19] and RHF/6-31G structural data of *syn*-1,1'-bicyclohexylidene (*syn*-1b; bond lengths in Å, valence angles in °).**[a]**

Structural parameter	**Single crystal X-ray data [19]**	**RHF/6-31G *syn*-1b**
C(1)-C(2)	1.339	1.337
C(2)-C(3)	1.507	1.520
C(3)-C(7)	1.524	1.541
C(7)-C(11)	1.527	1.533
C(1)-C(2)-C(3)	124.4	124.9
C(2)-C(3)-C(7)	113.1	111.3
C(3)-C(7)-C(11)	112.5	111.5
C(7)-C(11)-C(9)	107.6	111.1

[a]As a consequence of packing effects *syn*-4,4'-di-*tert*-butyl-bicyclohexylidene possesses C_1 instead of C_{2v} symmetry in the solid-state [19].

It is noteworthy that the energy difference between the *anti* and *syn* conformer of 4,4'-di-*tert*-butyl-bicyclohexylidene estimated from equilibration experiments [ratio *anti/syn* 0.83/0.17 (ΔG=0.95 kcal/mol, *vide supra*)] has been rationalised by invoking

non-bonded repulsive interactions between the *axial* hydrogen atoms [H(21)-H(22)] in the *syn* isomer (Figure 1b) [12].

Table 2 Total energy difference between *anti*-1a and *syn*-1b at various levels of theory.

Method	***anti*-1a**[a]	***syn*-1b**[a]	**ΔE_{tot} (kcal/mol)**[b]	**Ratio**[c] ***anti/syn***
RHF/6-31G	-465.87503441	-465.87504989	0.010	0.50/0.50
MP2/6-31G//RHF/6-31G	-466.97540077	-466.97556543	0.103	0.46/0.54
RHF/6-311G**//RHF/6-31G	-466.17089416	-466.17085765	-0.023	0.51/0.49
MP2/6-311G**//RHF/6-31G	-468.19547660	-468.19555785	0.051	0.48/0.52

[a]In Hartree (1 Hartree=627.5 kcal/mol). [b]1 cal=4.184 J. [c]Ratio *anti/syn* calculated using $\Delta E_{tot}(=E_{anti} - E_{syn})=\Delta G=-RT\ln K$ with T=300 K.

Since the structure of the bicyclohexylidene unit of the *anti* and *syn* conformers of 4,4'-di-*tert*-butyl-bicyclohexylidene, respectively, are similar to those calculated for *anti*-**1a** and *syn*-**1b** and the latter two possess nearly identical total energies, the proposed repulsive interactions cannot be responsible for their observed energy difference (see also Chapter 10).

*3.2. Vertical valence transitions of syn-1,1'-bicyclohexylidene (syn-**1b**)*

In Table 3 the MRDCI vertical valence transitions of *syn*-1,1'-bicyclohexylidene (*syn*-**1b**) are compiled and compared to those reported for *anti*-**1a** [8,9]. According to the results of Direct-CI calculations on the lowest valence transitions of *anti*-**1a** [9], the total deviation of *ca.* 3.5 eV from the experimental data ($\pi\rightarrow\pi^*$ transition; exp. 6.01 eV [1] *vs.* calc. Direct-CI 8.29 eV [9] and MRDCI 9.47 eV) can be separated into an error of *ca.* 2.3 eV due to the use of the 6-31G basis set and an error of *ca.* 1.2 eV due to the applied MRDCI frozen core approximation and configuration selection procedure. In the case of *anti*-**1a**, both the MRDCI as well as the Direct-CI method showed that the main configurations in the corresponding CI vectors are identical. Hence, we are confident that

the MRDCI method will provide reliable estimates for the transition energies, polarisation directions and CI vectors for the lowest valence transitions of *syn*-**1b** (*vide infra*).

The first transition of *syn*-**1b** has to be assigned to a $\pi\rightarrow\pi^*$ transition (9.46 eV; $1B_2$ symmetry, *f* 1.0185, HOMO→LUMO and c^2 0.93) and is similar to the first transition of *anti*-**1a** (9.47 eV; $1B_u$ symmetry, *f* 0.9401, HOMO→LUMO and c^2 0.92). For both compounds, the $\pi\rightarrow\pi^*$ transition is perfectly polarised along the carbon-carbon double bond.

In the case of *syn*-**1b**, however, the higher valence transitions differ markedly from those calculated for *anti*-**1a**. For *syn*-**1b**, the $\sigma\rightarrow\pi^*$ and $\pi\rightarrow\sigma^*$ transitions are interchanged with respect to those of *anti*-**1a** (*anti*-**1a**: $\sigma\rightarrow\pi^*$; 10.45 eV, $1B_g$ symmetry, *f* 0.0000, HOMO-1→LUMO and c^2 0.84, and $\pi\rightarrow\sigma^*$; 10.65 eV, $2B_u$ symmetry, *f* 0.1459, HOMO→LUMO+1 and c^2 0.87, and *syn*-**1b**: $\pi\rightarrow\sigma^*$; 10.42 eV, $2A_1$ symmetry, *f* <0.0001, HOMO→LUMO+1 and c^2 0.86, and $\sigma\rightarrow\pi^*$; 10.53 eV, $1B_1$ symmetry, *f* 0.0043, HOMO-1→LUMO and c^2 0.86). Furthermore, the oscillator strength (*f*) of the $\pi\rightarrow\sigma^*$ transition of *syn*-**1b** is decreased significantly compared to that of *anti*-**1a**. In addition, the direction of polarisation is changed from parallel along the carbon-carbon double bond for *anti*-**1a** to perpendicular to the carbon-carbon double bond as well as perpendicular to the plane defined by the carbon atoms C(1), C(2) and C(3) in the case of *syn*-**1b** (Table 3).

It should be stipulated that the absolute values of the calculated oscillator strengths (*f*) are not expected to be in agreement with experimental data, since only a 6-31G basis set was used in our calculations. However, they can be used for a qualitative assignment.

It is noteworthy that inclusion of polarisation functions on the carbon atoms in the MRDCI calculations (6-31G* basis set) does not significantly affect the transition energies, oscillator strengths (*f*) and the CI vectors for both *anti*-**1a** and *syn*-**1b** (Table 3). Clearly for an improved match between the theoretical and available experimental data, extended basis sets and larger active CI spaces are a prerequisite. However, for **1** these calculations are currently computationally not feasible. Nonetheless, our current MRDCI results demonstrate that the valence transitions of *anti*-**1a** and *syn*-**1b** will be markedly different.

Table 3 **The ground state and lowest excited states of *anti*-1,1'-bicyclohexylidene (*anti*-1a) and *syn*-1,1'-bicyclohexylidene (*syn*-1b); transition energies (eV), oscillator strengths (*f*), polarisation and state symmetry.[a,b]**

***anti*-1,1'-bicyclohexylidene (*anti*-1a)**				***syn*-1,1'-bicyclohexylidene (*syn*-1b)**			
Transition Energy[a,b]	***f***	**Polarisation[c]**	**State sym.**	**Transition Energy[a,b]**	***f***	**Polarisation[c]**	**State sym.**
9.47	0.9401	∥	$1B_u$	9.46	1.0185	∥	$1B_2$
(9.46)	(0.9855)			(9.41)	(1.0198)		
10.45	0.0000		$1B_g$	10.42	<0.0001	⊥⊥	$2A_1$
(10.66)	(0.0000)			(10.69)	(<0.0001)		
10.65	0.1459	∥	$2B_u$	10.53	0.0043	⊥	$1B_1$
(10.88)	(0.0847)			(10.73)	(0.0047)		
11.61	0.0000		$2B_g$	11.28	0.0988	⊥⊥	$3A_1$
(11.92)	(0.0000)			(11.54)	(0.0849)		
11.65	0.1361	⊥⊥	$3B_u$	11.93	<0.0001	∥	$2B_2$
(11.91)	(0.1110)			(12.07)	(0.0012)		
11.72	0.0000		$2A_g$	11.97	0.0109	⊥	$2B_1$
11.93	0.0000		$3A_g$	11.97	0.0619	∥	$3B_2$
11.99	0.0000		$4A_g$	11.99	0.0011	⊥	$3B_1$
12.05	0.1139	⊥	$1A_u$	12.01	0.0064	⊥⊥	$4A_1$
12.39	0.0513	∥	$4B_u$	12.58	0.0000		$1A_2$
12.48	0.0140	⊥	$2A_u$	12.78	0.0063	∥	$4B_2$

[a]Ground state energies of *anti*-**1a**: -466.01168043 a.u. and of *syn*-**1b**: -466.01241345 a.u. [b]Numbers between parentheses are calculated using a 6-31G* basis set. [c]Notation; ∥: polarised parallel to the double bond; ⊥: polarised perpendicular to the double bond in plane with the carbon atoms C(3) to C(6); ⊥⊥: polarised perpendicular to the double bond and perpendicular to the plane occupied by the carbon atoms C(3) to C(6) (see Figure 1).

4. Discussion

Taking into account an average error of *ca*. 3.5 eV for the calculated transition energies (*vide supra*) [9], our results suggest that for *anti*-**1a** two valence transitions will be observed at *ca.* 6.0 eV ($\pi\rightarrow\pi^*$, $1A_g\rightarrow1B_u$) and *ca.* 7.2 eV ($\pi\rightarrow\sigma^*$, $1A_g\rightarrow2B_u$) in reasonable agreement with experiment [1,3,4]. Since with standard solution UV

spectroscopy only valence transitions with energies below *ca.* 7.3 eV (λ >170 nm) can be measured, for *syn*-**1b** only one discernible valence transition is predicted at *ca.* 6.0 eV ($\pi\rightarrow\pi^*$, $1A_1\rightarrow1B_2$). The second transition with enough oscillator strength (*f*) will be observed at *ca.* 7.8 eV ($\pi\rightarrow\sigma^*$, $1A_1\rightarrow3A_1$), which, however, cannot be measured under ordinary conditions. Furthermore, the latter transition is not polarised along the carbon-carbon double bond, but both perpendicular to the carbon-carbon double bond and the plane defined by the carbon atoms C(1), C(2) and C(3) [Table 3].

The differences found between *anti*-**1a** and *syn*-**1b** can be rationalised by the change of molecular point group and the concomitant changes in their relevant MO's (Figure 2) [20]. A small effect of the change in geometry from the C_{2h} to the C_{2v} point group is discernible for the occupied MO's and on the LUMO of *anti*-**1a** and *syn*-**1b**. For example, the topology of the occupied MO's is changed, *i.e.* the HOMO-4 and HOMO-3, are interchanged. This, however, will have minor effects on the lowest transition energies, since configurations with excitations from these MO's to virtual MO's only possess a small contribution in the CI vector. However, the LUMO+1 and higher relevant virtual MO's of *anti*-**1a** and *syn*-**1b** are much more affected (Figure 2). The LUMO+1 of *syn*-**1b** is 0.45 eV lower in energy than of *anti*-**1a** and possesses different character. In the C_{2h} pointgroup, the LUMO+1 of *anti*-**1a** contains some π^* character, whereas in the case of *syn*-**1b** this is impossible due to its C_{2v} symmetry. It is expected that due to this smaller spatial extension the oscillator strength (*f*) of the first $\pi\rightarrow\sigma^*$ transition (HOMO→LUMO+1) is decreased for *syn*-**1b** (Table 3: *anti*-**1a**, $1A_g\rightarrow2B_u$, *f* 0.1459 and *syn*-**1b**, $1A_1\rightarrow2A_1$, *f* <0.0001). In tetramethylethene (**2**, D_2 symmetry), the order of excitations is the same as for *syn*-**1b**, *viz.* the first, second and third excitations are assigned to a $\pi\rightarrow\pi^*$, a $\pi\rightarrow\sigma^*$ and a $\sigma\rightarrow\pi^*$ transition, respectively, while for *anti*-**1a** the second and third transitions are interchanged [8,9]. The lowering of the $\pi\rightarrow\sigma^*$ transition energy of *syn*-**1b** with respect of that of *anti*-**1a** is rationalised by the changes in the LUMO+1 topology and energy (ΔE 0.45 eV). It is noteworthy that in comparison with the 6-31G results also with the 6-31G* basis set the HOMO-4 up to the HOMO and, especially, the LUMO up to the LUMO+4 possess identical symmetries (Figure 2).

The electron redistribution upon excitation is also influenced for *syn*-**1b**. As expected for the $\pi\rightarrow\pi^*$ transition ($1A_1\rightarrow1B_2$), no significant electron redistribution occurs (Table 4); the same result was found for *anti*-**1a**. For *anti*-**1a**, the $\pi\rightarrow\sigma^*$ transition ($1A_g\rightarrow2B_u$) has charge-transfer character, *i.e.* electron redistribution occurs from the olefinic carbon atoms [C(1) and C(2)] towards the *equatorial* hydrogen atoms [H(17) to H(20)] [9]. Upon excitation of *syn*-**1b** from the $1A_1$ ground state to the $2B_1$ excited state ($\pi\rightarrow\sigma^*$ transition, *f* 0.0109) a similar electron redistribution occurs. In contrast, the lowest lying discernible $\pi\rightarrow\sigma^*$ transition of *syn*-**1b** ($1A_1\rightarrow3A_1$ excitation), which possesses oscillator strength (*f* 0.0988), also has charge-transfer character, but from the olefinic carbon atoms [C(1) and C(2)] towards the *axial* hydrogen atoms H(13) to H(16) and H(21) to H(24) [see Figure 1].

Table 4 **Mulliken population analysis [18] of the ground state ($1A_1$) and Mulliken population differences of excited states $1B_2$, $3A_1$, $2B_1$ and $3B_2$ of *syn*-1,1'-bicyclohexylidene (*syn*-1b).**

***syn*-1b**	**State**				
Atom	**$1A_1$**	**$1B_2$[a]**	**$3A_1$[a]**	**$2B_1$[a]**	**$3B_2$[a]**
C(1),C(2)	5.99	-0.04	-0.24	-0.25	-0.17
C(3),C(4),C(5),C(6)	6.34	0.00	-0.01	0.03	0.01
C(7),C(8),C(9),C(10)	6.29	-0.02	-0.04	-0.03	-0.06
C(11),C(12)	6.30	-0.02	-0.01	0.04	-0.04
H(13),H(14),H(15),H(16)	0.84	0.02	0.08	-0.01	-0.01
H(17),H(18),H(19),H(20)	0.84	0.00	-0.01	0.12	0.01
H(21),H(22),H(23),H(24)	0.85	0.00	0.08	0.02	0.05
H(25),H(26),H(27),H(28)	0.85	0.02	-0.01	-0.01	0.03
H(29),H(30)	0.85	0.02	0.04	-0.00	0.03
H(31),H(32)	0.85	-0.01	-0.01	-0.01	0.13

[a]A positive number corresponds to an increase in electron population, while a negative number corresponds to a decrease in electron population.

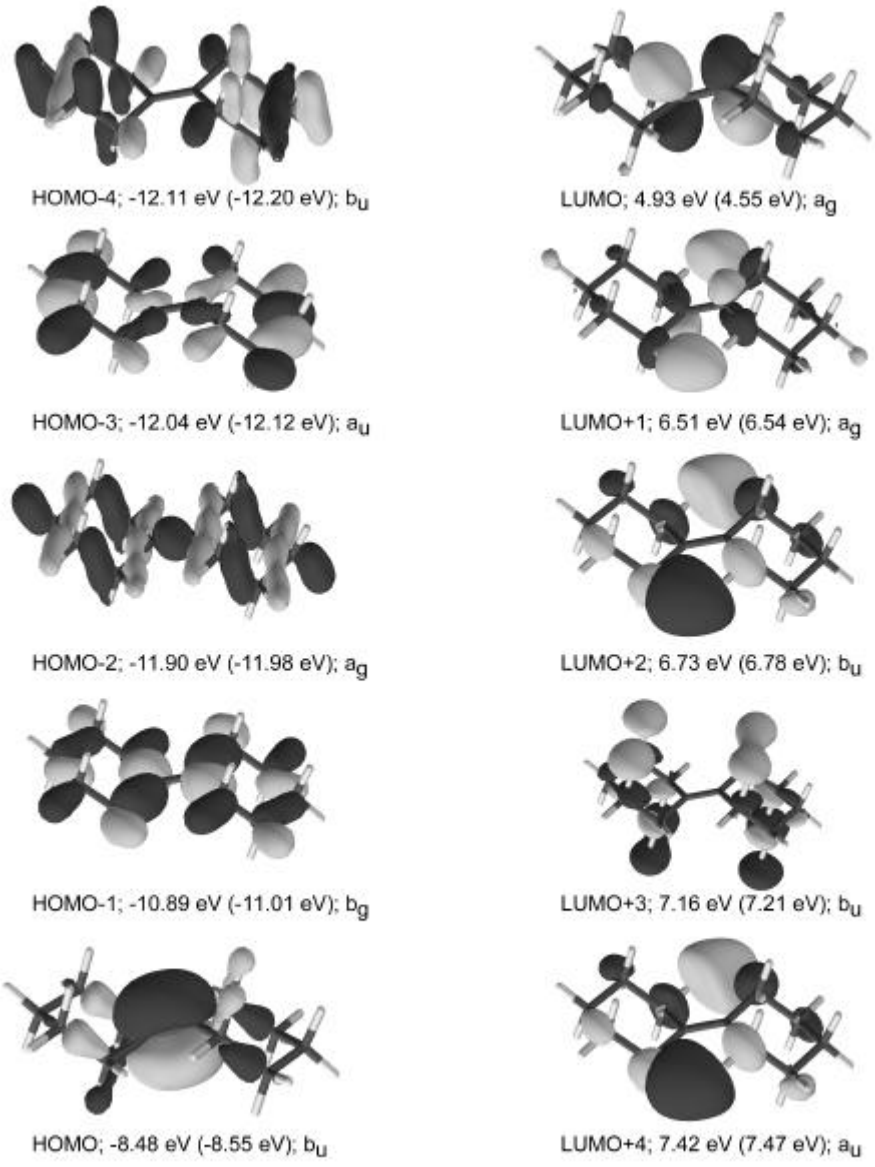

anti-**1a**

Figure 2 **6-31G MO contour plots (generated with Molden [20]) of the HOMO-4 to LUMO+4 of *anti*-1a and *syn*-1b with their energies and symmetries, respectively. Between parentheses 6-31G* MO energies are reported.**

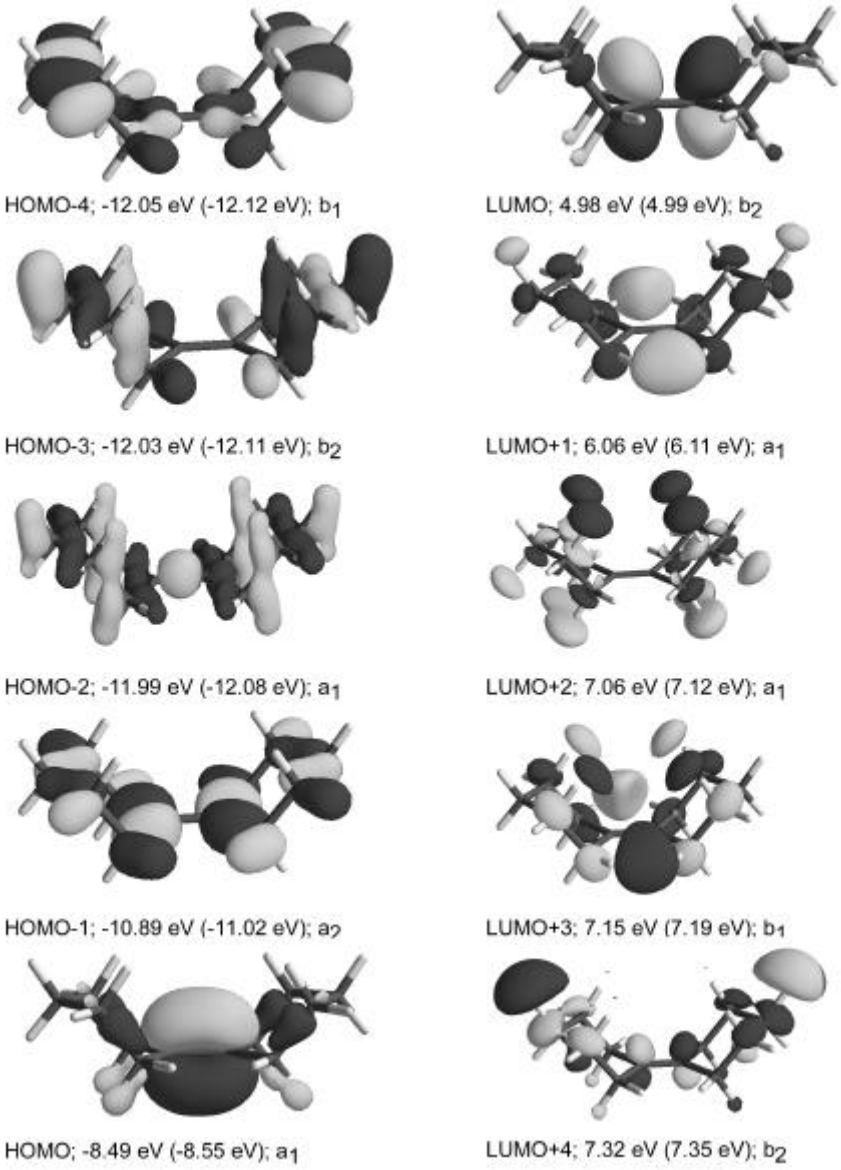

syn-**1b**

Figure 2 ***Continued***

5. Conclusions

The two conformers of bicyclohexylidene (**1**), *i.e. anti*-**1a** and *syn*-**1b**, possess nearly identical total energies. Therefore, in solution **1** is expected to be present in an equilibrium mixture consisting of almost equimolar amounts of *anti*-**1a** and *syn*-**1b**. As a consequence of the difference in molecular pointgroup between *anti*-**1a** (C_{2h}) and *syn*-**1b** (C_{2v}), their optical properties are markedly affected. For *anti*-**1a**, two valence absorption bands are calculated, *viz.* a $\pi\rightarrow\pi^*$ (*ca.* 6.0 eV, exp. 6.01 eV [1]) and $\pi\rightarrow\sigma^*$ (*ca.* 7.2 eV, exp. 6.85 eV [1]) transition, respectively [8,9]. In contrast for *syn*-**1b**, the MRDCI calculations predict only one valence absorption band corresponding to a $\pi\rightarrow\pi^*$ transition positioned at *ca.* 6.0 eV, which is polarised parallel to the carbon-carbon double bond. The next higher excitation ($\pi\rightarrow\sigma^*$ transition) of *syn*-**1b** will be found at *ca.* 7.8 eV and is polarised both perpendicular to the carbon-carbon double bond as well as to the plane occupied by the carbon atoms C(1), C(2) and C(3). Inclusion of polarisation functions on the carbon atoms in the MRDCI calculations (6-31G* basis set) does not significantly affect the calculated transition energies, oscillator strengths (*f*) and CI vectors for both conformers. Hence, our MRDCI results strongly suggest that the UV absorption spectrum of **1** in solution will consist of a superposition of the spectra of the distinct conformers *anti*-**1a** and *syn*-**1b**.

Acknowledgement

Financial support from NCF and Cray Research Inc for R.W.A. Havenith (NCF grant CRG 96-18) is gratefully acknowledged.

References

[1] M. Allan, P.A. Snyder and M.B. Robin, *J. Phys. Chem.*, **89** (1985) 4900.

[2] M.B. Robin, R.R. Hart and N.A. Kuebler, *J. Chem. Phys.*, **44** (1966) 1803.

[3] P.A. Snyder and L.B. Clark, *J. Chem. Phys.*, **52** (1970) 998.

[4] A. Yogev, J. Sagiv and Y. Mazur, *J. Am. Chem. Soc.*, **94** (1972) 5122.

[5] N. Veldman, A.L. Spek, F.J. Hoogesteger, J.W. Zwikker and L.W. Jenneskens, *Acta Crystallogr. C*, **50** (1994) 742.

[6] R.J. Buenker, S.D. Peyerimhoff and W. Butscher, *Mol. Phys.*, **35** (1978) 771.

[7] R.J. Buenker, S.-K. Shih and S.D. Peyerimhoff, *Chem. Phys.*, **36** (1979) 97.

[8] F.J. Hoogesteger, J.H. van Lenthe and L.W. Jenneskens, *Chem. Phys. Lett.*, **259** (1996) 178.

[9] R.W.A. Havenith, J.H. van Lenthe, L.W. Jenneskens and F.J. Hoogesteger, *Chem. Phys.*, **225** (1997) 139 (*cf.* Chapter 3).

[10] N.J. Turro, in: Modern molecular photochemistry (Benjamin/Cummings, Menlo Park CA, 1978).

[11] F.J. Hoogesteger, R.W.A. Havenith, J.W. Zwikker, L.W. Jenneskens, H. Kooijman, N. Veldman and A.L. Spek, *J. Org. Chem.*, **60** (1995) 4375.

[12] E.W.H. Asveld and R.M. Kellogg, *J. Org. Chem.*, **47** (1982) 1250.

[13] R.M. Kellogg, M. Noteboom and J.K. Kaiser, *Tetrahedron*, **32** (1976) 1641.

[14] M.F. Guest, J.H. van Lenthe, J. Kendrick, K. Schöffel, P. Sherwood and R.J. Harrison, *GAMESS-UK, a package of ab initio programs*, 1998.
With contributions from R.D. Amos, R.J. Buenker, M. Dupuis, N.C. Handy, I.H. Hillier, P.J. Knowles, V. Bonacic-Koutecky, W. von Niessen, V.R. Saunders and A.J. Stone.
It is derived from the original GAMESS code due to M. Dupuis, D. Spangler and J. Wendolowski, *NRCC Software Catalog*, Vol. 1, Program No. QG01 (GAMESS) 1980.

[15] R.J. Buenker, *Stud. Phys. Theor. Chem.*, **21** (1982) 17.

[16] R.J. Buenker and S.D. Peyerimhoff, *Theor. Chim. Acta*, **35** (1974) 33.

[17] S.R. Langhoff and E.R. Davidson, *Int. J. Quant. Chem.*, **8** (1974) 61.

[18] R.S. Mulliken, *J. Chem. Phys.*, **23** (1955) 1833.

[19] R. Mariezcurrena and L. Fornaro, *Acta Crystallogr. C*, **44** (1988) 2189.

[20] G. Schaftenaar, *Molden, CAOS/CAMM Center*, Nijmegen, The Netherlands, 1991.

Chapter 6

Long range through-bond interactions in functionalised oligo(cyclohexylidenes) and the photo-physical properties of 4,4'-bis(tetrahydro-4H-thiopyran-4-ylidene).[†]

[†] R.W.A. Havenith, J.H. van Lenthe, L.W. Jenneskens and A.W. Marsman, *to be submitted*

Abstract: Calculations on the smallest members of the oligo(cyclohexylidene) series (n=1-4) and on the tetrahydro-*4H*-thiopyran end-capped oligo(cyclohexylidene) series show that the strong through-bond coupling between their π bonds and sulphur lone pairs are mediated by the H(*ax*)-C-C-H(*ax*) structural sub-units and the π bonds connecting the cyclohexyl moieties. A comparison of the length dependency of the through-bond coupling *via* an oligo(cyclohexylidene) and an alkyl bridge shows that oligo(cyclohexylidenes) are more efficient in mediating through-bond couplings over large distances. The oligo(cyclohexylidene) bridge thus facilitates hole transfer processes between functional groups.

A first survey of the lowest valence transitions of 4,4'-bis(tetrahydro-*4H*-thiopyran-4-ylidene) show that these possess charge transfer character from the sulphur atoms towards the olefinic carbon atoms and the *axial* and *equatorial* hydrogen atoms. The through-bond orbital interactions have an effect on the electron redistribution that occurs when 4,4'-bis(tetrahydro-*4H*-thiopyran-4-ylidene) is excited to its first $\pi\rightarrow\pi^*$ excited state. The $\pi\rightarrow\pi^*$ transition possesses charge transfer character from the sulphur atoms towards the olefinic carbon atoms, due to the strong mixing of the sulphur lone pairs with the π bond.

1. Introduction

The oligo(cyclohexylidene) series containing a functionality at their α- and/or ω-termini have been established as novel molecular building blocks for supramolecular and functional materials [1-7]. One application of these oligomeric hydrocarbon spacers is their ability to hold two end groups at a well-defined spatial separation. Studies on similar bridges in electron transfer studies show that the spacer plays a crucial role in mediating long-range intramolecular electron transfer [6-13], *i.e.* the rate of electron transfer is highly dependent on the spacer-type and its length. It is thought that the rate enhancement of these bridge mediated electron transfer processes is due to the interaction of the orbitals of both chromophores with each other *via* coupling with orbitals on the spacer (through-bond coupling) [14-16].

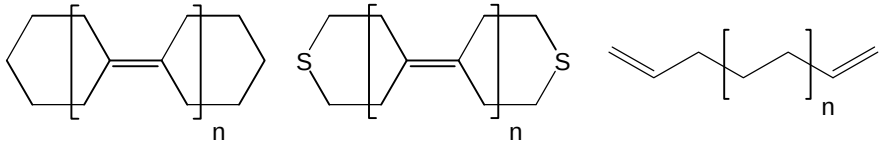

1(n) **2(n)** **3(n)**

Scheme 1 **Oligo(cyclohexylidenes) [1(n)] and tetrahydro-*4H*-thiopyran end-capped oligo(cyclohexylidenes) [2(n)]. The divinyl alkane [3(n)] oligomers are used as reference compounds.**

A model for the description of through-bond coupling was outlined by McConnell [17]. The splitting in energy between seemingly degenerate orbitals (ΔE) decays exponentially with the number of intervening σ bonds (N) according to equation (*1*).

$$\Delta E = Ae^{-b\frac{N}{2}} \qquad (1)$$

In equation (*1*), β is the attenuation coefficient (units: per bond) for hole and electron transfer, respectively. The smaller the value of β, the better hole (electron) transfer can occur over large distances [18-21].

This model has been applied to various systems, like the divinyl alkane [denoted by **3(n)**, see Scheme 1] oligomers [22]. To maximise the through-bond orbital interactions, the dihedral angle between the plane of each double bond and its respective allylic C-C bridge bond was fixed at 90º. The β values, calculated from equation (*1*) for consecutive members in the series [β(i,i+1)] can be used for comparing the length dependency of the through-bond coupling between functional groups bridged by various spacers. The β(i,i+1) values and the splitting in π MO energies, calculated (RHF/3-21G) for the **3(n)** series [22] show that the through-bond coupling between the vinyl substituents is measurable over 12 bonds as is shown in Table 1.[1]

Table 1 **The energy splitting of the ionisation potentials (RHF/3-21G) of the π bonds (eV) of 3(n), the number of intervening σ bonds, the β(i,i+1) and A values [22].**

Compound	ΔE(π) (eV)	# σ bonds	β(i,i+1)	A
3(1)	0.58	4	0.695	2.317
3(2)	0.29	6	0.588	1.681
3(3)	0.16	8	0.536	1.365
3(4)	0.09	10	0.532	1.338
3(5)	0.06	12	0.529	1.315
3(6)	0.03	14	0.528	1.305
3(7)	0.02	16		

The through-bond coupling between functional groups attached at the termini (α and ω) of the parent oligo(cyclohexylidenes) [**1(n)**, see Scheme 1] is determined by the symmetry and energy of the orbitals centred on that functional group [23]. The π-type lone pair orbitals of sulphur have the required symmetry and energy to couple with the oligo(cyclohexylidene) bridge [24], and the tetrahydro-*4H*-thiopyran end-capped

[1] The original β(i,i+1) values in reference [22] are half of those reported in Table 1, because the division by 2 in equation (*1*) was later added [21].

oligo(cyclohexylidenes) [**2(n)**, see Scheme 1] can thus serve as an efficient spacer in molecules for mediating electron transfer processes.

Photo-electron spectroscopy studies and *ab initio* calculations (NBO analyses) on the shorter members of the oligo(cyclohexylidene) [**1(2)**] and the tetrahydro-*4H*-thiopyran end-capped derivatives [**2(1)** and **2(2)**] [23,24] show that the oligo(cyclohexylidene) framework indeed mediate electronic interactions. The sulphur lone pairs couple with the σ bonds of the H(*ax*)-C-C-H(*ax*) sub-units and the π bonds of the intervening oligo(cyclohexylidene) bridge [24]. Interestingly, the splitting of the energy of the sulphur lone pairs [ΔE(LpS)] of adjacent members of the thiopyran end-capped derivatives [**2(1)**: 0.36 eV, 7.66 Å; **2(2)**: 0.32 eV, 11.88 Å] is only diminished by 0.04 eV, suggesting a very weak distance dependency of the orbital interactions. If this weak distance dependency occurs for extended members of this series, the tetrahydro-*4H*-thiopyran end-capped oligo(cyclohexylidenes) will possess molecular wire characteristics.

We will now focus on the length dependency of the through-bond interactions in the oligo(cyclohexylidene) series. RHF/6-31G* calculations on the extended homologues in the **1(n)** and the **2(n)** series will determine if the interactions between the functional groups are retained, despite the long distance. The coupling of the orbitals on the chromophores with the intervening bridge will be studied using the natural bond orbital (NBO) [25,26] approach [27]. We will present the β values of equation (*1*) for both series to compare the length dependency of the through-bond coupling in the oligo(cyclohexylidenes) with those obtained for the **3(n)** series. The influences of the sulphur substitution and the through-bond interactions on the lowest valence transitions of **2(1)** are calculated using the MRDCI methodology.

2. Computational details

All geometries were optimised using the GAMESS-UK [28] package at the RHF/6-31G* level of theory. A previous study of **1(1)** and **2**(**1**) shows that this level of theory is adequate. The geometries of **1(1)** and **2(1)** obtained at this level of theory are in

excellent agreement with available single X-ray data [24,29]. Ionisation potentials were obtained using Koopmans' theorem [30].

For analysing the contributions of through-space and through-bond interactions, the procedure first suggested by Heilbronner and Schmelzer [31] and later extended by Imamura *et al.* [32], was used, using natural bond orbitals (NBO's) [25-27]. In this analysis, the interaction between a subset of NBO's is estimated by setting all off-diagonal elements between the pairs of NBO's not included in this subset to zero. A diagonalisation of the resulting Fock matrix gives the MO's in NBO basis and their energies for the case that only the selected interactions are operational [22,27,33,34]. The NBO analyses were performed using the Weingold NBO 3.0 program [35] as implemented in GAMESS-UK.

For an assignment of the ionisation potentials, the MO's with the highest contribution of the sulphur lone pair NBO's ($2c^2$) were assigned as the sulphur lone pairs. In the same way, the outermost π orbitals were identified in the **1(n)** series.

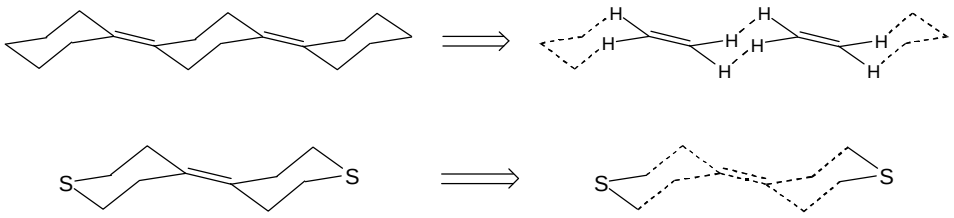

Scheme 2 **Schematic drawing of the geometries considered in the ghost-centre calculations.**

Ghost-centre calculations [36] were performed for **1(2)** and **2(1)**, to establish whether through-space or through-bond interactions are operational. In calculations for **1(2)**, the π bonds of **1(2)** are replaced by ethene molecules, while the other atoms of **1(2)** are replaced by ghost-centres with the same basis functions as on the atoms. The distance of the π bonds of both ethene molecules is thus the same as those in **1(2)**. In Scheme 2, a schematic drawing is given of the relative orientation of the two ethene molecules in the ghost-centre calculation. For **2(1)**, the sulphur atoms are replaced by two dimethylsulfide

molecules, while the intervening atoms are replaced by ghost-centres with the appropriate basis functions (Scheme 2).

Excited state calculations for 4,4'-bis(tetrahydro-4H-thiopyran-4-ylidene)

The lowest valence transitions of 4,4'-bis(tetrahydro-*4H*-thiopyran-4-ylidene) [**2(1)**] were calculated using the Direct MRDCI [37] approach as implemented in GAMESS-UK. The calculations were performed at the RHF/6-31G* geometry, using the 6-31G* orbitals. The active space in the CI calculations consisted of the highest 29 occupied MO's (58 electrons) and 148 virtual orbitals. For the choice of the reference configurations in the final CI calculation, first an MRDCI calculation was performed with the reference configurations chosen as single and double excitations from the highest 7 occupied to the lowest 5 unoccupied orbitals of the appropriate symmetry. The four lowest roots of each symmetry were calculated. The most important configurations (c^2>0.01) of those lowest four roots of each symmetry were then taken as the reference configurations in the final MRDCI calculations.

The configuration selection procedure [38] in the final MRDCI calculations resulted in the selection of 98673 configuration state functions (CSFs) of A_g symmetry (13 reference configurations), 127864 CSFs of A_u (5 reference configurations) and 144728 CSFs of B_u symmetry (9 reference configurations). The CI energies were corrected for size-consistency errors by the Davidson method [39,40].

3. Results and discussion

3.1. SCF molecular orbital energies

The π MO energies of **1(n)** and **2(n)**, together with their assignment as the outermost π bonds or sulphur lone pairs of **1(n)** or **2(n)**, respectively, are presented in Table 2. The ionisation potentials of **1(1)**, **1(2)**, **2(1)** and **2(2)** are in excellent agreement with the experimental ones, measured by photo-electron spectroscopy [24]. A splitting of

the energy levels of the π bonds is discernible. A strong mixing of all π bonds occurs in both the **1(n)** and **2(n)** series. In the case of **2(n)**, the sulphur lone pairs also mix strongly with the π bonds of the intervening oligo(cyclohexylidene) bridge, as is indicated by the contribution of the sulphur lone pair NBO's in all π type MO's (Table 2).

The ghost-centre calculation [36] (*cf.* Chapter 3), performed for **1(2)**, shows that the energy difference between the π orbitals of the two ethene molecules is small (0.05 eV). In the case of **2(1)**, the energy of the sulphur lone pairs is split by less than 0.01 eV. The through-space interaction is thus negligible for even the smallest derivatives in both series.

Table 2 **The π MO and sulphur lone pair orbital energies (eV) of compounds 1(n) and 2(n). The total contribution (c^2) from both outermost π orbitals and sulphur lone pairs, in the case of 1(n) and 2(n), respectively, in the particular MO is indicated between parentheses.[a]**

	1(1)	**1(2)**	**1(3)**	**1(4)**	
HOMO	-8.58 (0.80)	-8.35 (0.74)*	-8.25 (0.40)*	-8.21 (0.23)	
HOMO-1		-8.91 (0.79)*	-8.65 (0.76)*	-8.49 (0.57)*	
HOMO-2			-9.06 (0.38)	-8.84 (0.54)*	
HOMO-3				-9.12 (0.20)	
	2(0)	**2(1)**	**2(2)**	**2(3)**	**2(4)**
HOMO	-9.09 (0.87)*	-8.76 (0.51)*	-8.60 (0.26)	-8.48 (0.13)	-8.39 (0.06)
HOMO-1	-9.55 (0.90)*	-9.12 (0.89)*	-8.89 (0.69)*	-8.74 (0.47)*	-8.63 (0.28)
HOMO-2		-9.53 (0.38)	-9.21 (0.62)*	-8.99 (0.62)*	-8.85 (0.52)*
HOMO-3			-9.49 (0.20)	-9.27 (0.42)	-9.07 (0.49)*
HOMO-4				-9.45 (0.14)	-9.31 (0.31)
HOMO-5					-9.42 (0.12)

[a]The orbitals marked with an asterisk are assigned to the outermost π orbitals in the case of **1(n)** and to the sulphur lone pairs in the case of **2(n)**.

3.2. NBO analyses

The relevant NBO's for the through-bond interactions are indicated in Scheme 3. For the analysis of the through-bond interactions in the case of **1(n)**, 6 consecutive steps are taken, starting with *1*) no interaction (self-energies of the NBO's). In the succeeding steps, the following interactions between NBO's are added to the preceding one: *2*) the π bonds (through-space interaction), *3*) the inner σ C-C bonds, *4*) the outer σ C-C bonds, *5*) the C-H(*ax*) bonds and *6*) all NBO's (Scheme 3a). In the case of the series **2(n)**, 5 consecutive steps are considered, *viz. 1*) no interaction (self-energies of the NBO's), *2*) the π bonds and the sulphur lone-pairs (through-space interaction), *3*) the σ C-C bonds, *4*) the C-H(*ax*) bonds and *5*) all NBO's (Scheme 3b).

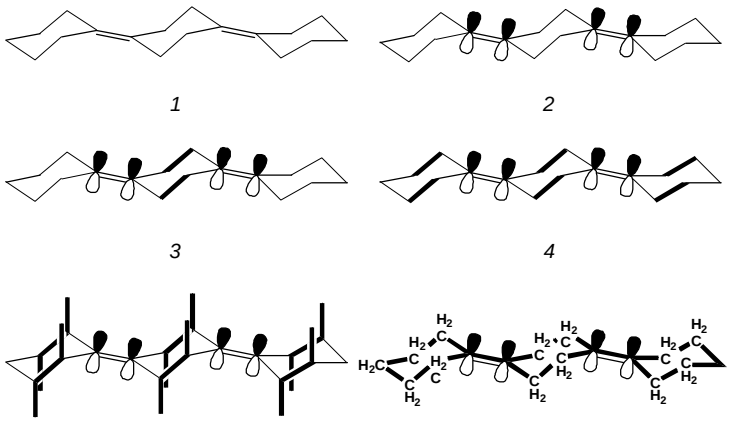

Scheme 3a **The interacting NBO's for 1(n) are indicated by bold lines in the 6 consecutive steps.**

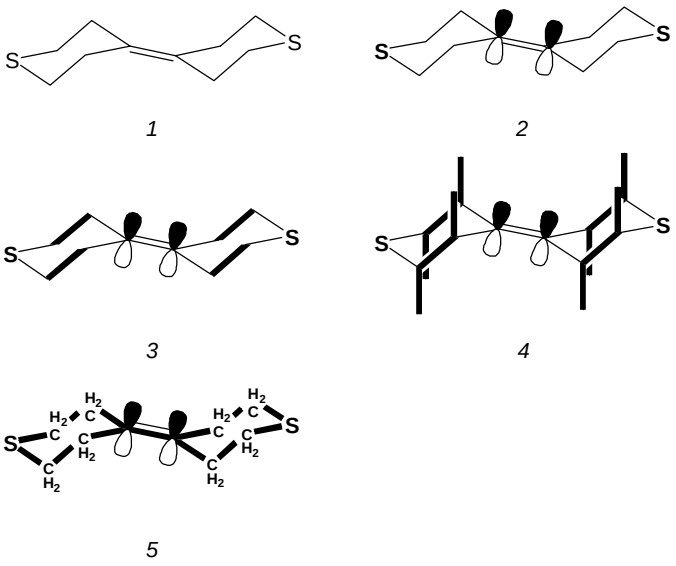

Scheme 3b **The interacting NBO's for 2(n) are indicated by bold lines in the 5 consecutive steps.**

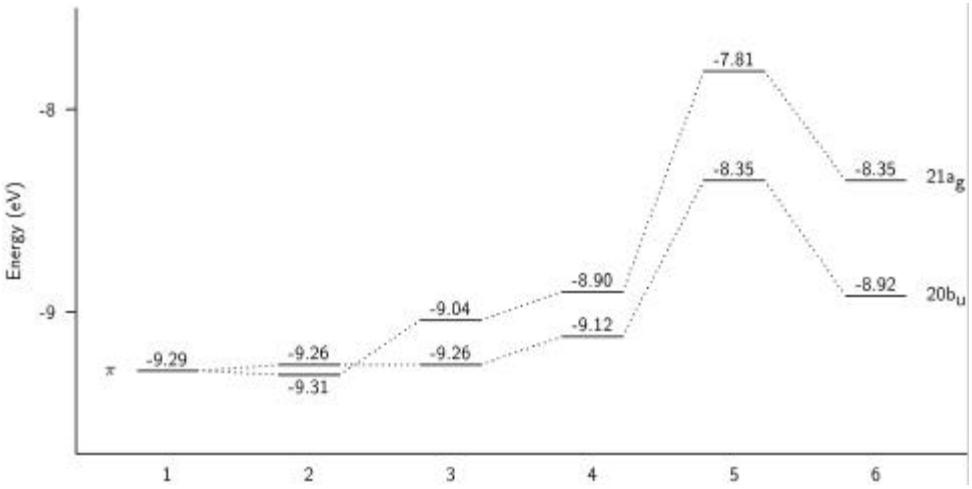

Figure 1 **The NBO interaction diagram of the π bonds of 1(2).**

In Figure 1, the orbital energies of the π MO's of **1(2)** after each step in the NBO analysis are indicated. The energies of the localised π bonds of **1(2)** are degenerate (step *1*). After through-space interaction (step *2*), the energy levels are split by only 0.05 eV, in line with the result obtained by the ghost-centre calculations (0.05 eV). The splitting increases to 0.22 eV as a consequence of the interaction with the intervening C-C single bonds (step *3*). Both levels are destabilised by an interaction with the other C-C σ bonds, but the splitting remains the same. A splitting of 0.54 eV is obtained when the C-H(*ax*) bonds get an interaction with the π bonds and the C-C σ bonds (step *5*). A total splitting of 0.57 eV is observed when all NBO's interact (step *6*). After interaction with the σ C-C bonds and the σ C-H(*ax*) bonds, the splitting between the energy levels of the π MO's is close to that after interaction with all NBO's, indicating that the splitting is caused mainly by interaction with these σ bonds.

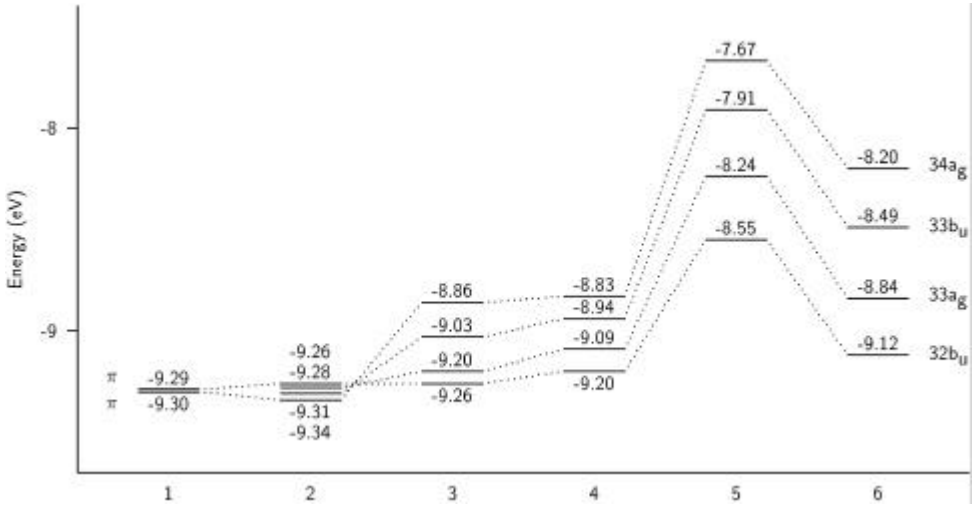

Figure 2 The NBO interaction diagram of the π bonds of 1(4).

In the case of **1(4)**, the same pattern is seen (Figure 2). Through-space interactions are negligible (step *2*), interaction with only the C-C bonds causes a small splitting (step *4*), and large splittings are obtained after interaction with the C-C and C-H(*ax*) structural units (step *5*).

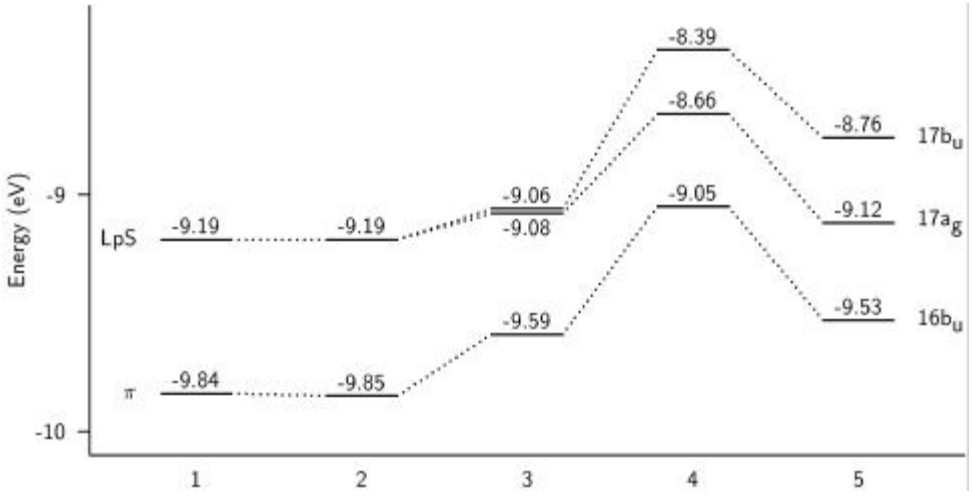

Figure 3 The NBO interaction diagram of the π bonds and the sulphur lone pairs of 2(1).

For **2(1)**, through-space interactions are also negligible. The sulphur lone pairs remain degenerate after interaction with only the C-C single bonds (step *3*). For the parent compounds, this interaction results already in a small splitting of the π MO energies. The splitting between the energy levels of the sulphur lone pairs is again caused by interaction with both the C-C and C-H(*ax*) units (step *4*, ΔE=0.36 eV).

In the case of **2(4)**, the same patterns as were found for **1(4)** and **2(2)** are discernible (Figure 4). The π orbitals split in energy after interaction with the C-C units (step *3*), while the sulphur lone pairs remain degenerate. After interaction with the C-C and C-H(*ax*) units (step *4*), the sulphur lone pairs mix with the olefinic bonds resulting in an energy splitting of 0.19 eV. The splitting between the sulphur lone pairs when all NBO's are considered (step *5*), is 0.23 eV. Thus, similar to the **1(n)** series, the through-bond interactions in the **2(n)** series are mediated by the H(*ax*)-C-C-H(*ax*) structural units of and the π bonds between the intervening oligo(cyclohexylidene) bridge.

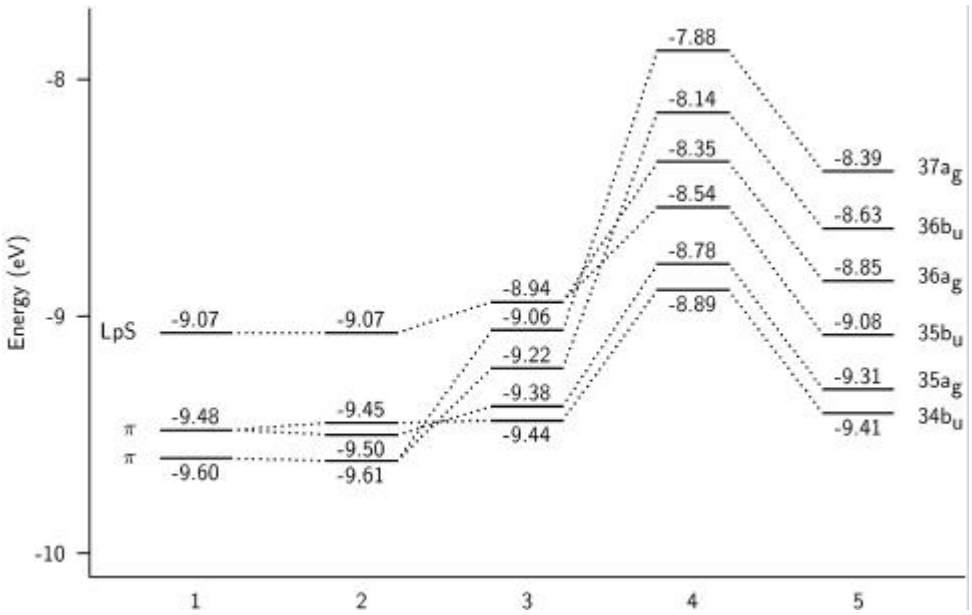

Figure 4 The NBO interaction diagram of the π bonds and sulphur lone pairs of 2(4).

3.3. Length dependency of the through-bond orbital coupling between the sulphur lone pairs

The small decrease in the splittings of the sulphur lone pair energies as a function of distance suggests a very weak length dependency of the through-bond interactions. To compare the oligo(cyclohexylidene) derivatives with the divinyl alkane series in mediating through-bond interactions, its β values of equation (*1*) were calculated. They are calculated from the splitting of **1(n)** and **2(n)** and those of the next homologue **1(n+1)** and **2(n+1)** and are denoted as β(i,i+1). The constant A in equation (*1*) is calculated with this β(i,i+1) value. The β(i,i+1) values for the consecutive members of the series **1(n)** and **2(n)** are tabulated in Table 3 and 4, respectively, together with the orbital splitting of the outermost π bonds in the case of **1(n)** and of the sulphur lone pairs in the case of **2(n)** (*cf.* Table 2).

Similar β(i,i+1) values for **1(n)** and **2(n)** are found, as expected, as the same orbitals are involved in the through-bond interactions. The constants A calculated for both

series are fairly constant, suggesting that the exponential decay of the through-bond interactions is a good first order approximation.

Table 3 **The energy splitting of the ionisation potentials of the outermost π bonds (eV) of 1(n), the number of intervening σ bonds, the β(i,i+1) values, A and the distance between the two π bonds (Å).**

Compound	ΔE(π) (eV)	# of σ bonds	β(i,i+1)	A	π-π distance (Å)
1(2)	0.564 (0.46)[a]	3	0.18	0.74	2.98
1(3)	0.395 (0.40)[a]	7	0.06	0.48	7.19
1(4)	0.352	11			11.42

[a]Experimental values from references [23,24] are indicated between parentheses .

Table 4 **The energy splitting of the ionisation potentials of the sulphur lone pairs (eV) of 2(n), the number of intervening σ bonds, the β(i,i+1) values, A and the distance between the two sulphur atoms (Å).**

Compound	ΔE(LpS) (eV)	# of σ bonds	β(i,i+1)	A	S-S distance (Å)
2(0)	0.464 (0.45)[a]	3	0.12	0.56	3.49
2(1)	0.364 (0.4)[a]	7	0.07	0.46	7.66 (7.70)[b]
2(2)	0.317 (0.3)[a]	11	0.11	0.59	11.88
2(3)	0.252	15	0.06	0.40	16.11
2(4)	0.224	19			20.33

[a]Experimental values from reference [24] are indicated between parentheses . [b]Experimental value derived from a single X-ray analysis [24].

The calculated β(i,i+1) values for both oligo(cyclohexylidene) series are all very small compared to those of **3(n)** (Table 1), which was one of the best bridges for mediating through-bond interactions according to this model. Thus the oligo(cyclohexylidene) bridge is even more efficient than an alkyl spacer in mediating through-bond interactions. The through-bond interactions in the oligo(cyclohexylidene) series are thus less dependent of the length of the bridge and are mediated over longer distances than by an alkyl spacer. Hence, oligo(cyclohexylidenes) are very efficient in

mediating orbital interactions between appropriate end groups and they thus facilitate hole transfer over large distances.

A weak distance dependency of the rate of electron transfer is found for assemblies of **2(n)** [with n=0-2] on a gold surface [6]. Hence, these molecules possess thus good conductor characteristics.

3.4. The lowest valence transitions of anti-4,4'-bis(tetrahydro-4H-thiopyran-4-ylidene) [2(1)]

The strong mixing of the sulphur lone pairs with the π bond of **2(1)** can have a pronounced effect on its photo-physical properties. The lowest valence transitions of the *anti* conformer of 4,4'-bis(tetrahydro-*4H*-thiopyran-4-ylidene) [**2(1)**] were calculated using the Direct MRDCI approach to probe the effect of through-bond interactions on its UV spectrum. The excitation energies are tabulated in Table 5, together with the oscillator strength (*f*), polarisation direction and their assignment. Only the B_u excited states are interesting, as the transition moments for the excitation towards the lower A_u excited states are very small. It was noted in a previous study, that an average error of *ca.* 3.5 eV is made by this approach [36]. However, a comparison of the calculated transition energies with the experimental ones indicates that the error made in this case is somewhat larger, *ca.* 4.2 eV.

According to our calculations, two absorptions are expected in solution UV spectroscopy. This excitation corresponds to the LpS→π* ($1B_u$; 9.99 eV; *f* 0.5504; experimental 5.7 eV). The second excitation corresponds to a π→π* ($2B_u$; 11.78 eV; *f* 0.5661; experimental 6.2 eV) transition, respectively. The third transition with a considerable oscillator strength is that towards the $3B_u$ excited state (15.80 eV; *f* 0.2625), corresponding to a LpS→σ* transition. The first π→σ* transition is the excitation towards the $4B_u$ state (16.52 eV; *f* 0.0370). Both transition energies are too high to be observable in solution UV spectroscopy.

Table 5 **The lowest valence transitions of 4,4'-bis(tetrahydro-*4H*-thiopyran-4-ylidene) [2(1)].**

Transition energy (eV)	State symmetry	Oscillator strength (*f*)	Polarisation[a]	Assignment[b]
9.99	$1B_u$	0.5504	∥	HOMO→LUMO
11.78	$2B_u$	0.5661	∥	HOMO-2→LUMO
12.72	$1A_u$	0.0004	⊥	0.42 (HOMO-1→LUMO+2)
				0.24 (HOMO→LUMO+1)
13.11	$2A_u$	0.0042	⊥	HOMO-6→LUMO
14.40	$3A_u$	0.0002	⊥	0.48 (HOMO-2→LUMO+1)
				0.35 (HOMO-1→LUMO+5)
15.80	$3B_u$	0.2625	∥	HOMO→LUMO+3
16.16	$4A_u$	0.0005	⊥	0.41 (HOMO-2→LUMO+2)
				0.24 (HOMO→LUMO+1)
				0.17 (HOMO-3→LUMO+1)
16.52	$4B_u$	0.0370	⊥⊥	0.63 (HOMO-2→LUMO+3)
				0.19 (HOMO-1→LUMO+4)

[a]Notation; ∥: polarised parallel to the double bond; ⊥: polarised perpendicular to the double bond in plane with the carbon atoms C(3) to C(6); ⊥⊥: polarised perpendicular to the double bond and perpendicular to the plane occupied by the carbon atoms C(3) to C(6) (see Figure 5) [b]In case of multi-reference character of the excited state, the c^2 are tabulated.

The experimental energy difference of 0.5 eV between the first and second transition energies is not reproduced at the MRDCI level of theory. A difference of 1.79 eV is found. This error can probably be attributed to the configuration selection procedure. From the total of 10 812 082 configurations, only 144 728 were treated in the CI expansion. For the $1B_u$ and $2B_u$ state, an error of 877 and 1088 mHartree is estimated, respectively. As both values differ, a larger difference between the $1B_u$ and $2B_u$ state energy is expected. These calculations should therefore be considered as a first stab at the analysis of the excited states of **2(1)**.

The electron population redistributions for excitation towards the first four B_u states are tabulated in Table 6. A large electron population redistribution occurs upon the excitations towards the $1B_u$ (LpS→π^*; 9.99 eV; *f* 0.5504) and $2B_u$ (π→π^*; 11.78 eV; *f*

0.5661) states. The electron population on the sulphur atoms decreases, while that on the olefinic carbon atoms C(1) and C(2) and the hydrogen atoms H(13)-H(16) (*axial*) and H(25)-H(28) (*equatorial*) increases (see for atom numbering Figure 5). The electron population decrease on the sulphur atoms upon excitation towards the $2B_u$ state (HOMO-2→LUMO; $\pi\rightarrow\pi^*$; 11.78 eV; *f* 0.5661) is smaller than upon excitation towards the $1B_u$ state (HOMO→LUMO; LpS→π^*; 9.99 eV; *f* 0.5504), as the HOMO-2 possesses more π character than the HOMO. The mixing of the sulphur lone pair orbitals with the π bond, which is a consequence of the through-bond orbital coupling, is thus clearly visible in the electron redistribution upon excitation.

Similar to 1,1'-bicyclohexylidene that rapidly interconverts from its *anti*- into its *syn*-conformer [41], **2(1)** is also highly mobile in solution and in the gas-phase [24]. The calculated energy difference between the *anti*- and *syn*-conformers of **2(1)** is 0.08 kcal/mol. The topology of the highest occupied and lowest unoccupied molecular orbitals of *anti*- and *syn*-**2(1)** are similar to those of **1(1)**. Thus, *anti*-*syn* isomerism is expected to have the same effect on the (gas-phase) UV spectrum as in the case of **1(1)** [41] (see also Chapter 5). Hence, EELS measurements should be performed.

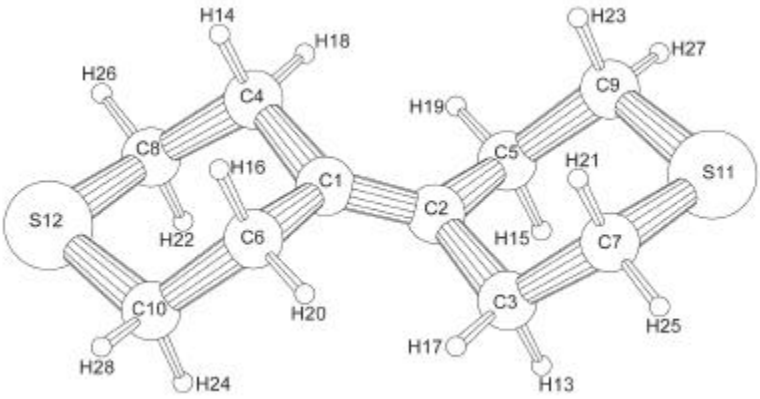

Figure 5 **The RHF/6-31G* optimised structure of 4,4'-bis(tetrahydro-*4H*-thiopyran-4-ylidene) [2(1)].**

Table 6 Mulliken population analysis [42] of the ground state and Mulliken population differences for the excited states of 2(1).

Atom[a]	**State**				
	$1A_g$	$1B_u$[b]	$2B_u$[b]	$3B_u$[b]	$4B_u$[b]
C(1),C(2)	5.983	0.087	0.061	-0.055	-0.084
C(3),C(4),C(5),C(6)	6.338	-0.009	-0.007	-0.028	-0.022
C(7),C(8),C(9),C(10)	6.458	-0.007	-0.008	0.005	0.001
S(11),S(12)	15.896	-0.172	-0.161	-0.080	-0.063
H(13),H(14),H(15),H(16)	0.820	0.025	0.028	0.001	0.001
H(17),H(18),H(19),H(20)	0.827	0.010	0.012	0.063	0.058
H(21),H(22),H(23),H(24)	0.811	-0.005	-0.001	0.023	0.030
H(25),H(26),H(27),H(28)	0.805	0.031	0.028	0.005	0.003

[a]Atom numbering as indicated in Figure 5. [b]For the excited states a positive number indicates an increase in electron population, while a negative number corresponds to a decrease in electron population.

4. Conclusions

Ab initio SCF MO calculations on oligo(cyclohexylidenes) and tetrahydro-*4H*-thiopyran end-capped oligo(cyclohexylidenes) show that through-bond interactions are operational. In the case of the tetrahydro-*4H*-thiopyran end-capped oligo(cyclohexylidenes), the sulphur lone pairs mix strongly with the π bonds connecting the cyclohexyl moieties and with the σ bonds of the cyclohexyl moieties. NBO analyses suggest that the interactions are mediated by the H(*ax*)-C-C-H(*ax*) structural sub-units of the cyclohexyl rings.

The β values between consecutive members of the tetrahydro-*4H*-thiopyran end-capped oligo(cyclohexylidenes) series are all very small, indicating that functional groups separated by long oligo(cyclohexylidene) spacers interact with each other. Tetrahydro-*4H*-thiopyran end-capped oligo(cyclohexylidenes) can thus facilitate hole transfer between functional groups over large distances.

A first survey of the excited state properties of 4,4'-bis(tetrahydro-*4H*-thiopyran-4-ylidene) show that the through-bond orbital interactions affect the electron redistribution

which occurs upon the $\pi \rightarrow \pi^*$ excitation. As a consequence of the strong mixing of the sulphur lone pairs with the π bond, the $\pi \rightarrow \pi^*$ transition possesses charge transfer character from the sulphur atoms towards the olefinic carbon atoms. It is expected that *anti-syn* isomerism has the same effect on the UV spectra of both conformers as it has on those of 1,1'-bicyclohexylidene.

References

[1] F.J. Hoogesteger, J.M. Kroon, L.W. Jenneskens, E.J.R. Südholter, T.J.M. de Bruin, J.W. Zwikker, E. ten Grotenhuis, C.H.M. Marée, N. Veldman and A.L. Spek, *Langmuir*, **12** (1996) 4760.

[2] F.J. Hoogesteger, R.W.A. Havenith, J.W. Zwikker, L.W. Jenneskens, H. Kooijman, N. Veldman and A.L. Spek, *J. Org. Chem.*, **60** (1995) 4375.

[3] E. ten Grotenhuis, A.W. Marsman, F.J. Hoogesteger, J.C. van Miltenburg, J.P. van der Eerden, L.W. Jenneskens, W.J.J. Smeets and A.L. Spek, *J. Cryst. Growth*, **191** (1998) 834.

[4] A.W. Marsman, E.D. Leusink, J.W. Zwikker, L.W. Jenneskens, W.J.J. Smeets and A.L. Spek, *Chem. Mater.*, **11** (1999) 1484.

[5] F.J. Hoogesteger, C.A. van Walree, L.W. Jenneskens, M.R. Roest, J.W. Verhoeven, W. Schuddeboom, J.J. Piet and J.M. Warman, *Chem. Eur. J.*, **6** (2000) 2948.

[6] E.P.A.M. Bakkers, A.W. Marsman, L.W. Jenneskens and D. Vanmaekelbergh, *Angew. Chem. Int. Ed.*, **39** (2000) 2297.

[7] E.P.A.M. Bakkers, A.L. Roest, A.W. Marsman, L.W. Jenneskens, L.I. de Jong-van Steensel, J.J. Kelly and D. Vanmaekelbergh, *J. Phys. Chem. B*, **104** (2000) 7266.

[8] G.L. Closs, L.T. Calcaterra, N.J. Green, K.W. Penfield and J.R. Miller, *J. Phys. Chem.*, **90** (1986) 3673.

[9] A.D. Joran, B.A. Leland, G.G. Geller, J.J. Hopfield and P.B. Dervan, *J. Am. Chem. Soc.*, **106** (1984) 6090.

[10] M.R. Wasielewski, M.P. Niemczyk, W.A. Svec and E.B. Pewitt, *J. Am. Chem. Soc.*, **107** (1985) 1080.

[11] C.A. Stein, N.A. Lewis and G.J. Seitz, *J. Am. Chem. Soc.*, **104** (1982) 2596.

[12] M. Antolovich, P.J. Keyte, A.M. Oliver, M.N. Paddon-Row, J. Kroon, J.W. Verhoeven, S.A. Jonker and J.M. Warman, *J. Phys. Chem.*, **95** (1991) 1933.

[13] P. Pasman, G.F. Mes, N.W. Koper and J.W. Verhoeven, *J. Am. Chem. Soc.*, **107** (1985) 5839.

[14] R. Hoffmann, A. Imamura and W.J. Hehre, *J. Am. Chem. Soc.*, **90** (1968) 1499.

[15] R. Hoffmann, *Acc. Chem. Res.*, **4** (1971) 1.

[16] M.N. Paddon-Row, *Acc. Chem. Res.*, **15** (1982) 245.

[17] H.M. McConnell, *J. Chem. Phys.*, **35** (1961) 508.

[18] M.N. Paddon-Row and S.S. Wong, *Chem. Phys. Lett.*, **167** (1990) 432.

[19] K.D. Jordan and M.N. Paddon-Row, *J. Phys. Chem.*, **96** (1992) 1188.

[20] S. Broo and S. Larsson, *Chem. Phys.*, **148** (1990) 103.

[21] M.J. Shephard and M.N. Paddon-Row, *Chem. Phys. Lett.*, **301** (1999) 281.

[22] M.J. Shephard, M.N. Paddon-Row and K.D. Jordan, *J. Am. Chem. Soc.*, **116** (1994) 5328.

[23] A.W. Marsman, R.W.A. Havenith, S. Bethke, L.W. Jenneskens, R. Gleiter and J.H. van Lenthe, *Eur. J. Org. Chem.*, (2000) 2629.

[24] A.W. Marsman, R.W.A. Havenith, S. Bethke, L.W. Jenneskens, R. Gleiter, J.H. van Lenthe, M. Lutz and A.L. Spek, *J. Org. Chem.*, **65** (2000) 4584.

[25] J.P. Foster and F. Weinhold, *J. Am. Chem. Soc.*, **102** (1980) 7211.

[26] A.E. Reed and F. Weinhold, *J. Chem. Phys.*, **78** (1983) 4066.

[27] M.N. Paddon-Row and K.D. Jordan, *J. Am. Chem. Soc.*, **115** (1993) 2952.

[28] M.F. Guest, J.H. van Lenthe, J. Kendrick, K. Schöffel, P. Sherwood and R.J. Harrison, *GAMESS-UK, a package of ab initio programs*, 2000.
With contributions from R.D. Amos, R.J. Buenker, M. Dupuis, N.C. Handy, I.H. Hillier, P.J. Knowles, V. Bonacic-Koutecky, W. von Niessen, V.R. Saunders and A.J. Stone.
It is derived from the original GAMESS code due to M. Dupuis, D. Spangler and J. Wendolowski, *NRCC Software Catalog*, Vol. 1, Program No. QG01 (GAMESS) 1980.

[29] N. Veldman, A.L. Spek, F.J. Hoogesteger, J.W. Zwikker and L.W. Jenneskens, *Acta Crystallogr. C*, **50** (1994) 742.

[30] T.A. Koopmans, *Physica*, **1** (1933) 104.

[31] E. Heilbronner and A. Schmelzer, *Helv. Chim. Acta*, **58** (1975) 936.

[32] A. Imamura and M. Ohsaku, *Tetrahedron*, **37** (1981) 2191.

[33] M.J. Shephard, M.N. Paddon-Row and J.D. Jordan, *Chem. Phys.*, **176** (1993) 289.

[34] M.N. Paddon-Row and M.J. Shephard, *J. Am. Chem. Soc.*, **119** (1997) 5355.

[35] E.D. Glendening, A.E. Reed, J.E. Carpenter and F. Weinhold, *NBO 3.0 program, natural bond orbital/natural population analysis/natural localized molecular orbital programs*.

[36] R.W.A. Havenith, J.H. van Lenthe, L.W. Jenneskens and F.J. Hoogesteger, *Chem. Phys.*, **225** (1997) 139 (*cf.* Chapter 3).

[37] B. Engels, V. Pleß and H.-U. Suter, *Direct MRD-CI, University of Bonn*, Bonn, Germany, 1993.

[38] R.J. Buenker and S.D. Peyerimhoff, *Theor. Chim. Acta*, **35** (1974) 33.

[39] S.R. Langhoff and E.R. Davidson, *Int. J. Quant. Chem.*, **8** (1974) 61.

[40] R.J. Buenker, S.-K. Shih and S.D. Peyerimhoff, *Chem. Phys.*, **36** (1979) 97.

[41] R.W.A. Havenith, L.W. Jenneskens and J.H. van Lenthe, *Chem. Phys. Lett.*, **282** (1998) 39 (*cf.* Chapter 5).

[42] R.S. Mulliken, *J. Chem. Phys.*, **23** (1955) 1833.

Chapter 7

1,3,5-Cyclohexatriene captured in computro; the concept of aromaticity.[†]

[†] J.H. van Lenthe, R.W.A. Havenith, F. Dijkstra and L.W. Jenneskens, *to be submitted*

Abstract: The determination of the extra stability of benzene, due to resonance/delocalised π-electrons, is not straightforward, *e.g.* the energy of benzene, described by two Kekulé structures, should be compared to that of 'hypothetical' 1,3,5-cyclohexatriene, described by only one Kekulé structure. Using Valence Bond (VB) theory, the energies and geometries of two-Kekulé-structure benzene and one-Kekulé-structure 1,3,5-cyclohexatriene have been calculated. The vertical resonance energy of benzene is only -9.6 kcal/mol. Geometry optimisation of one-Kekulé-structure 1,3,5-cyclohexatriene leads to a D_{3h} symmetric structure with alternating bond lengths located 7.4 kcal/mol above benzene (-TRE). A calculation on deformed benzene (two Kekulé structures) in the 1,3,5-cyclohexatriene optimised geometry shows that it is still stabilised by resonance by 6.2 kcal/mol and is located only 1.2 kcal/mol above benzene itself. Upon geometry optimisation, D_{6h} symmetric benzene results. The resonance between the two Kekulé structures is thus necessary for the D_{6h} symmetric geometry of benzene.

1. Introduction

'Bicarburet of hydrogen' nowadays referred to as benzene (C_6H_6) continuously surprises the scientific community [1,2], since it was first isolated by Faraday in 1825 [3,4]. Despite its unsaturated character its properties differ from those of (conjugated) alkenes [5]. In fact, benzene has a very distinct chemical reactivity.

With the advance of quantum chemistry the peculiar behaviour of benzene could be qualitatively rationalised using a Valence Bond (VB) treatment, *i.e.* by resonance between two Kekulé structures which provides extra stabilisation. In a Molecular Orbital (MO) approach the properties of benzene could be explained by π-electron delocalisation along its carbon perimeter. This has led to the famous Hückel 4n+2/4n rules, *i.e.* monocyclic conjugated circuits ([n]-annulenes) with 4n+2 (*aromatic* character) and 4n (*anti-aromatic* character) π-electrons (n = 0, 1, 2, etc.) are thermodynamically stabilised and destabilised, respectively [5]. The extra stabilisation of benzene due to the resonance between its two Kekulé structures or, equivalently, to its delocalised π system, is called the resonance (RE) or delocalisation energy. As a consequence benzene has a hexagonal geometry (D_{6h} symmetry) with bond lengths (1.399 Å [6]) intermediate between regular single and double carbon-carbon bond lengths.

The determination of the resonance energy of benzene, which represents the energy criterion for aromaticity, is thus an important, but not straightforward issue. The problem is the inaccessibility of appropriate reference compounds [7]. For example, 1,3,5-cyclohexatriene with the same geometry as benzene, but lacking resonance/π-electron delocalisation would be an appropriate reference. However, it does not exist! The energy difference between benzene and this hypothetical 1,3,5-cyclohexatriene gives the vertical resonance energy (VRE). To circumvent this problem it was proposed to use polyenes as a reference [8], *i.e.* the energy of benzene is compared to that of again a hypothetical cyclic polyene, 1,3,5-cyclohexatriene with D_{3h} symmetry. Its energy is estimated by taking thrice the C=C and C-C increment [8]. This energy difference gives the theoretical resonance energy (TRE). In this case also a change in geometry ($D_{6h} \rightarrow D_{3h}$) is involved.

Whereas the two reference points required for the determination of VRE or TRE of benzene are experimentally inaccessible, the best approach towards these reference compounds is by applying *Ab Initio* Valence Bond (VB) theory. A prerequisite is that optimised 1,3,5-cyclohexatriene (D_{3h} symmetry) is within reach.

Here we report the results of VB calculations on benzene and the elusive reference points, *viz.* 1,3,5-cyclohexatriene in both the benzene as well as its optimised ('true' 1,3,5-cyclohexatriene) geometries. Besides giving values for the resonance energies VRE and TRE, the results also shed light on the recent proposal that the hexagonal geometry of benzene is a consequence of the symmetrising force of the σ-skeleton instead of resonance/delocalisation of the π-electrons [9,10].

2. Methods

Within the VB model the wave function describes the desired double and single bonds; the π-system is described within the non-orthogonal VB framework using p-like orbitals on the six carbon atoms. The σ-system consists of delocalised doubly occupied orbitals. In all calculations all orbitals are completely optimised.

Since each bond in VB is described by a singlet coupled pair of orbitals, the reference points 1,3,5-cyclohexatriene in the benzene geometry (D_{6h} symmetry) and in its optimised geometry (D_{3h} symmetry) with double bonds between the carbon-atoms (1,2), (3,4) and (5,6), can be described by the following wave function:

$$\Psi_1 = \left| s_{core}(p_1\overline{p}_2 - \overline{p}_1 p_2)(p_3\overline{p}_4 - \overline{p}_3 p_4)(p_5\overline{p}_6 - \overline{p}_5 p_6) \right| = \left| s_{core}(1,2)(3,4)(5,6) \right|$$

Thus the wave function in either case consists of only *one* Kekulé structure. In contrast, the wave function of regular benzene (D_{6h} symmetry) and benzene deformed (D_{3h} symmetry) in the optimised geometry of 1,3,5-cyclohexatriene will be obtained by adding the *second* Kekulé structure, giving

$$\Psi_2 = N\left(\left| s_{core}(1,2)(3,4)(5,6) \right| + \left| s_{core}(2,3)(4,5)(6,1) \right| \right)$$

Note that two Kekulé structures are *not* orthogonal to each other (for benzene, the overlap is 0.66). This is both a consequence of the orbital overlap and an intrinsic property of the Rumer spin functions. Hence, the formal single bonds of 1,3,5-cyclohexatriene (one-Kekulé-structure calculations) will possess double bond character. So 1,3,5-cyclohexatriene is polyene-like.

In our VB description of benzene, the three Dewar benzene structures, *viz.* three additional covalent structures which contribute for less than 6-7% each [11,12] are excluded, to focus on the effect of resonance interactions between the possible Kekulé structures.

The VB wave functions will be denoted by the symmetry of the geometry and the number of structures employed. Thus a regular benzene calculation is denoted by D_{6h}-**2**. To obtain an estimate of the VRE, a one-Kekulé-structure calculation has been performed, *viz.* denoted by deformed 1,3,5-cyclohexatriene (D_{6h}-**1**). For the calculation of the TRE, the geometry of 1,3,5-cyclohexatriene (D_{3h}-**1**) has been optimised. A calculation on deformed benzene in the optimised 1,3,5-cyclohexatriene geometry (D_{3h}-**2**) has been performed to judge whether resonance is still important upon deformation of benzene.

In our VB approach, the p-orbitals are allowed to delocalise, though they are still predominantly atomic in nature (*cf.* Cooper *et al.* [11]). Thus completely optimised non-orthogonal atomic orbitals are used which have tails on the other atoms. This model was first used by Coulson and Fischer in their description of the H_2 molecule [13]. The geometries of benzene (D_{6h}-**2**, Ψ_2) and 1,3,5-cyclohexatriene (D_{3h}-**1**, Ψ_1) were optimised using gradient techniques [14]; a 6-31G basis set [15] was used. The calculations are performed using the *Ab Initio* Valence Bond program TURTLE [16], as integrated in the GAMESS-UK package [17].

3. Results and discussion

*3.1. The geometries and resonance energies of (deformed) benzene (D_{6h}-**2**, D_{3h}-**2**) and (deformed) 1,3,5-cyclohexatriene (D_{6h}-**1**, D_{3h}-**1**)*

The optimised geometries of benzene (D_{6h}-**2**) and its reference compound 1,3,5-cyclohexatriene (D_{3h}-**1**) are presented in Table 1, together with their total energies and the energy of their most stable Kekulé structure.

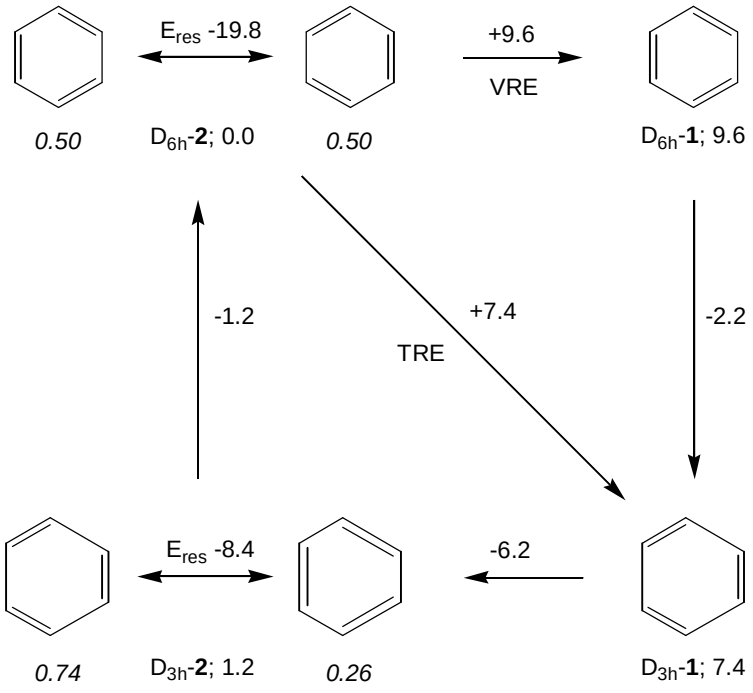

Scheme 1 **The thermocycle of benzene, their relative energies (kcal/mol) and the weights (in *italics*) of the Kekulé structures.**

Table 1 **The optimised structures of benzene (D_{6h}-2) and 1,3,5-cyclohexatriene (D_{3h}-1) together with their total VB energy (in Hartree) and energy of their most stable Kekulé structure (in Hartree), and those of their deformed counterparts D_{6h}-1 and D_{3h}-2.**

Molecule	C_1-C_2(Å)	C_2-C_3(Å)	Total energy	Most stable structure energy
benzene (D_{6h}-**2**)[1]	1.399	1.399	-230.693447	-230.661873
1,3,5-cyclohexatriene (D_{3h}-**1**)[2] deformed	1.369	1.433	-230.681589	-230.681589
1,3,5-cyclohexatriene (D_{6h}-**1**)	1.399	1.399	-230.678149	-230.678149
deformed benzene (D_{3h}-**2**)	1.369	1.433	-230.691547	-230.678195

In our calculations, the following results are obtained (Scheme 1). Benzene (D_{6h}-**2**) has a geometry with carbon-carbon bond lengths of 1.399 Å in excellent agreement with the experimental value (1.399 Å) [6]. Geometry optimisation of 1,3,5-cyclohexatriene (D_{6h}-**1**) starting at the benzene (D_{6h}-**2**) geometry leads to 1,3,5-cyclohexatriene (D_{3h}-**1**) with alternating bond lengths of 1.369 Å and 1.433 Å (Table 1), *i.e.* 1,3,5-cyclohexatriene (D_{3h}-**1**) is captured in computro (Scheme 1)! This relaxation of the 1,3,5-cyclohexatriene geometry (D_{6h}-**1**) from D_{6h} symmetry to D_{3h} symmetry (D_{3h}-**1**) is only moderately exothermic (-2.2 kcal/mol, Scheme 1). The calculated alternating bond lengths are in reasonable agreement with experimental values found in linear 1,3,5-hexatriene (1.368 Å and 1.458 Å [18]). The resemblance between the optimised geometry of 1,3,5-cyclohexatriene (D_{3h}-**1**) and related bond lengths in 1,3,5-hexatriene confirms the polyene character of the former.

Upon inclusion of resonance, deformed benzene (D_{3h}-**2**) is located 1.2 kcal/mol above benzene. Geometry optimisation leads immediately back to D_{6h}-**2**. These results indicate that resonance between the two Kekulé structures is necessary for obtaining the D_{6h} symmetric geometry of benzene (*cf.* [19]).

[1] Other structural features of D_{6h}-**2**: C-H 1.073 Å; ∠ C-C-H 120.0º.

[2] Other structural features of D_{3h}-**1**: C-H 1.073 Å; ∠ C_1-C_2-H 120.6º; ∠ C_2-C_3-H 119.4º.

According to Pauling, the resonance energy (RE) of a molecule is defined as the energy difference between the total energy of the molecule and the energy of its most stable Kekulé structure [20]. For benzene (D_{6h}-**2**), both structures are degenerate and have equal weights. A RE value of -19.8 kcal/mol is found (Scheme 1). Upon deformation of benzene towards the 1,3,5-cyclohexatriene geometry (D_{3h}-**2**), the weights of both structures become 0.74 and 0.26 (Scheme 1). The Pauling RE of deformed benzene (D_{3h}-**2**) is still -8.4 kcal/mol. While a significant resonance stabilisation is present in deformed benzene (D_{3h}-**2**), it is located above D_{6h} benzene (D_{6h}-**2**, Scheme 1). The small endothermicity (1.2 kcal/mol, Scheme 1) of the deformation of benzene to the 1,3,5-cyclohexatriene optimised structure (D_{6h}-**2** $\rightarrow$ D_{3h}-**2**) and the fact that resonance still is important in deformed benzene (D_{3h}-**2**) suggest that the (magnetic) properties of deformed benzene are similar to those of benzene (D_{6h}-**2**) itself. Indeed, for even stronger distortions of the benzene geometry towards a D_{3h} structure with alternating bond lengths, the magnetic properties, are nearly identical to those of benzene [21].

A VRE of only -9.6 kcal/mol is found for benzene (D_{6h}-**2**) (Scheme 1). The VRE of deformed benzene (D_{3h}-**2**) is only 3.4 kcal/mol lower than that of benzene (D_{6h}-**2**), *viz.* -6.2 kcal/mol. According to our VB calculations, the TRE of benzene is only -7.4 kcal/mol (Scheme 1). These values for both the VRE and TRE are considerably lower than most previously reported values (range 5 - 95 kcal/mol [7,22-24]). This discrepancy can be attributed to the fact that in previous calculations the VRE and TRE were calculated using either calculations with pre-determined ethene π orbitals [23] or CASSCF wave functions that were transformed to a VB space of all covalent VB determinants [22]. Hence the 1,3,5-cyclohexatrienes (D_{6h}-**1** and D_{3h}-**1**) were accessed with non-optimised orbitals. In the most recent VB calculations [24] 175 different (ionic) structures for benzene (D_{6h}-**2**) while for (deformed) 1,3,5-cyclohexatriene (D_{6h}-**1** and D_{3h}-**1**) only 27 (ionic) structures were taken into account. This may well be an unbalanced view, and *e.g.* affect the energies.

The calculated VRE of benzene is also considerably lower than the resonance energy according to the Pauling definition. The optimisation of the wave function in the case of the one-structure calculation lowers the energy by 10.2 kcal/mol in comparison

with the energy of one single structure in the corresponding two-structure calculation. We attribute this to the fact that deformed 1,3,5-cyclohexatriene (D_{6h}-**1**) does not possess isolated double bonds but possesses polyene character.

4. Conclusions

The Valence Bond calculations show that benzene is stabilised with respect to the elusive reference molecule 1,3,5-cyclohexatriene (D_{3h}-**1**) by 7.4 kcal/mol (TRE), which is much smaller than most earlier suggestions. 1,3,5-Cyclohexatriene (D_{3h}-**1**) is accessed in computer experiments. At this geometry, benzene still possesses a considerably degree of π-electron delocalisation. The second Kekulé structure is responsible for the relaxation of D_{3h}-**2** to benzene, thus resonance is necessary for obtaining the D_{6h} symmetric geometry of benzene.

References

[1] P.J. Garratt, Aromaticity, (Wiley, New York, 1986).

[2] V.I. Minkin, M.N. Glukhovtsev and B.Y. Simkin, Aromaticity and anti-aromaticity, (Wiley, New York, 1994).

[3] M. Faraday, *Phil. Trans.*, (1825) 440.

[4] R. Kaiser, *Angew. Chem.*, **80** (1968) 337.

[5] T.M. Krygowski, M.K. Cyrañski, Z. Czarnocki, G. Häfelinger and A.R. Katritzky, *Tetrahedron*, **56** (2000) 1783.

[6] J.H. Callomon, E. Hirota, K. Kuchitsu, W.J. Lafferty, A.G. Maki, C.S. Pote, I. Buck and B. Starck, Vol. 7, *Structure data of free polyatomic molecules* in Landolt-Börnstein, numerical data and functional relationships in science and technology (Springer-Verlag, Berlin, 1976).

[7] R. Janoschek, *J. Mol. Struct. (Theochem)*, **229** (1991) 197.

[8] M.J.S. Dewar and C. de Llano, *J. Am. Chem. Soc.*, **91** (1969) 789.

[9] S. Shaik, P.C. Hiberty, L. Jean Michel and G. Ohanessian, *J. Am. Chem. Soc.*, **109** (1987) 363.

[10] S. Shaik, A. Shurki, D. Danovich and P.C. Hiberty, *J. Mol. Struct. (Theochem)*, **398-399** (1997) 155.

[11] D.L. Cooper, J. Gerratt and M. Raimondi, *Nature*, **323** (1986) 699.

[12] F. Dijkstra and J.H. van Lenthe, *Int. J. Quant. Chem.*, **74** (1999) 213.

[13] C.A. Coulson and I. Fischer, *Philosophical Magazine*, **40** (1949) 386.

[14] F. Dijkstra and J.H. van Lenthe, *J. Chem. Phys.*, **113** (2000) 2100.

[15] W.J. Hehre, R. Ditchfield and J.A. Pople, *J.Chem.Phys.*, **56** (1972) 2257.

[16] J. Verbeek, J.H. Langenberg, C. Byrman, F. Dijkstra and J.H. van Lenthe, *TURTLE a VBSCF program*, 1989-2000.

[17] M.F. Guest, J.H. van Lenthe, J. Kendrick, K. Schöffel, P. Sherwood and R.J. Harrison, *GAMESS-UK, a package of ab initio programs*, 2000.
With contributions from R.D. Amos, R.J. Buenker, M. Dupuis, N.C. Handy, I.H. Hillier, P.J. Knowles, V. Bonacic-Koutecky, W. von Niessen, V.R. Saunders and A.J. Stone.
It is derived from the original GAMESS code due to M. Dupuis, D. Spangler and J. Wendolowski, *NRCC Software Catalog*, Vol. 1, Program No. QG01 (GAMESS) 1980.

[18] J. Kao and N.L. Allinger, *J. Am. Chem. Soc.*, **99** (1977) 975.

[19] E.D. Glendening, R. Faust, A. Streitwieser, K.P.C. Vollhardt and F. Weinhold, *J. Am. Chem. Soc.*, **115** (1993) 10952.

[20] L. Pauling and G.W. Wheland, *J. Chem. Phys.*, **1** (1933) 280.

[21] U. Fleischer, W. Kutzelnigg, P. Lazzeretti and V. Mühlenkamp, *J. Am. Chem. Soc.*, **116** (1994) 5298.

[22] F. Bernardi, P. Celani, M. Olivucci, M.A. Robb and G. Suzzi-Valli, *J. Am. Chem. Soc.*, **117** (1995) 10531.

[23] H. Kollmar, *J. Am. Chem. Soc.*, **101** (1979) 4832.

[24] Y. Mo, W. Wu and Q. Zhang, *J. Phys. Chem.*, **98** (1994) 10048.

Chapter 8

Aromaticity of pyrene and its cyclopentafused congeners; resonance and NICS criteria. An ab initio Valence Bond analysis in terms of Kekulé resonance structures.[†]

[†] R.W.A. Havenith, J.H. van Lenthe, F. Dijkstra and L.W. Jenneskens, submitted for publication in *J. Phys. Chem. A*

Abstract: The effect of cyclopentafusion on the aromatic properties of pyrene and its cyclopentafused congeners has been studied by calculating resonance energies using the Valence Bond (VB) method, and Nucleus Independent Chemical Shifts using DIGLO. The VB resonance energy is only slightly affected by cyclopentafusion. The resonance interactions between Kekulé resonance structures that lead to six π electron (benzene-like) conjugated circuits have the largest contributions to the resonance energy, in favour of Clar's model. For all compounds these contributions are of similar magnitude. Hence, according to the resonance criterion, all compounds have the same aromatic character.

In contrast, the total NICS values show a decrease of aromatic character of the compounds in the series upon the addition of externally fused five-membered rings. However, in line with the resonance criterion, the diamagnetic part of the shielding tensor perpendicular to the molecular framework is nearly constant for all compounds, provided that comparable gauge origins are chosen. Thus, care should be taken by comparing the aromatic character of rings of different molecules by considering only their total NICS values.

1. Introduction

Polycyclic aromatic hydrocarbons (PAHs) with external cyclopentafused five-membered rings, such as the cyclopentafused pyrene derivatives (Scheme 1), belong to the class of non-alternant polycyclic aromatic hydrocarbons and may exhibit unusual (photo)-physical properties, *e.g.* anomalous fluorescence and high electron affinities [1,2].

Several qualitative models, *e.g.* Platt's ring perimeter model [3], Clar's model [4] and Randi¶'s conjugated circuits model [5-7], have either been or are frequently used for the rationalisation of the properties and the reactivity of PAHs. According to Platt's ring perimeter model [3], the aromatic hydrocarbon should be divided into two parts: a perimeter and an inner core. The perimeter should be considered as a [n] annulene, while the inner core represents only a perturbation. The properties of the hydrocarbon are then interpreted as those of the [n] annulene, using the Hückel [4n+2] rule.

Another view offers Clar's model [4] of aromatic hydrocarbons. In this model aromaticity is regarded as a local property. The Kekulé resonance structure with the largest number of aromatic sextets, *i.e.* benzene-like moieties, is preferred. The other rings in the PAH are less aromatic and are chemically more reactive.

The conjugated circuits model of Randi¶ [5-7] takes both Clar's model and Platt's ring perimeter model into consideration. All distinct conjugated circuits, *i.e.* cyclic arrays of sp^2 hybridised carbon atoms, in all Kekulé resonance structures are considered with equal weight. This model is used for estimating the resonance energy of a PAH. All conjugated circuits have a contribution, depending on the number of π electrons. Those consisting of [4n+2] π electrons [R(n)] have a stabilising (negative) contribution, while the [4n] conjugated circuits [Q(n)] have a destabilising (positive) contribution. The parameters R(n) and Q(n) were chosen in order to reproduce the resonance energy [6] of small aromatic hydrocarbons obtained by using either Valence Bond (VB) calculations [8] or by comparing the total energies of the PAH with an appropriate polyene reference compound [9]. All these qualitative models rationalise the properties of aromatic and anti-aromatic hydrocarbons in terms of the Hückel [4n+2] and [4n] rules.

The extra stability of a PAH, due to π electron delocalisation, can also be determined, computationally or experimentally, by either considering homodesmotic relationships [10] or by the reaction enthalpy of the reaction of the PAH towards suitable chosen reference compounds [11]. For example, for pyrene (**1**) the aromatic stabilisation energy (ASE), which serves as a measure of the resonance energy, can be calculated as the energy difference between the methyl substituted derivative and its quinoid derivative containing an exo methylene substituent.

Another approach to assess the aromatic properties of a PAH is by considering its magnetic properties. As a consequence of induced ring currents in their π systems [12,13], the magnetic properties of aromatic compounds differ with respect to those of non-conjugated alkenes. Hence, magnetic properties [10] (large anisotropy of the magnetic susceptibility, deshielded ring protons and negative Nucleus Independent Chemical Shift (NICS) values [14]) are also frequently used as aromaticity criteria.

Aromaticity is associated with cyclic electron delocalisation [10]. This results from resonance between two or more Kekulé resonance structures. A striking example is the structure of benzene, which cannot be described by one valence bond structure. Hückel theory and any other molecular orbital theory are one determinant approaches and thus do not provide any information about the importance of the different structures. In contrast, VB theory can address the interaction between Kekulé resonance structures since the wave function is written as a linear combination of these structures. Following the proposal by Pauling [15], the resonance energy (E_{res}) of an aromatic hydrocarbon is calculated as the difference between the total VB energy and the energy of the most stable structure ($E_{res}=E_{tot}-E_{lowest}$). In addition, the weights of the different Kekulé resonance structures are accessible which designate the importance of a particular structure in the wave function.

In a related study on the cyclopentafused pyrene congeners [16], in which regular *ab initio* methods were used (RHF/6-31G* and B3LYP/6-31G*), we found that cyclopentafusion has a large effect on their magnetic properties; a decrease of the aromatic character upon cyclopentafusion was found. The aromatic stabilisation energies (ASE's) were unaffected although the number of π electrons is increasing in this series.

These effects prompted us to study the effect of cyclopentafusion in the cyclopentafused pyrene series on the interaction between the different Kekulé resonance structures and its effect on the resonance energy and so its effect on their aromatic properties. VB theory enables us to partition the resonance energy into the contributions of the different conjugated circuits (*vide infra*). In this way, the aromatic properties of the individual rings can be studied using the resonance criterion, and can be compared to the magnetic criteria for aromaticity. The results can be used for validating the fundamentals of the empirical models for describing PAHs.

2. Methods

2.1. Computational details

All geometries were optimised using the GAMESS-UK [17] package at the RHF/6-31G level.[1] The equilibrium geometry of **7** was found to be bowl-shaped (*vide infra*) [16]. This means that in a treatment of the conjugated system in this geometry, σ orbitals cannot be excluded, as the strict σ/π separation is destroyed. The deviation from the planar form of **7** is rather small (12.4º, see Figure 1h). Previous VB studies of bent-benzenes showed that the description of the π system does not change much for bending angles up to 50º [18]. Thus the VB results obtained for the planar transition state will not deviate much from those of bowl-shaped **7**, while the calculation on planar **7** is computationally much cheaper.

The VB calculations were performed with the TURTLE [19] program package. In the spirit of Pauling [20], we considered only the Kekulé resonance structures (*vide infra*). The π system was described by strictly atomic, non-orthogonal p-orbitals, which

[1] The geometries obtained at the RHF/6-31G level of theory are in excellent agreement with those obtained at the RHF/6-31G* and B3LYP/6-31G* levels of theory [16]. In line are also the magnetic properties calculated at the RHF/6-31G, RHF/6-31G* and B3LYP/6-31G* geometries, indicating that the RHF/6-31G basis set gives an adequate description of the compounds.

were optimised for benzene (*vide infra*). The σ core was taken from a preceding RHF/6-31G calculation.

Nucleus Independent Chemical Shift (NICS) values in the ring centres [14] were calculated using the Direct IGLO [13,21] program, at the RHF/6-31G geometry using the IGLO-III basis set. The chemical shift shielding tensor is given as a sum of the diamagnetic and paramagnetic part by the IGLO program.

2.2. Nomenclature of Valence Bond structures

Before considering the possible valence bond structures for pyrene (**1**) and its cyclopentafused derivatives, the possibilities for benzene are presented. For benzene, five covalent structures are possible. Two of these are represented by the Kekulé resonance structures, in which the π bonds coincide with the σ bonds. Three other covalent structures exist, *viz.* the Dewar benzene structures. In these structures, two of the three π bonds coincide with the σ bonds, while the third π bond connects the opposite site of the hexagon. The wave function of benzene is made up for more than 70% of the two Kekulé resonance structures [18]. Thus the three Dewar benzene structures have only minor contributions.

For pyrene (**1**) 1430 covalent structures can be generated. Only six structures have all π bonds along the σ bonds. These six structures are the Kekulé resonance structures of pyrene. In the case of *tetra*cyclopenta[*cd*,*fg*,*jk*,*mn*]pyrene (**7**), 208012 covalent structures can be generated. Only ten Kekulé resonance structures exist for this molecule. It is expected that only the Kekulé resonance structures are important in the description of these molecules and that the other structures can be ignored.

2.3. Choice of the p-orbitals

A VB calculation, in which the p-orbitals are optimised, is time consuming. For example in the case of cyclopenta[*cd*]pyrene (**2**), it takes two orders of magnitude more CPU time than a VB calculation with predetermined orbitals. The latter took 4 hours of

CPU time on a SGI-R10K. Therefore, all VB calculations were performed with predetermined (optimised for benzene) strictly atomic p-orbitals. To validate the applicability of these frozen p-orbitals, they were also optimised for **2**, *viz.* the smallest molecule in this series with low symmetry (C_s). The results show that the structure energies, their weights and the resonance energy (E_{res}) are only marginally affected (Table 1).

Table 1 **The weights and energies of the Kekulé resonance structures of 2 calculated using the benzene optimised p-orbitals and the optimised p-orbitals of 2 (Scheme 1).**

	Benzene optimised p-orbitals		**2 optimised p-orbitals**	
Structure	**Weight**	**E (a.u.)**	**Weight**	**E (a.u.)**
2A	0.216	-686.845553	0.216	-686.845623
2B	0.189	-686.837622	0.189	-686.837677
2C	0.193	-686.833741	0.193	-686.833809
2D	0.240	-686.847528	0.240	-686.847621
2E	0.083	-686.802083	0.083	-686.802107
2F	0.079	-686.802020	0.079	-686.802076
Total E (a.u.)[a]	-686.940798		-686.940936	
E_{res} (kcal/mol)	58.53		58.56	

[a]RHF/6-31G total energy of **2**: -687.242053 a.u.

2.4. Partitioning of the resonance energy

Besides an estimate of the total resonance energy ($E_{res}=E_{tot}-E_{lowest}$), which is a measure of the aromatic character of the compound, the VB calculations also provide coefficients and interaction matrix elements of the individual resonance structures. This enables the identification of the most important resonance interactions between Kekulé resonance structures and in this way the most aromatic subsystems.

In order to analyse the individual contributions of different conjugated circuits to the resonance energy, the **H** matrix has to be transformed to an orthogonal basis. Thus, the structures are orthogonalised (Löwdin orthogonalisation [22]) and the **H** matrix is

transformed to this orthogonal basis, yielding $\mathbf{H}^{\perp}$. The total energy can then be partitioned in the weighted diagonal contributions of the structures and the weighted resonance contributions between them:

$$E = \sum_i \sum_j c_i c_j H_{ij}^{\perp} = \sum_i c_i c_i H_{ii}^{\perp} + \sum_i \sum_{j>i} 2 c_i c_j H_{ij}^{\perp} \qquad (1)$$

where c_i is the coefficient of structure i in the wave function.

The sum of these resonance contributions is another measure of the resonance energy (E^m_{res}); namely with respect to the weighted mean value of the energy of all structures. This mean resonance energy is thus more negative (stabilising) than the Pauling resonance energy (E_{res}) [15]. The E^m_{res} values for **1-7** follow the same trend as the E_{res} values (Table 2). This means that E^m_{res} can serve as a measure for the resonance energy E_{res}. The contribution to E^m_{res} of a particular interaction between two structures is two times the weighted resonance contribution ($2c_i c_j H_{ij}^{\perp}$). The differences between a pair of Kekulé resonance structures elucidate the conjugated circuit in which the π electrons are delocalised by resonance.

3. Results and discussion

3.1. The RHF/6-31G geometries of the cyclopentafused pyrene derivatives

Whereas the optimised geometries of **1-6** were all found to be planar, that of **7** is bowl-shaped (Figure 1). The planar geometry of **7** is the transition state for bowl-to-bowl interconversion; an energy barrier of only 3.20 kcal/mol (RHF/6-31G level of theory; RHF/6-31G* 3.8 kcal/mol; B3LYP/6-31G* 2.9 kcal/mol [16]) is found.

In pyrene (**1**) a short C5-C7 bond length of 1.34 Å (Figure 1a) is found. The bond lengths in the biphenyl-like sub-structure are all *ca.* 1.40 Å, whereas the C4-C5 bond length is substantially longer, *viz.* 1.44 Å. The RHF/6-31G geometry of **1** is in excellent agreement with that found by a single-crystal X-ray analysis at 93 K [23] (Figure 1a).

Cyclopentafusion has only a minor influence on the bond lengths of the pyrene substructure (see for example cyclopenta[*cd*]pyrene (**2**), Figure 1b). For all five-membered rings similar structural features are found, *viz.* typical single and double bond lengths of *ca.* 1.49 Å and *ca.* 1.36 Å, respectively (Figures 1c-g).

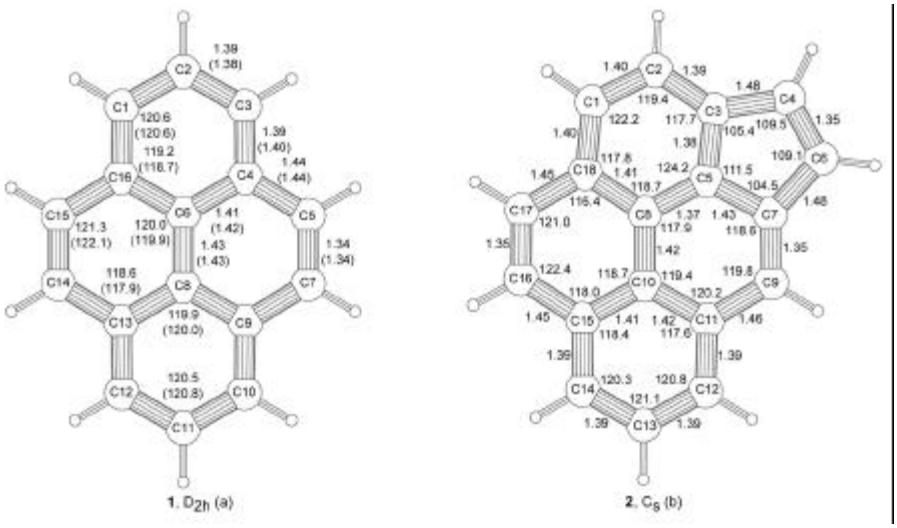

Figure 1 **Salient RHF/6-31G structural features of pyrene (1) (a) (experimental values between parentheses [23]), cyclopenta[*cd*]pyrene (2) (b), *di*cyclopenta[*cd,mn*]- (3) (c) and *di*cyclopenta[*cd,jk*]- (4) (d), *dic*yclopenta[*cd,fg*]-pyrene (5) (e), *tris*cyclopenta[*cd,fg,jk*]pyrene (6) (f), planar *tetra*cyclopenta[*cd,fg,jk,mn*]pyrene (7) (g) and a side-view on the equilibrium structure of *tetra*cyclopenta-[*cd,fg,jk,mn*]pyrene (h). Bond lengths are in Å and valence angles in °.**

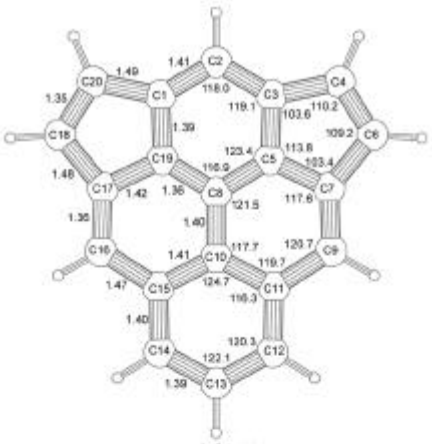

3, C_{2v} (c)

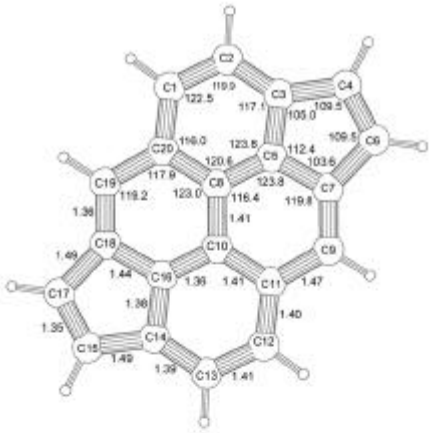

4, C_{2h} (d)

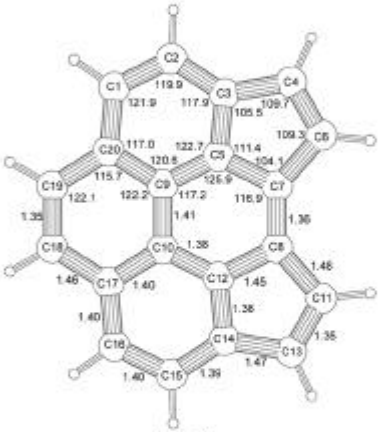

5, C_{2v} (e)

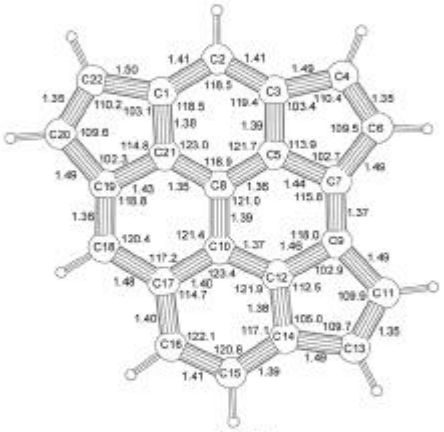

6, C_s (f)

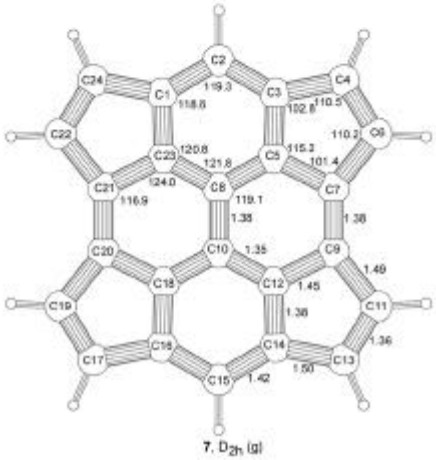

7, D_{2h} (g)

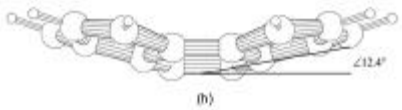

(h)

*3.2. Valence Bond description of pyrene (**1**)*

The weights and relative energies of the Kekulé resonance structures **A-F** (Scheme 1) of pyrene (**1**) are presented in Table 2. The larger weights of **A-D** compared to those of **E** and **F**, indicate that **A-D** are more important in the VB description of **1**. The total resonance energy (E_{res}) of **1** equals -62.34 kcal/mol (Table 3), indicating a high degree of stabilisation with respect to the most stable Kekulé resonance structure of **1**.

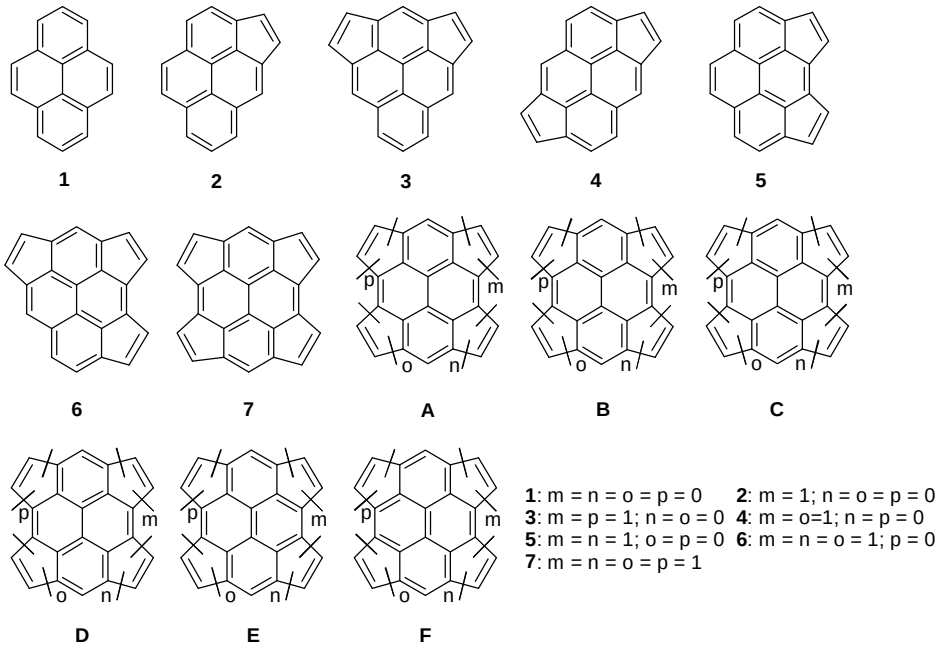

Scheme 1 **The structures of 1-7 and a schematic representation of their pyrene-type Kekulé resonance structures.**

The partitioning of the resonance energy (Table 4) reveals a large contribution of -16.92 kcal/mol to the mean resonance energy (E^{m}_{res}) from the resonance interactions between **A**↔**C**, **A**↔**D**, **B**↔**C** and **B**↔**D**. The resonance interaction between **A** and **C** (Scheme 1) leads to a six π electron (benzene-like) conjugated circuit in the top six-

membered ring of **1** (Scheme 2). Electron delocalisation within a six π electron conjugated circuit in the top and bottom six-membered rings is further a consequence of the resonance interaction between the structures **A**↔**D**, **B**↔**C** and **B**↔**D**. The interactions **A**↔**E** and **B**↔**F** (Schemes 1 and 2) lead to a conjugated circuit in the right and left central six-membered ring, respectively, and have a contribution of -9.66 kcal/mol to E^m_{res}. The sum of all E^m_{res} contributions of the resonance interactions within the top and bottom six-membered rings is -67.68 kcal/mol (67.1%), while that of the central six-membered rings is -19.32 kcal/mol (19.1%). Other resonance interactions, *e.g.* **A**↔**F**, leading to a 14 π electron conjugated circuit (Schemes 1 and 2), are responsible for the remaining part of E^m_{res}, and contribute to a lesser extent (13.8%) to the total resonance energy.

Table 2 **Weights of Kekulé resonance structures of compounds 1-7 and their relative energy between parentheses (in kcal/mol[a], Scheme 1).**

Compound	A	B	C	D	E	F
1 (D_{2h})	0.200	0.200	0.214	0.214	0.086	0.086
	(0.00)	(0.00)	(0.71)	(0.71)	(21.99)	(21.99)
2 (C_s)	0.216	0.189	0.193	0.240	0.083	0.079
	(1.24)	(6.22)	(8.65)	(0.00)	(28.52)	(28.56)
3 (C_{2v})	0.203	0.203	0.217	0.217	0.079	0.079
	(0.00)	(0.00)	(0.47)	(0.47)	(26.49)	(26.49)
4 (C_{2h})	0.203	0.203	0.176	0.267	0.075	0.075
	(7.81)	(7.81)	(16.62)	(0.00)	(36.52)	(36.52)
5 (C_{2v})	0.239	0.174	0.218	0.218	0.082	0.069
	(0.00)	(11.50)	(6.20)	(6.20)	(33.50)	(35.93)
6 (C_s)	0.223	0.189	0.243	0.198	0.076	0.068
	(0.75)	(6.52)	(0.00)	(7.90)	(34.26)	(36.23)
7 (D_{2h})[b]	0.208	0.208	0.222	0.222	0.068	0.068
	(0.00)	(0.00)	(0.13)	(0.13)	(35.19)	(35.19)

[a]Energy of the Kekulé resonance structure with the lowest energy: **1A/B**: -611.187290 a.u.; **2D**: -686.847528 a.u.; **3A/B**: -762.485737 a.u.; **4D**: -762.505755 a.u.; **5A**: -762.505340 a.u.; **6C**: -838.142596 a.u. and **7A/B**: -913.774319 a.u. [b]Transition state for bowl-to-bowl interconversion.

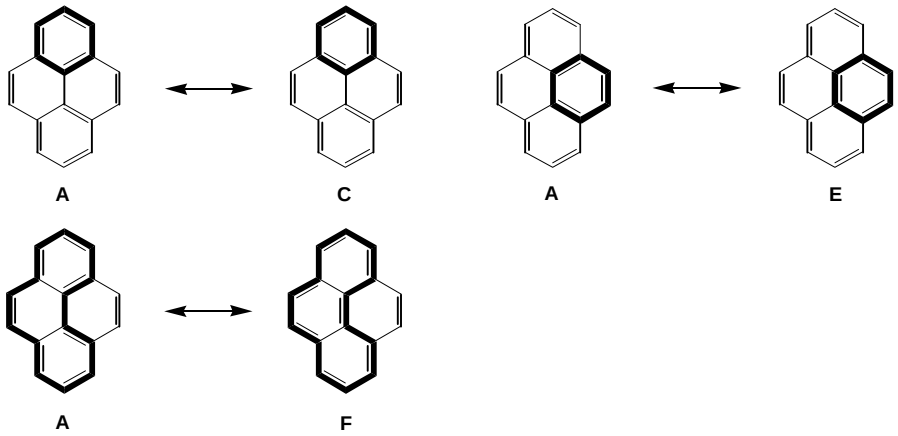

Scheme 2 **Resonance between the structures 1A and 1C, 1A and 1E and 1A and 1F, leading to benzene-like resonance in the top six π electron, central six π electron and 14 π electron conjugated circuits, respectively.**

Table 3 **Total energies of compounds 1-7 (a.u.) and their resonance energies (kcal/mol).**

Compound[a]	RHF	VB	E_{res} [b]	E^{m}_{res} [b]	E_{rel} [c]
1 (6)	-611.555550	-611.286631	-62.34	-100.90	
2 (6)	-687.242053	-686.940798	-58.53	-101.10	
3 (6)	-762.918242	-762.584880	-62.21	-101.77	4.70
4 (7)	-762.922606	-762.592661	-54.54	-101.49	1.96
4 (6)	-762.922606	-762.592523	-54.45	-101.32	
5 (7)	-762.925727	-762.595225	-56.40	-101.79	0.00
5 (6)	-762.925727	-762.595050	-56.29	-101.54	
6 (8)	-838.595341	-838.236025	-58.63	-102.68	
7 (10)	-914.259921	-913.873884	-62.48	-104.20	
7 (6)	-914.259921	-913.873345	-62.14	-103.44	

[a]The number of Kekulé resonance structures is indicated between parentheses. [b]For comparison the resonance energies of benzene, calculated with localised p-orbitals (6-31G basis set) and two structures, are E_{res} = -27.74 kcal/mol and E^{m}_{res} = -44.16 kcal/mol. [c]Calculated at the RHF/6-31G level of theory, in kcal/mol relative to the energy of **5**.

Table 4 **The contributions of the interactions between the orthogonalised structures to the resonance energy (E^m_{res}) for pyrene (1) in kcal/mol [$2c_i c_j H_{ij}^{\perp}$].**

	A	**B**	**C**	**D**	**E**
B	-0.08				
C	-16.92	-16.92			
D	-16.92	-16.92	0.29		
E	-9.66	-0.18	-3.20	-3.20	
F	-0.18	-9.66	-3.20	-3.20	-0.96

3.3. The effect of cyclopentafusion

In a previous study, it was shown that the aromatic stabilisation energies (ASE's) of the compounds **1-7** are all nearly equal [16], *i.e.* cyclopentafusion has no effect on the resonance energy. This conclusion is confirmed by the VB calculations. The resonance energy (both E_{res} and E^m_{res}) of the compounds **1-7** are all of the same magnitude (Scheme 1 and Table 3).

Upon the addition of externally fused five-membered rings, the weights of the pyrene sub-structures are only marginally affected (Table 2). The contributions of the different conjugated circuits to E^m_{res} show for all compounds the same trends; the six π electron (benzene-like) conjugated circuits in the top and bottom six-membered rings (**A**↔**C**, **B**↔**D**, **A**↔**D**, **B**↔**C**) have the highest contribution to E^m_{res}, independent of cyclopentafusion. The energy of the Kekulé resonance structures is only moderately affected by cyclopentafusion. The structures with the lowest number of formal double bonds in the five-membered rings are energetically favoured (Table 2 and Scheme 1).

Table 5 **The contributions of the interactions between the orthogonalised structures to the resonance energy (E^{m}_{res}) for cyclopenta[*cd*]pyrene (2), *di*cyclopenta[*cd,mn*]-pyrene (3), *di*cyclopenta[*cd,jk*]- (4) and *di*cyclopenta[*cd,fg*]pyrene (5) in kcal/mol [$2c_i c_j H_{ij}^{\perp}$].**

Cyclopenta[*cd*]pyrene (**2**)						
	A	**B**	**C**	**D**	**E**	
B	-0.09					
C	-16.82	-15.68				
D	-18.32	-17.54	0.30			
E	-10.05	-0.18	-2.99	-3.37		
F	-0.19	-9.04	-2.93	-3.27	-0.87	
*Di*cyclopenta[*cd,mn*]pyrene (**3**)						
	A	**B**	**C**	**D**	**E**	
B	-0.09					
C	-17.54	-17.00				
D	-17.00	-17.54	0.30			
E	-9.61	-0.19	-3.11	-3.14		
F	-0.19	-9.61	-3.14	-3.11	-0.81	
*Di*cyclopenta[*cd,jk*]pyrene (**4**)						
	A	**B**	**C**	**D**	**E**	**F**
B	-0.08					
C	-15.65	-15.65				
D	-19.01	-19.01	0.31			
E	-9.32	-0.18	-2.71	-3.39		
F	-0.18	-9.32	-2.71	-3.39	-0.77	
G	-0.08	-0.08	-0.04	-0.13	-0.03	-0.03
*Di*cyclopenta[*cd,fg*]pyrene (**5**)						
	A	**B**	**C**	**D**	**E**	**F**
B	-0.09					
C	-18.58	-16.17				
D	-18.58	-16.17	0.31			
E	-10.63	-0.18	-3.16	-3.16		
F	-0.14	-8.13	-2.89	-2.89	-0.78	
G	-0.16	-0.03	-0.09	-0.09	0.01	-0.17

The interactions between two Kekulé resonance structures with the lowest number of double bonds within the five-membered rings have the largest contribution to E^{m}_{res}. For example for **2**, both the interactions **A**↔**D** and **B**↔**C** lead to benzene-like resonance in the bottom six membered ring. The structures **A** and **D** have both one double bond in the five-membered ring, while the structures **B** and **C** have two double bonds (Scheme 1). The structures **A** and **D** have therefore a lower energy compared to structures **B** and **C** (Table 2), and consequently their contribution to E^{m}_{res} is larger (Table 5). The same reasoning also rationalises the differences between the contribution to E^{m}_{res} of the resonance interactions within the central six-membered rings (Table 5 and Scheme 1). Thus, the small differences in the contributions of similar conjugated circuits to E^{m}_{res} in the series can be related to the energy differences between the Kekulé resonance structures.

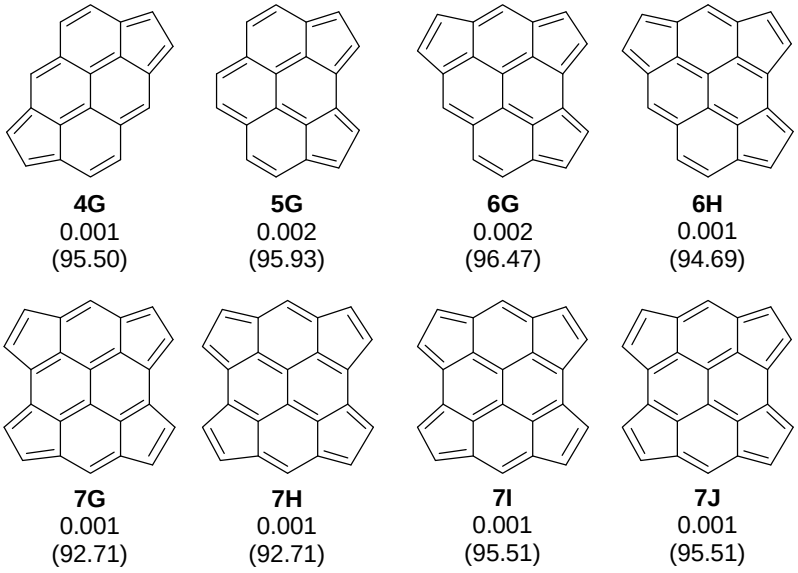

Scheme 3 **The remaining Kekulé resonance structures of 4, 5, 6 and 7 with their weights and their relative energies.**

In addition to the six pyrene sub-structures, compounds **4-7** possess the Kekulé resonance structures depicted in Scheme 3. However, their contribution to E^{m}_{res} is only small; they have negligible weights. Further support for the marginal influence of these resonance structures on E_{res} and E^{m}_{res} comes from VB calculations performed for **4**, **5** and **7** with only the inclusion of the pyrene sub-structures. A decrease of E_{res} of only *ca.* 0.4 kcal/mol is observed (Table 3) and the structure weights are unaffected. Hence, all compounds should be seen as substituted pyrene derivatives.

3.4. Resonance energy (E_{res}) as a measure of stability?

The relative energy of the isomers **3-5** and their resonance energy are presented in Table 3. As noted previously [16], the relative stability order of **5**>**4**>**3** does not follow the trend in the order of the resonance energy (E_{res}) of **3**>**5**>**4**.

A comparison of the energies of the most stable Kekulé resonance structures (Scheme 1 and Table 2) of **3-5** shows that the energy of the most stable structure of **3** (**A**/**B**) is 12.3 kcal/mol higher than that of **5** (**A**). The energy difference between **4D** and **5A** is only -0.26 kcal/mol. Since **3-5** contain the same number of π electrons the significant energy difference between **3A/B** and **5A** has to originate from the skeleton.

The strain energy for these isomers has been deduced from homodesmotic reactions and distorted cyclopenta[*cd*]pyrene isomers, fixed in a geometry to match those of **3-5** [16], The strain energy of **3** is 5.2 kcal/mol higher than that of **5**.

Thus, the relative stability of the *di*cyclopentafused-pyrene isomers cannot be deduced from a consideration of the resonance energy alone (see also reference [24]).

3.5. Magnetic properties versus the Valence Bond results

Magnetic properties of polycyclic aromatic compounds are frequently used as aromaticity criteria [10,14]. The NICS values calculated at the ring centres for the compounds **1-7** are depicted in Scheme 4. Large negative NICS values are found for the top and bottom six-membered rings. The NICS values for these rings are shifted 10 ppm

upfield with respect to the NICS values of the central six-membered rings, which is in line with the resonance criterion, derived above.

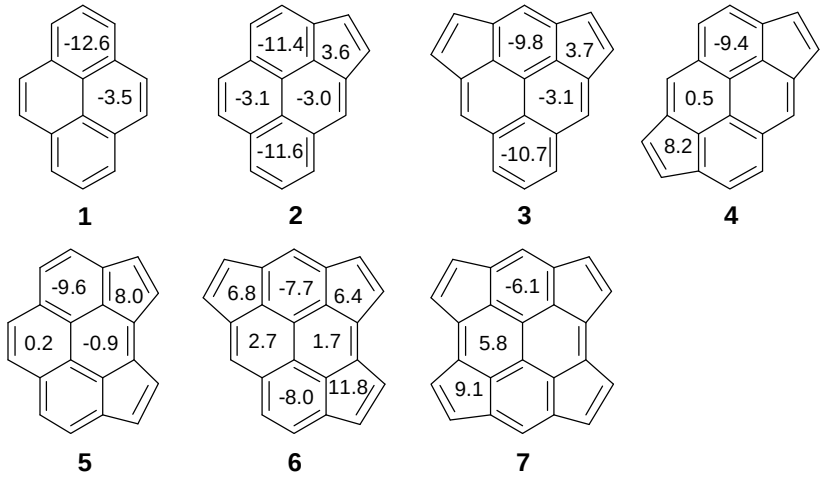

Scheme 4 The NICS values of compounds 1-7 at the ring centres.

Upon the addition of externally fused five-membered rings, the NICS values at the ring centres suggest a reduction of the aromatic character in this series. The resonance criterion (both E_{res} and E^{m}_{res}), however, does not suggest that the aromatic character of **1-7** decreases. To resolve this apparent discrepancy, one should consider the origin of the NICS criterion. Kutzelnigg *et al.* [13] showed that in the case of D_{6h} benzene, the paramagnetic contribution to the out-of-plane component of the magnetic susceptibility due to the π electrons vanishes, if the gauge origin is chosen in the ring centre. This concept was extended and referred to as the Nucleus Independent Chemical Shift (NICS) [14]. The diamagnetic contribution of the chemical shielding tensor perpendicular to the molecular framework ($NICS^{d}_{\perp}$) is indicative for the induced ring currents. For benzene, the NICS and the $NICS^{d}_{\perp}$ are equal. Unfortunately, for systems that do not possess this high symmetry, the paramagnetic contribution does not vanish and $NICS^{d}_{\perp}$ may deviate from the total NICS value. In order to get an estimate of the induced ring current when applying an external magnetic field, the $NICS^{d}_{\perp}$ values should be considered. In addition,

for a meaningful comparison of different $NICS^{d}_{\perp}$ values, the gauge origins should be comparable, as the diamagnetic and paramagnetic contributions are gauge dependent, while the total shielding is not. As a result of the gauge dependence, the meaning of absolute $NICS^{d}_{\perp}$ values has disappeared, and the $NICS^{d}_{\perp}$ values can only be used for comparing the aromatic character of similar rings of different molecules.

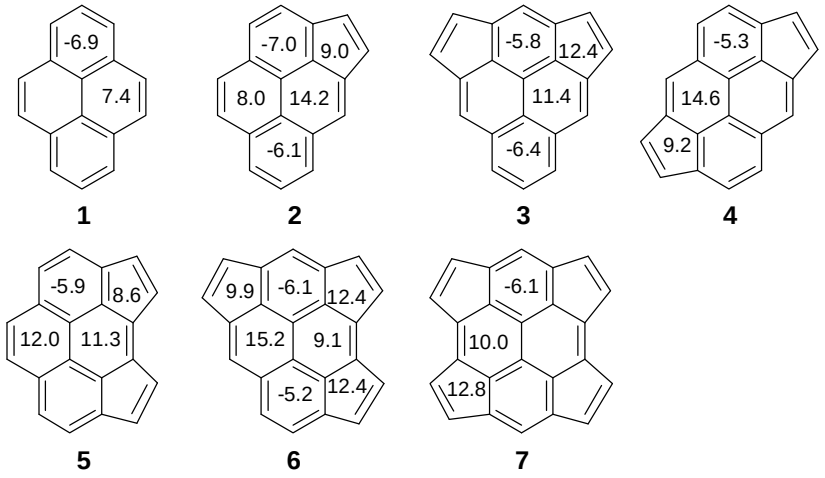

Scheme 5 **The diamagnetic part of the shielding tensor perpendicular to the molecular plane ($NICS^{d}_{\perp}$) of the NICS values of compounds 1-7 calculated at the ring centres. The gauge origins of the localised MO's are chosen as the charge centroids of all drawn bonds. A single line denotes a LMO in the plane of the molecule and a double line denotes two banana bonds, one above and one below the plane of the molecule.**

The IGLO procedure requires localised molecular orbitals (LMO's). These LMO's are indicated by **all** drawn bonds in Scheme 5. The employed localisation procedure allows σ/π mixing, resulting in banana bonds for double bonds. The gauge origins in our IGLO calculations are chosen as the charge centroids of these LMO's. Several subgroups with comparable gauge origins can be identified. The gauge origins for the top and bottom six-membered rings are evenly distributed. The values of the $NICS^{d}_{\perp}$

of these six-membered rings are of equal magnitude (Scheme 5), in line with the resonance criterion. The gauge origins are not comparable for the central six-membered rings and the five-membered rings, as the number of endo-cyclic double bonds, of which the charge centroids are chosen as the gauge origins, is not the same for all rings. The central six-membered rings can be divided into three subgroups and the five-membered rings into two, according to the number of endo-cyclic double bonds. The first subgroup of the central six-membered rings is composed by the right ring of **1**, the left ring of **2**, the right ring of **6** and the left ring of **7**, all containing three endo-cyclic double bonds. The subgroup of two endo-cyclic double bonds contains the right ring of **3** and both central rings of **5**. The last subgroup of one endo-cyclic double bond consists of the right ring of **2** and the left rings of **4** and **6**. In a similar way, the five-membered rings of **2**, **4**, **5** and the left ring of **6** can be grouped together and those of **3** and **7** and the right rings of **6**. The $NICS^{d}_{\perp}$ values of the rings within each subgroup have comparable magnitudes (Scheme 5). From this point of view, the magnetic criteria also suggest that cyclopentafusion does not affect the aromatic character of the pyrene skeleton in line with E_{res} and E^{m}_{res}.

It can therefore be concluded that the diamagnetic part of the chemical shielding tensor of the NICS values perpendicular to the molecular framework is indicative for resonance in a particular ring, but for comparing these values, equivalent gauge origins should be ensured. Hence, a comparison of total NICS values should be cautiously applied.

3.6. The Valence Bond results in relation to the empirical models

Since the contributions to the resonance energy for electron delocalisation around the ring perimeter are negligible, no support for Platt's ring perimeter model [3] is found. For example, the contribution to E^{m}_{res} from resonance between the structures **5A** and **5G** (Schemes 1 and 3) is only -0.16 kcal/mol (Table 5).

The VB calculations show that the Kekulé resonance structures with the maximum number of aromatic sextets have the lowest energy. The resonance interactions

in these sextets have the largest contribution to the resonance energy, in line with Clar's model [4].

The resonance energies obtained for this series using the conjugated circuits model are not in agreement with those obtained from the VB calculations (Table 6). The differences in resonance energy of these compounds are a consequence of the existence of [4n] π electron conjugated circuits, according to the conjugated circuits model. In contrast, the VB calculations show that for all compounds only the pyrene sub-structures are important. Thus the assumption of equal importance of all conjugated circuits leads to substantial errors in the derived resonance energy.

Table 6 **Resonance energy (kcal/mol) of the compounds 1-7 as estimated from the conjugated circuits model.**

Compound	Resonance Energy[a]	Resonance Energy
1	12R(1)+8R(2)+6R(3)/6	-49.95
2	12R(1)+8R(2)+6R(3)/6	-49.95
3	12R(1)+8R(2)+6R(3)/6	-49.95
4	12R(1)+8R(2)+6R(3)+12Q(4)/7	-40.45
5	12R(1)+8R(2)+6R(3)+2Q(3)+8Q(4)+2Q(5)/7	-40.24
6	12R(1)+8R(2)+6R(3)+4Q(3)+20Q(4)+2Q(5)/8	-32.28
7	12R(1)+8R(2)+6R(3)+12Q(3)+28Q(4)+4Q(5)/10	-21.95

[a]R(n) and Q(n) represent [4n+2]-, with n=1,3 and [4n], with n=1,5 π-electron conjugated circuits, respectively. The E_{res} values of R(n) and Q(n) were taken from reference [6] [stabilisation is denoted by a negative contribution to the resonance energy; R(1) -20.04 kcal/mol, R(2) -5.67 kcal/mol; R(3) -2.31 kcal/mol; Q(1) 36.90 kcal/mol; Q(2) 10.38 kcal/mol; Q(3) 3.46 kcal/mol and Q(4) 1.38 kcal/mol. Q(5) is assumed to be 0.00 kcal/mol].

4. Conclusions

VB calculations with the inclusion of all Kekulé resonance structures on the cyclopentafused pyrene derivatives show that cyclopentafusion has only a modest effect on their resonance energies (both E_{res} and E^{m}_{res}), in line with their aromatic stabilisation energies. Only small differences in weights of the pyrene sub-structures are found. The six

π electron (benzene-like) conjugated circuits have the largest contribution to the resonance energy. The contributions to the resonance energy of these six π electron conjugated circuits are of nearly equal magnitude within this series. Cyclopentafusion only affects the energies of the pyrene sub-structures. Kekulé resonance structures in which the five-membered rings participate in π electron delocalisation are unimportant, in line with Clar's model of aromatic hydrocarbons.

Care should be taken in comparing the aromatic character of rings of different molecules by considering the total NICS values. The diamagnetic part of the shielding tensor perpendicular to the molecular framework is nearly constant throughout the series, provided that similar gauge origins are chosen.

References

[1] For example: C. Gooijer, I. Kozin, N.H. Velthorst, M. Sarobe, L.W. Jenneskens and E.J. Vlietstra, *Spectrochim. Acta, Part A*, **54** (1998) 1443 and references cited.

[2] M. Sarobe, Polycyclic aromatic hydrocarbons under high temperature conditions. Consequences for carbon build up during combustion and fullerene formation processes, Ph.D. Thesis, Utrecht University, Utrecht, The Netherlands (1998).

[3] J.R. Platt, *J. Chem. Phys.*, **22** (1954) 1448.

[4] E. Clar, Polycyclic Hydrocarbons, (Academic Press Inc., London, 1964).

[5] M. Randi¶, *Chem. Phys. Lett.*, **38** (1976) 68.

[6] M. Randi¶, *Tetrahedron*, **33** (1977) 1905.

[7] M. Randi¶, *J. Am. Chem. Soc.*, **99** (1977) 444.

[8] W.C. Herndon and M.L.J. Ellzey, *J. Am. Chem. Soc.*, **96** (1974) 6631.

[9] M.J.S. Dewar and C. de Llano, *J. Am. Chem. Soc.*, **91** (1969) 789.

[10] A review of different aromaticity criteria: P. von R. Schleyer and H. Jiao, *Pure & Appl. Chem.*, **68** (1996) 209.

[11] Y. Mo, H. Jiao, Z. Lin and P. von R. Schleyer, *Chem. Phys. Lett.*, **289** (1998) 383.

[12] L. Pauling, *J. Chem. Phys.*, **4** (1936) 673.

[13] U. Fleischer, W. Kutzelnigg, P. Lazzeretti and V. Mühlenkamp, *J. Am. Chem. Soc.*, **116** (1994) 5298.

[14] P. von R. Schleyer, C. Maerker, A. Dransfeld, H. Jiao and N.J.R. van Eikema Hommes, *J. Am. Chem. Soc.*, **118** (1996) 6317.

[15] L. Pauling and G.W. Wheland, *J. Chem. Phys.*, **1** (1933) 362.

[16] R.W.A. Havenith, H. Jiao, L.W. Jenneskens, J.H. van Lenthe, M. Sarobe, P. von R. Schleyer, M. Kataoka, A. Necula and L.T. Scott, *manuscript in preparation* (2000).

[17] M.F. Guest, J.H. van Lenthe, J. Kendrick, K. Schöffel, P. Sherwood and R.J. Harrison, *GAMESS-UK, a package of ab initio programs*, 2000.
With contributions from R.D. Amos, R.J. Buenker, M. Dupuis, N.C. Handy, I.H. Hillier, P.J. Knowles, V. Bonacic-Koutecky, W. von Niessen, V.R. Saunders and A.J. Stone.
It is derived from the original GAMESS code due to M. Dupuis, D. Spangler and J. Wendolowski, *NRCC Software Catalog*, Vol. 1, Program No. QG01 (GAMESS) 1980.

[18] F. Dijkstra and J.H. van Lenthe, *Int. J. Quant. Chem.*, **74** (1999) 213.

[19] J. Verbeek, J.H. Langenberg, C.P. Byrman, F. Dijkstra and J.H. van Lenthe, *TURTLE, an ab initio VB/VBSCF program*, 1988-2000.

[20] L. Pauling, The nature of the chemical bond and the structure of molecules and crystals: An introduction to modern structural chemistry, third ed., (Cornell University Press, Ithaca, New York, 1960).

[21] U. Meier, C. van Wüllen and M. Schindler, *J. Comp. Chem.*, **13** (1992) 551.

[22] P.O. Löwdin, *Rev. Mod. Phys.*, **39** (1967) 259.

[23] C.S. Frampton, K.S. Knight, N. Shankland and K. Shankland, *J. Mol. Struct.*, **520** (2000) 29.

[24] G. Subramanian, P. von R. Schleyer and H. Jiao, *Angew. Chem. Int. Ed. Engl.*, **35** (1996) 2638.

Chapter 9

Dis-rotatory versus con-rotatory electrocyclic ring opening of Dewar benzene. The con-rotatory pathway is preferred and does not involve trans-benzene.[†]

[†] R.W.A. Havenith, L.W. Jenneskens and J.H. van Lenthe, *J. Mol. Struct. (Theochem)*, **492** (1999) 217-224

Abstract: For the electrocyclic ring opening of Dewar benzene (**2**) into benzene (**1**) both a *dis-rotatory* and *con-rotatory* pathway with distinct transition states, **TS1** and **TS2**, respectively, are found at the CASSCF(10,10)/6-311G** level of theory. The importance of the CASSCF(10,10) active space for the proper description of **TS1** and **TS2** is illustrated by similar calculations using a smaller active space, *viz.* CASSCF(2,2), CASSCF(4,4) and CASSCF(6,6). Although **TS2** represents a true saddle point, **TS1** appears to be a higher order saddle point at these levels of theory. Single-point multi-reference SDCI (MRCI) calculations at the CASSCF(10,10)/6-311G** geometries and natural orbitals were performed at all stationary points to obtain more reliable total energies. In contrast to common believe, **TS2** lies below **TS1** (by 6.62 kcal/mol), *i.e.* the *con-rotatory* process is favoured. Moreover, CASSCF(10,10)/6-311G** Intrinsic Reaction Coordinate (IRC) calculations show that upon *con-rotatory* electrocyclic ring opening **2** does not give the extraordinarily strained *trans*-benzene (**3**), *i.e. cis, cis, trans*-cyclohexa-1,3,5-triene. The conversion of **3** into **1** and *vice versa* is a distinct process on the C_6H_6 potential energy surface.

1. Introduction

Among the theoretical concepts, which relate organic reaction mechanisms and stereochemistry that of pericyclic reactions developed by Woodward and Hoffmann has revolutionised chemistry [1-9]. This is illustrated by a quotation from their review: *"…..nor can violations be expected of so fundamental a principle of maximum bonding. All the more is it then important to give consideration to some reactions, which might appear on casual inspection to contravene orbital symmetry conservation.…."* A seminal example of a violation is the isomerisation of Dewar benzene (**2**) to benzene (**1**) [9]. Thermally allowed *con-rotatory* electrocyclic ring opening of **2** was predicted to give the extraordinarily strained *cis, cis, trans*-1,3,5-cyclohexatriene, *viz. trans*-benzene (**3**) [1,5,6,9]. Hence, the thermal stability of **2**, which is *ca.* 70 kcal/mol less stable than **1**, is generally explained by invoking that isomerisation of **2** into **1** has to occur *via* a thermally forbidden *dis-rotatory* pathway.

Recently this view was challenged. In a paper, in which the two modes of electrocyclic ring opening of **2** into **1** were studied at the *ab initio* Generalised Valence Bond level of theory with one pair (GVB) using a 6-31G* basis set [10,11], the commonly accepted C_{2v} transition state for the *dis-rotatory* pathway was found to be a second-order saddle point [two imaginary frequencies (n_{imag}=2); -613.7 and -402.6 cm^{-1}]. Instead a C_s transition state (n_{imag}=1; -486.1 cm^{-1}) positioned 3.7 kcal/mol below the C_{2v} saddle point was identified, as expected for the thermally allowed *con-rotatory* electrocyclic ring opening of **2**! To establish if the *con-rotatory* pathway connects **2** either to **3** [1,5,6,9] or directly to **1**, RHF/3-21G and GVB/3-21G intrinsic reaction coordinate (IRC) calculations were done. Whereas at the RHF/3-21G level **2** converted into **3** and subsequently into **1**, at the GVB/3-21G level **2** gave **1** without the clear-cut intermediacy of **3** [10,11].

To shed light on this important issue we have performed *ab initio* calculations using a 6-311G** [12] basis set and the largest complete active space (CAS) [13] currently computationally feasible to assure that diradical character will be properly accounted for in the case of symmetry-forbidden reactions. To ensure that the conversion from **1** into **2** and possibly that of **2** into **3** [11] are continuously described at the CASSCF

level ten molecular orbitals (MO's) were chosen for the CASSCF active space [CASSCF(10,10)]. In the case of **1** the CASSCF active space comprises the five highest occupied MO's, *i.e.* the $\pi(a_u)$ MO, the two degenerate $\sigma(e_g)$ MO's and the two degenerate $\pi(e_g)$ MO's. Along the reaction pathway connecting **1** and **2** bent benzene analogues are envisaged in which σ MO's and π MO's will mix. Hence, the use of smaller CASSCF active spaces may give erroneous results (*vide infra*).

2. Computational details

Stationary points were identified at the CASSCF(10,10)/6-311G** level (hereafter [CAS]) taking into consideration ten molecular orbitals (MO's) and ten electrons using GAMESS-UK [14]. The ten MO's, *viz.* five from the occupied and five from the virtual space, were chosen to include at least all three occupied π-MO's and two σ-MO's in the case of **1**. Subsequently, single-point multi-reference SDCI (MRCI) [15,16] calculations at the CASSCF(10,10)/6-311G** geometries and natural orbitals (hereafter [+MRCI]) were performed to include dynamical correlation energy and, hence, to obtain more reliable total energies. In the [+MRCI] calculations all valence electrons are active in the CI space and all doubly excited CASSCF configurations are taken as references. The single-point [+MRCI] total energies are corrected for size consistency errors by the Davidson method [17,18].

The CASSCF(10,10)/6-311G** transition states **TS1** and **TS2** for the *dis-rotatory* and *con-rotatory* electrocyclic ring opening of **2** into **1**, respectively, were also located at the CASSCF(2,2)/-, CASSCF(4,4)/- and CASSCF(6,6)/6-311G** level of theory in order to verify if **TS1** and **TS2** are true transition states upon use of a smaller CASSCF active space.

Magnetic susceptibilities (χ), absolute shieldings (σ) and Nucleus Independent Chemical Shifts (NICS) [19] for **1** and **3** were calculated at the CASSCF(10,10)/6-311G** geometries using the Direct IGLO method [20] and the IGLO III basis set [21].

3. Results and discussion

3.1. The CASSCF active space

Although for a proper description of the *dis-rotatory* electrocyclic ring opening of **2** into **1** a CASSCF(2,2) active space should suffice, it was shown in the original paper that at the GVB/6-31G*, *i.e.* CASSCF(2,2)/6-31G*, level of theory the C_{2v} transition state (**TS1**) represents a higher order saddle point (n_{imag}=2) whereas the *con-rotatory* transition state (C_s, **TS2**) was a true saddle point (n_{imag}=1) [11]! Therefore, we were prompted to study the character of **TS1** and **TS2** as a function of the size of the CASSCF active space. To this end **TS1** and **TS2** were located with a CASSCF(2,2), CASSCF(4,4), CASSCF(6,6) and CASSCF(10,10) active space using the 6-311G** basis set. The *con-rotatory* (C_s, **TS2**) transition state was found to be a true saddle point (n_{imag}=1) at all these levels of theory. In line with the CASSCF(2,2)/6-31G* results [11], the *dis-rotatory* (C_{2v}, **TS1**) transition state proved to be a higher order saddle point at the CASSCF(2,2)/- and CASSCF(4,4)/6-311G** levels of theory with n_{imag}=2 and n_{imag}=2, respectively. It is noteworthy, that at the CASSCF(6,6)/6-311G** level of theory, a symmetry broken solution exists (C_{2v} to C_1) for **TS1**. This indicates that a CASSCF(6,6) wave function is insufficient for the description of this saddle point. As will be discussed in detail below, true transition states were readily located at the CASSCF(10,10)/6-311G** [CAS] level of theory for the *dis-rotatory* (C_{2v}, **TS1**) and *con-rotatory* (C_s, **TS2**) electrocyclic ring opening of **2** into **1**. This underlines the importance of the size of the active space for a proper description of the interconversion of **2** into **1** and *vice versa*.

*3.2. Benzene (**1**), Dewar benzene (**2**) and trans-benzene (**3**)*

The [CAS] geometries of **1** and **2** are presented in Figure 1 (see Table 1 for [CAS] and [+MRCI] total energies). It is noteworthy that [CAS] **1** calculated in D_{6h} symmetry possesses three imaginary frequencies (n_{imag}=3), which upon symmetry breaking from D_{6h} to D_{2h} disappear (n_{imag}=0). Notwithstanding, the [+MRCI] energy

difference between D_{6h} **1** and D_{2h} **1** is only 0.00007 a.u., *viz.* 0.04 kcal/mol. For **1** an active space of ten MO's is clearly not well balanced! This exemplifies the problem of describing a potential energy surface with one CASSCF active space. It is substantiated by a CASSCF(6,6)/6-311G** calculation of D_{6h} **1** in which only π MO's are in the active space (n_{imag}=0). Notwithstanding, the [CAS] geometry of **1** is only slightly affected by this artificial symmetry breaking. Carbon-carbon bond length differences of 0.02 Å are found (1.39 Å *vs.* 1.41 Å), while the valence angles deviate only *ca.* 0.5° from the ideal 120° (Figure 1).

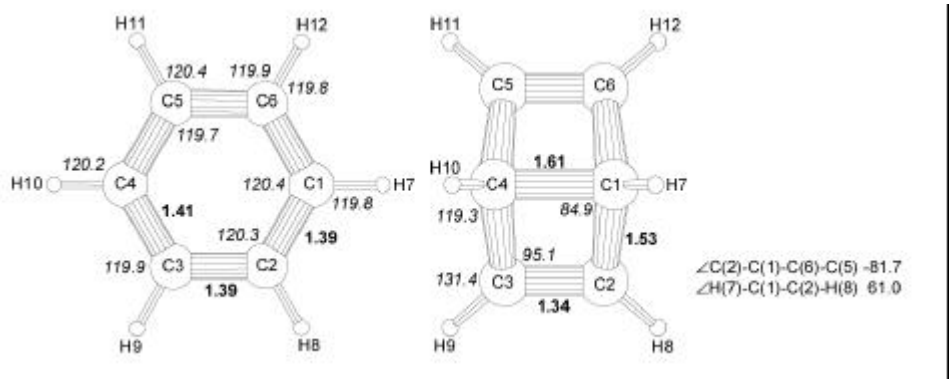

Figure 1 **[CAS] structures of benzene (1, D_{2h}) and Dewar benzene (2, C_{2v}) (bond lengths in Å, valence and dihedral angles in °).**

With the exception of the sp^3-sp^3 carbon-carbon single bond length C(1)-C(4), which is calculated to be *ca.* 0.04 Å longer, the [CAS] geometry of C_{2v} **2** is in good agreement with experimental data obtained by electron diffraction [22]. Furthermore in line with expectation [10,11,23-25], **2** is 76.36 kcal/mol ([+MRCI]) less stable than **1**.

According to the Woodward and Hoffmann rules [1,5,6,9] *con-rotatory* electrocyclic ring opening of **2** gives the highly strained *trans*-benzene (**3**) as the initial product. The latter, due to its strained character is expected to isomerise to **1** by π-bond rotation [10,11]. Hence, **3** was located at the [CAS] level of theory. Compound **3** (C_2 symmetry) was identified as a [CAS] local minimum and shown to be positioned 22.94 kcal/mol and 99.30 kcal/mol ([+MRCI]) above **2** and **1**, respectively (Table 1). In line

with available data [11], considerable bond length alternation is found in its carbon framework; for the sp^2-sp^2 carbon-carbon single bonds values of 1.50 Å [C(1)-C(2)] and 1.49 Å [C(3)-C(4) and C(5)-C(6)], and for the sp^2-sp^2 carbon-carbon *cis*-double bonds [C(1)-C(6) and C(2)-C(3)] a value of 1.36 Å was found. In contrast the carbon-carbon *trans*-double bond [C(4)-C(5)] is considerably longer, *viz.* 1.41 Å. The dihedral angle H(10)-C(4)-C(5)-H(11) is -179.0°, *i.e.* H(10) and H(11) of the *trans*-double bond C(4)-C(5) are close to *anti-periplanar* (Figure 2). According to the [+MRCI] natural orbital occupations of 1.83 and 0.16 electrons found for **3**, it represents a closed shell species despite its strained character.

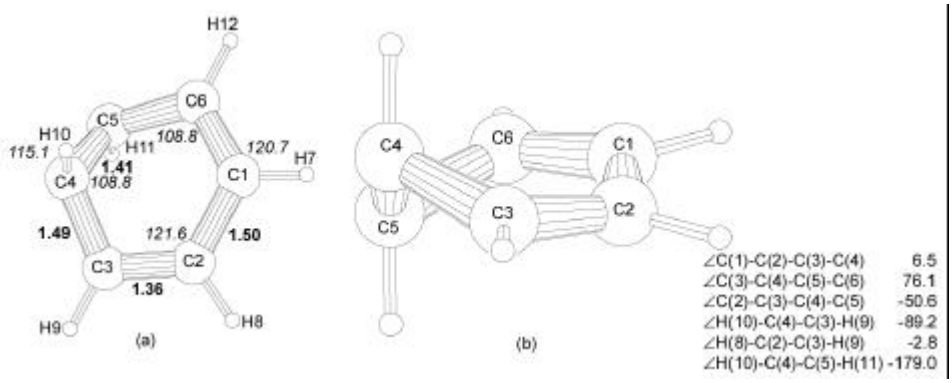

Figure 2 **[CAS] structure of *cis, cis, trans*-1,3,5-cyclohexatriene (3, C_2) (bond lengths in Å, valence and dihedral angles in °). a) top view; b) side view.**

Since benzene (**1**) represents the archetypal aromatic compound possessing a ring current, it is of interest to compare the magnetic properties of **1** with those of **3**. Recently, it was proposed that the Nucleus Independent Chemical Shifts (NICS) [19] at the ring centre and 0.5 Å above the plane are valuable probes for aromaticity. IGLO calculations [IGLO/basis III//CASSCF(10,10)/6-311G**] [21] revealed that **1** and **3** have markedly different magnetic properties. The calculated magnetic susceptibilities (χ) suggest that **3**, in contrast to **1**, does not possess a ring current [χ: **1**, *out-of-plane* component χ_{zz} -107.5 (exp. -94.6 [21]) and *average in-plane* component $\chi_{ip}=1/2(\chi_{xx}+\chi_{yy})$ -39.2 (exp. -34.9 [21]) ppm cgs and **3**, *out-of-plane* component χ_{zz} -49.6 and *average in-plane* component

$\chi_{ip}=1/2(\chi_{xx}+\chi_{yy})$ -33.6 ppm cgs] [21], and is thus non-aromatic. This is further corroborated by the NICS [19] values calculated [IGLO/basis III//CASSCF(10,10)/6-311G**] [21] at the ring centres of **1** (NICS -9.9, *aromatic*) and **3** (NICS -0.9, *non-aromatic*). The NICS values 0.5 Å above the plane leads to a similar conclusion (**1** NICS -11.5, *aromatic* and **3** NICS -2.0, *non-aromatic*).

*3.3. Isomerisation of trans-benzene (**3**) into benzene (**1**)*

For the isomerisation of **3** into **1** a [CAS] transition state (**TS3**; C_2 symmetry) which corresponds to π-bond rotation [11] along C(4)-C(5) could be located. In going from **3** to **TS3**, the bond length of the *trans*-double bond [C(4)-C(5)] increases from 1.41 Å to 1.49 Å and the dihedral angle H(10)-C(4)-C(5)-H(11) changes from -179.0° into 147.9° (Figures 2 and 3). An [+MRCI] activation barrier of 8.03 kcal/mol was found (Table 1), which is higher than the CASSCF(6,6)/6-31G* estimate (2.95 kcal/mol) [11], but lower than the related barrier for the isomerisation of *trans*- to *cis*-cyclohexene (range 10-15 kcal/mol [18,26]). Since upon π-bond rotation the HOMO and LUMO interchange, **TS3** is expected to possess diradical character. Indeed, [+MRCI] natural orbital occupations of 1.29 and 0.70 electrons were found.

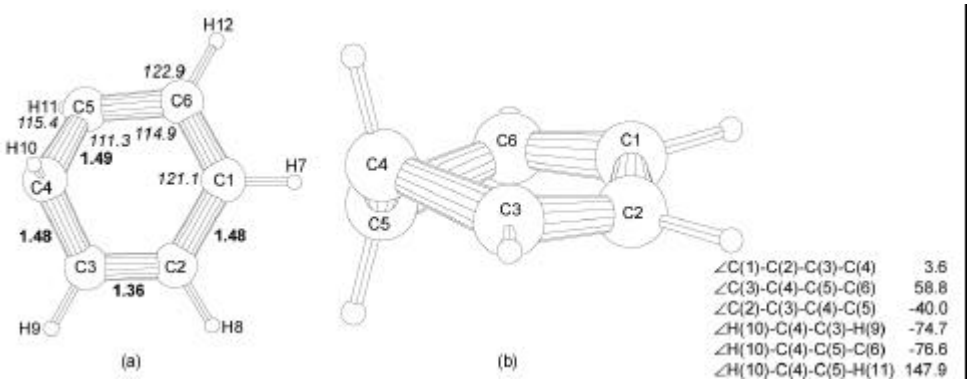

Figure 3 **[CAS] structure of the transition state connecting *cis, cis, trans*-1,3,5-cyclohexatriene and benzene (TS3, C_2) (bond lengths in Å, valence and dihedral angles in °). a) top view; b) side view.**

Table 1 **[CAS] and [+MRCI] total energies and [+MRCI] energy differences (ΔE) for the *dis*-rotatory and *con*-rotatory electrocyclic ring opening, respectively, of 2, and the π-bond rotation of 3 to 1.**

Compounds (point group)	[CAS][a]	n_{imag}[b]	[+MRCI][a]	ΔE[c]
Minima				
benzene (**1**, D_{2h})[d]	-230.878640997	0	-231.590344665	0.00
Dewar benzene (**2**, C_{2v})	-230.717796389	0	-231.468665814	76.36
trans-benzene (**3**, C_2)	-230.707764963	0	-231.432103408	99.30
Transition states				
dis-rotatory **TS1** (C_{2v})[e]	-230.671378734	1 (-633)	-231.406164496	115.58
con-rotatory **TS2** (C_s)	-230.699415546	1 (-530)	-231.416716700	108.96
p-bond rotation **TS3** (C_2)	-230.699597450	1 (-606)	-231.419307232	107.33
IRC point (C_s)[f]				
H(10)-C(4)-C(5)-H(11) 122.1°	-230.705304129	1 (-105)	-231.419537430	107.18

[a][CAS] and [+MRCI] total energies (in a.u.) are uncorrected for zero-point motion (see Text). [b]n_{imag}; number of imaginary frequencies (values in cm^{-1} between parentheses). [c]ΔE; relative [+MRCI] energies (in kcal/mol) with respect to **1**. [d]See Text. [e]For **TS1** symmetry-breaking from C_{2v} (n_{imag}=1; -633 cm^{-1}) to C_2 (n_{imag}=1; -641 cm^{-1}) occurs at the [CAS] level. However, their [+MRCI] energy difference is only 0.0013 a.u., *viz.* 0.82 kcal/mol (see Text for [CAS] D_{6h} **1**)[d]. [f][+MRCI]; natural orbital occupations, 1.60 and 0.39; See also Text.

*3.4. Dis-rotatory versus con-rotatory electrocyclic ring opening of Dewar benzene (**2**) into benzene (**1**)*

At variance with the previous GVB/6-31G* results, which gave for the *dis-rotatory* pathway a C_{2v} second-order saddle point [11], a proper [CAS] C_{2v} transition state [**TS1**; n_{imag}=1, -633 cm^{-1} (Figure 4, Table 1 and section "The CASSCF active space") could be located. In agreement with its symmetry-forbidden character [1,5,6,9], **TS1** possesses diradical character ([+MRCI]; natural orbital populations, 1.40 and 0.51 electrons). From consideration of the symmetries of the CASSCF MO's, it follows that

the orbital crossing occurs after the transition state **TS1** is passed [10]. The imaginary frequency corresponds to a *dis-rotatory* electrocyclic ring opening; **TS1** connects **2** to **1** with an [+MRCI] activation barrier of 39.22 kcal/mol [Table 1; experiment: range 25-36 kcal/mol [23-25]].

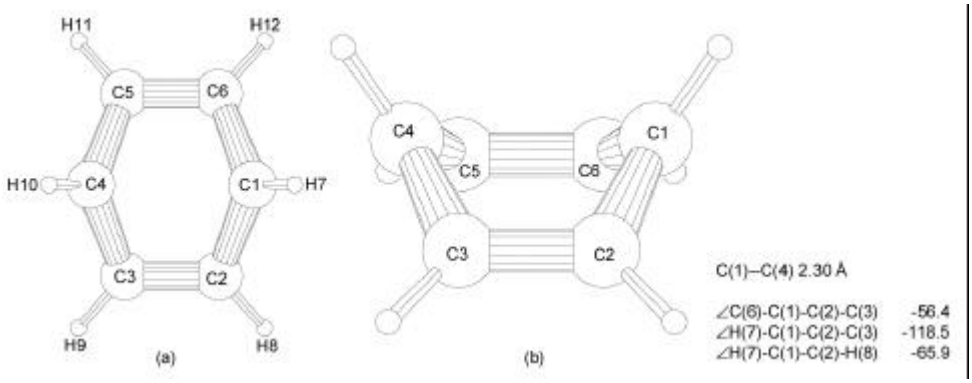

Figure 4 **[CAS] structure of the transition state for the *dis*-rotatory electrocyclic ring opening of Dewar benzene (TS1, C_{2v}) (bond lengths in Å, valence and dihedral angles in °). a) top view; b) side view.**

Subsequently, the [CAS] transition state for *con-rotatory* electrocyclic ring opening of **2** was located. A proper C_s transition state (**TS2**; n_{imag}=1; -530 cm^{-1}) was found positioned 32.60 kcal/mol [+MRCI] above **2**, but 6.62 kcal/mol [+MRCI] below **TS1** (Figure 5 and Table 1). Moreover, the [+MRCI] natural orbital occupations of 1.78 and 0.21 electrons indicate that **TS2** is a closed shell species. In analogy to **TS1**, also in the case of **TS2** orbital crossing takes place after the transition state is passed. Its imaginary frequency corresponds to the *con-rotatory* movement of H(7) and H(10); C(1) and C(4) move into the direction of the plane determined by C(2), C(3), C(5) and C(6).

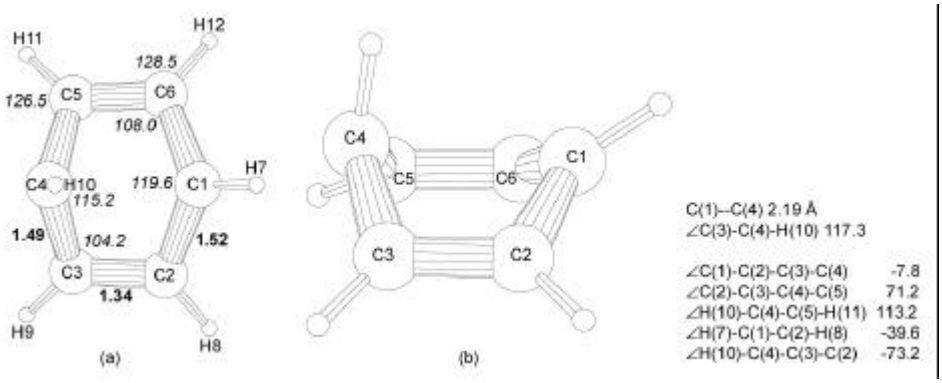

Figure 5 **[CAS] structure of the transition state for the con-rotatory electrocyclic ring opening of Dewar benzene (TS2, C_s) (bond lengths in Å, valence and dihedral angles in °). a) top view; b) side view.**

To determine if **TS2** connects either **2** to **3** or **2** directly to **1**, [CAS] IRC calculations were performed; the change of the dihedral angle H(10)-C(4)-C(5)-H(11) was followed. If **TS2** with H(10)-C(4)-C(5)-H(11) 113.2° goes to **3**, this dihedral angle has to change into -179.0° (Figure 2). However, without symmetry-breaking from C_s to C_2, H(10)-C(4)-C(5)-H(11) increases from 113.2° to 122.1° and, subsequently, smoothly decreases to 0°, *i.e.* **TS2** connects **2** directly to **1**! This is supported by an analysis of the force matrix at the IRC point with H(10)-C(4)-C(5)-H(11)=122.1° {[+MRCI] energy positioned 7.88 kcal/mol above **3** and 0.15 kcal/mol below **TS3** (Figure 6 and Table 1)}. One imaginary frequency (n_{imag}=1; -105 cm^{-1}) is found, which corresponds to the movement of C(1) and C(4) towards the plane determined by C(2), C(3), C(5) and C(6). The movement of H(7) and H(10), *viz.* the change of dihedral angle H(10)-C(4)-C(5)-H(11), required for the conversion of **TS2** to **3** corresponds to a positive vibration (382 cm^{-1}) and thus represents an energetically uphill process.

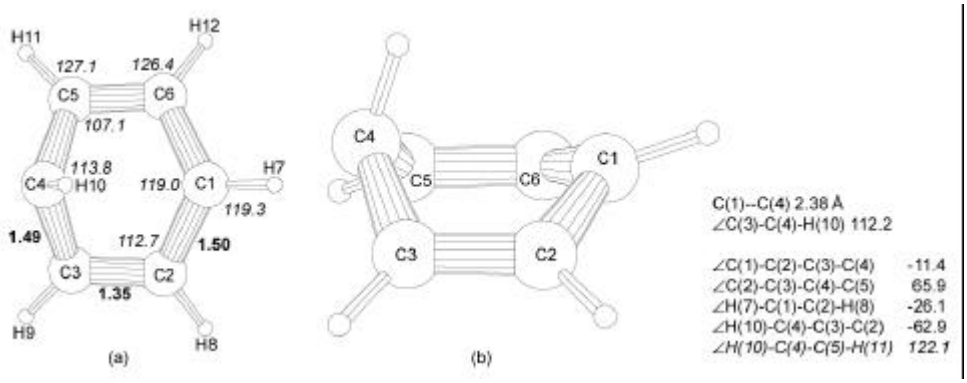

Figure 6 **[CAS] structure of the IRC point (C_s) with dihedral angle H(10)-C(4)-C(5)-H(11) 122.1° (bond lengths in Å and valence and dihedral angles in °). a) top view; b) side view.**

4. Conclusions

For the electrocyclic ring opening of **2** both *dis-rotatory* and *con-rotatory* pathways with distinct transition states **TS1** and **TS2**, respectively, are accessible at the CASSCF(10,10)/6-311G** [CAS] level of theory. The importance of the size of the CASSCF active space with regard to the proper description of especially **TS1** and **TS2** is illustrated by the systematic evaluation of the character of **TS1** and **TS2** located with CASSCF(2,2), CASSCF(4,4), CASSCF(6,6) and CASSCF(10,10) active spaces, respectively. With these smaller active spaces **TS2** represents a true saddle point, whereas **TS1** is calculated to be a higher order saddle point. In contrast to common believe, the *con-rotatory* pathway is favoured, *i.e.* **TS2** lies 6.62 kcal/mol ([+MRCI]) below **TS1**. Moreover, IRC calculations show that *con-rotatory* electrocyclic ring opening converts **2** directly into **1**. Consequently, the conversion of **3** into **1** represents a distinct process on the C_6H_6 potential energy surface.

Acknowledgements

Partial financial support from NCF and Cray Research Inc. for R.W.A. Havenith (NCF grant CRG 96.18) and the gift of a copy of the direct SCF version of IGLO (DIGLO) by Dr. U. Fleischer (Ruhr-Universität Bochum, Germany) are gratefully acknowledged.

References

[1] T.L. Gilchrist and R.C. Storr, Organic reactions and orbital symmetry, (Cambridge University Press, Cambridge, 1979).

[2] R. Hoffmann and R.B. Woodward, *J. Am. Chem. Soc.*, **87** (1965) 2046.

[3] R. Hoffmann and R.B. Woodward, *J. Am. Chem. Soc.*, **87** (1965) 4388.

[4] R. Hoffmann and R.B. Woodward, *J. Am. Chem. Soc.*, **87** (1965) 4389.

[5] K.N. Houk, Y. Li and J.D. Evanseck, *Angew. Chem. Int. ed. Engl.*, **31** (1992) 682.

[6] K.N. Houk, Y. Li and J.D. Evanseck, *Angew. Chem.*, **104** (1992) 711.

[7] R.B. Woodward and R. Hoffmann, *J. Am. Chem. Soc.*, **87** (1965) 395.

[8] R.B. Woodward and R. Hoffmann, *J. Am. Chem. Soc.*, **87** (1965) 2511.

[9] R.B. Woodward and R. Hoffmann, The conservation of orbital symmetry, (Verlag Chemie GmbH, Academic Press Inc., New York USA, 1971).

[10] M.J.S. Dewar, G.P. Ford and H.S. Rzepa, *J. Chem. Soc., Chem. Commun.*, (1977) 728.

[11] R.P. Johnson and K.J. Daoust, *J. Am. Chem. Soc.*, **118** (1996) 7381.

[12] R. Krishnan, J.S. Binkley, R. Seeger and J.A. Pople, *J. Chem. Phys.*, **72** (1980) 650.

[13] B.O. Roos, Ab initio methods in quantum chemistry, Part II, (John Wiley & Sons Ltd., Chichester, UK; pp. 399-445, 1987).

[14] M.F. Guest, J.H. van Lenthe, J. Kendrick, K. Schöffel, P. Sherwood and R.J. Harrison, *GAMESS-UK, a Package of Ab Initio Programs*, 1998.
With contributions from R.D. Amos, R.J. Buenker, M. Dupuis, N.C. Handy, I.H. Hillier, P.J. Knowles, V. Bonacic-Koutecky, W. von Niessen, V.R. Saunders and A.J. Stone.

It is derived from the original GAMESS code due to M. Dupuis, D. Spangler and J. Wendolowski, *NRCC Software Catalog*, Vol. 1, Program No. QG01 (GAMESS) 1980.

[15] P.E.M. Siegbahn, *J. Chem. Phys.*, **72** (1980) 1647.

[16] V.R. Saunders and J.H. van Lenthe, *Mol. Phys.*, **48** (1983) 923.

[17] S.R. Langhoff and E.R. Davidson, *Int. J. Quant. Chem.*, **8** (1974) 61.

[18] J. Verbeek, J.H. van Lenthe, P.J.J.A. Timmermans, A. Mackor and P.H.M. Budzelaar, *J. Org. Chem.*, **52** (1987) 2295.

[19] P. von R. Schleyer, C. Maerker, A. Dransfeld, H. Jiao and N.J.R. van Eikema Hommes, *J. Am. Chem. Soc.*, **118** (1996) 6317.

[20] U. Meier, C. van Wüllen and M. Schindler, *J. Comp. Chem.*, **13** (1992) 551.

[21] U. Fleischer, W. Kutzelnigg, P. Lazzeretti and V. Mühlenkamp, *J. Am. Chem. Soc.*, **116** (1994) 5298.

[22] E.A. McNeill and F.R. Scholer, *J. Mol. Struct.*, **31** (1976) 65.

[23] R. Breslow, J. Napierski and A.H. Schmidt, *J. Am. Chem. Soc.*, **94** (1972) 5906.

[24] J.F.M. Oth, *Recl. Trav. Chim. Pays-Bas*, **87** (1968) 1185.

[25] H.C. Volger and H. Hoogeveen, *Recl. Trav. Chim. Pays-Bas*, **86** (1967) 830.

[26] R.P. Johnson and K.J. DiRico, *J. Org. Chem.*, **60** (1995) 1074.

Chapter 10

Notes and outlook

1. The predictive power of *ab initio* theory

In the previous chapters, various predictions have been put forward about the properties and reactivity of molecules. In the mean time, experiments have been conducted to verify these predictions. In this chapter, these recent results are summarised and compared to the predictions done in the preceding chapters.

1.1. The UV spectra of anti- and syn-4,4'-di-tert-butyl-bicyclohexylidene

In chapter 5, the UV spectrum of *syn*-1,1'-bicyclohexylidene (*syn*-**1a**) is predicted to be different from that of *anti*-1,1'-bicyclohexylidene (*anti*-**1b**). It is argued that the origin of their different spectroscopic properties must be found in the differences between the unoccupied molecular orbitals. The occupied molecular orbitals of both compounds are similar, so we expect the same PES data and different UV spectra.

Anti- (*anti*-**2a**) and *syn*-4,4'-di-*tert*-butyl-bicyclohexylidene (*syn*-**2b**) have been synthesised, according to literature procedures [1], and their PES and UV spectrum have been recorded. The PES spectrum of the *anti* and *syn* conformer (shown in Figure 1) are indeed identical [2]. Their UV spectra (solvent *n*-hexane), shown in Figure 2, are markedly different. For *anti*-4,4'-di-*tert*-butyl-bicyclohexylidene (*anti*-**2a**), two bands are observed at 217.5 nm (5.7 eV) and 193.7 nm (6.4 eV), while for the *syn*-conformer (*syn*-**2b**) only one band is observed at 210.1 nm (5.9 eV), in accordance with the *ab initio* MRDCI calculations. The calculated oscillator strengths are not expected to be in accord with the experimental ones, as only a modest 6-31G basis set was used in the calculations. It should be noted that the observation of the high-energy (low wavelength) absorptions is on the borderline of the possibilities, *i.e.* the solvent also absorbs in this region. Therefore, it is desirable that the gas-phase UV spectra using EELS (see for example [3]) should be recorded for these compounds.

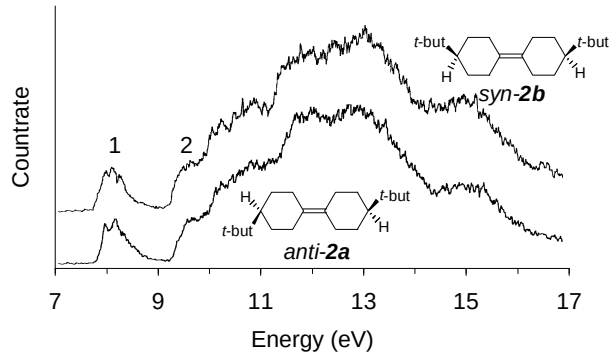

Figure 1 **The PES spectra of *anti*- and *syn*-4,4'-di-*tert*-butyl-bicyclohexylidene [2].**

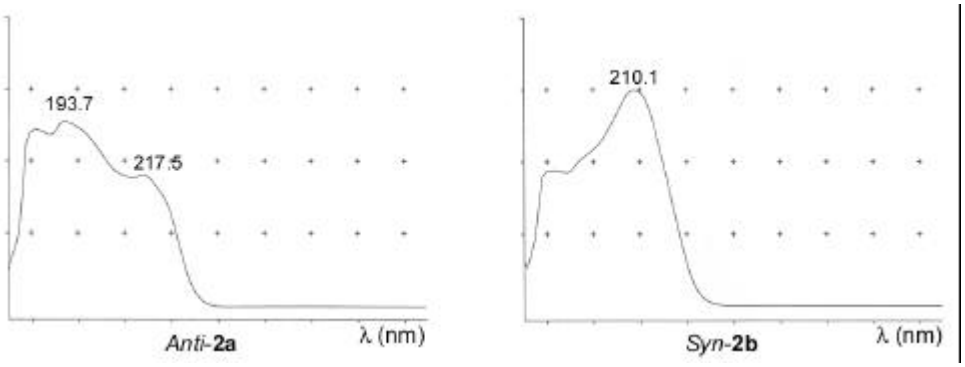

Figure 2 **The UV solution spectra of *anti*- (*anti*-2a) and *syn*4,4'-di-*tert*-butyl-bicyclohexylidene (*syn*-2b, solvent: *n*-hexane).**

1.2. Is trans-benzene a Möbius benzene?

According to the results, described in chapter 9, the unknown *cis, cis, trans*-1,3,5-cyclohexatriene (*trans*-benzene, **3**, see Figure 2 of Chapter 9) is a stationary point at the C_6H_6 potential energy surface. It was often suggested that *trans*-benzene has the topology of a Möbius benzene [4-6], since its p-orbitals are rotated with respect to each other in the Heilbronner sense [7]. However, both the magnetic properties (NICS -0.9, see Chapter 9) and the π molecular orbital topology of *trans*-benzene (butadiene-like and a

distorted ethene-like π bond) indicate that *trans*-benzene does not represent a Möbius benzene [8].

1.3. The electrocyclic ring opening of 1-chlorobicyclo[2.2.0]hexadiene and 1,4-dichlorobicyclo[2.2.0]hexadiene

In chapter 9, the results of our calculations reveal that the thermal electrocyclic ring opening of Dewar benzene can proceed *via* both the *dis-rotatory* (**TS1**) and the *con-rotatory* transition state **TS2**, in contrast to previous contentions based upon the Woodward and Hoffmann rules [9]. The *con-rotatory* transition state (**TS2**) lies 6.6 kcal/mol below the *dis-rotatory* transition state (**TS1**), and will thus be preferred. The accessibility of two distinct reaction pathways suggests that the substitution pattern at the carbon atoms C(1) and C(4) of Dewar benzene (see Figure 1 of Chapter 9) can affect the reaction path and thus the reaction kinetics. Indeed a large difference in reaction kinetics has been found for electrocyclic ring opening of 1-chlorobicyclo[2.2.0]hexadiene (**4**) and 1,4-dichlorobicyclo[2.2.0]hexadiene (**5**) [10]. Whereas compound **4** rearranges at room temperature, compound **5** requires heating. For **4** and **5** an activation enthalpy of 19.1 kcal/mol and 30.5 kcal/mol, respectively, is found. This difference could not be explained if only the *dis*-rotatory pathway is operational.

Calculations at the MRCI/6-311G**//CASSCF(6,6)/6-311G** level of theory show that **4** follows a *con-rotatory* pathway (*via* **TS4**, n_{imag}=1, -406.0 cm^{-1}, see Figure 3), while **5** follows the *dis-rotatory* (*via* **TS5**, n_{imag}=1, -673.0 cm^{-1}, see Figure 3) pathway [11] (see Scheme 1). No *dis-rotatory* transition state could be located for **4** and no *con-rotatory* transition state exists for **5**. Hence, these calculations indeed strongly suggest that the substitution pattern of the C(1)-C(4) bond markedly affects the reaction coordinate.

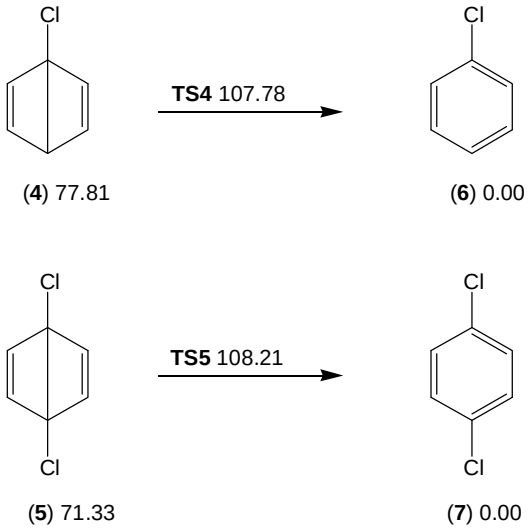

Scheme 1 **The relative energies (kcal/mol) of the electrocyclic ring opening reactions of 1-chlorobicyclo[2.2.0]hexadiene (4) and 1,4-dichlorobicyclo[2.2.0]hexadiene (5).**

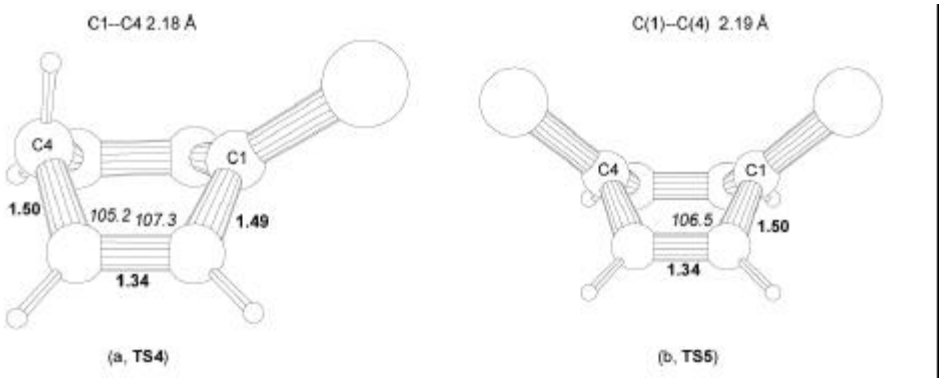

Figure 3 **The transition states for the ring opening of the chloro substituted Dewar benzenes. (a) the *con-rotatory* TS4, connecting 4 with monochlorobenzene, (b) the *dis-rotatory* TS5, connecting 5 with 1,4-dichlorobenzene.**

The activation energy for the conversion of **4** into 1-chlorobenzene (calculated 29.97 kcal/mol, see Scheme 1; experimental 19.1 kcal/mol [10]) is indeed lower than that

for Dewar benzene into benzene (calculated 32.60 kcal/mol, see Table 1, Chapter 9; experimental 23.0 kcal/mol [10]). A Mulliken population analysis shows that no radical charge redistribution occurs upon the introduction of the chloro-atom. Thus, mixing with a charge-transfer state, as suggested earlier [10], to stabilise **TS4** does not occur. In addition, the C(1)-C(4) distance is not affected by chloro-substitution (see Figure 5 of Chapter 9), and **TS4** possesses the same biradical character as **TS2** according to the natural orbital populations (**TS4**: 1.73 and 0.26 electrons; **TS2**: 1.78 and 0.21 electrons).

For **TS5**, the C(1)-C(4) distance (2.19 Å) is shortened compared to that of **TS1** (2.30 Å, see Figure 4 of Chapter 9). Similar to **TS1**, **TS5** possesses biradical character, *viz.* **TS5** has natural orbital occupations of 1.50 and 0.49. The activation energy is 36.88 kcal/mol. This calculated value of the activation energy is 6.91 kcal/mol higher than that found for the reaction of **4**, in reasonable agreement with the experimental value of 11.4 kcal/mol [10]. Hence, the difference in reaction kinetics presumably originates from the difference in reaction path.

2. Outlook

The examples in the previous section, where some of the predictions, made in this thesis, were verified, further show that *ab initio* theory is indeed a valuable and reliable tool for the survey of ground- and excited states of large organic molecules and of potential energy surfaces. This thesis shows that the application of quantum chemistry in organic chemistry has a promising future; real problems, originating in the laboratory, can be solved or rationalised by calculations if performed at an adequate level.

The development of applied quantum chemistry in organic chemistry is dependent on the computer technology. Until recently, the computer industry focused on the speed of individual CPU's. Currently, there is a shift towards the development of large massively parallel machines with huge amounts of memory and disk space. Hence, methods that can easily be parallelised, are the methods of the future. Examples of these methods are Hartree-Fock, DFT, CCSD(T) and valence bond methods. Probably Hartree-Fock will not be the most frequently used method in the future; Hartree-Fock theory

neglects electron correlation. Geometry optimisations will be carried out using DFT methods; CCSD(T) calculations will be performed for getting reliable estimates of the energy. CCSD(T) calculations will also be used for the calculation of (response) properties of molecules. The huge amounts of available memory and disk space make the use of sufficiently large basis sets for chemical accuracy (±1 kcal/mol) possible.

Valence bond theory will gain in popularity, as chemists are attracted to the easy interpretability of the results. VB calculations on moderately sized molecules, not only molecules with π systems, can be performed in reasonable amounts of time on massive parallel machines. The inclusion of electron correlation, by for example the use of correlated structures, will turn this qualitative model into a quantitative one.

However, before we will reach Utopia, a lot of difficulties have to be solved. For example, DFT methods currently tend to prefer delocalised structures. This preference leads to substantial errors in the prediction of for example the energy difference between $C_{10}H_{10}$ isomers [12]. Particularly poor is the qualitatively wrong description of the potential energy curve for the dissociation of radical cations by DFT [13-16]. For example the reaction product of the dissociation of $H_3N\text{-}NH_3^+$ is according to DFT $2NH_3^{0.5+}$ instead of NH_3 and NH_3^+. A qualitatively correct description for this dissociation process is obtained when the exact, *i.e.* Hartree-Fock exchange is used. Thus, the current exchange functionals are far from the exact ones. Unfortunately, it still appears to be very difficult to correct this problem.

For the description of excited states, DFT also seems to work satisfactorily, as long as the transitions do not possess charge transfer character [17]. Probably this error is related to the qualitatively wrong description of potential energy surfaces of radical cations. Hence, DFT should be applied with caution for the calculation of many excited state properties and geometries. Thus CI (both non-selected and selected) and CASPT2 methods still have their place. To keep control over the number of configurations in the CI calculations on systems with a large number of electrons and molecular orbitals, methods should be developed which are able to freeze unimportant orbitals. One can think of a localisation of the orbitals and freeze the orbitals, not relevant for the calculation.

Already a parallel version of the DIESEL-CI program [18] exists. Test calculations on 1,4-dimethylidene-cyclohexane (12 099 236 configuration state functions) show that this program scales reasonably well with an increasing number of processors. The test calculations were performed on an Origin 2000 machine (128 300 MHz R12K CPU's (600 Mflop/s) and 65 GB memory) which is located at SARA at Amsterdam. The wall-time of the two CPU calculation was 151 356 s, while the four CPU calculation took 79 446 s. Thus 97.4% of the code is parallelised, leading to a maximum speed-up for this job by a factor of 39. Hence, only *ca.* 32 CPU's can effectively be used. Thus *e.g.* MRDCI calculations can easily be performed on large molecules (*ca.* 500 orbitals) and on parallel machines. However, before these calculations use all CPU's of the new supercomputer (1024 R14K CPU's [1000 Mflop/s]), a lot of programming has still to be done.

References

[1] R.M. Kellogg, M. Noteboom and J.K. Kaiser, *Tetrahedron*, **32** (1976) 1641.

[2] A.W. Marsman, R.W.A. Havenith, S. Bethke, L.W. Jenneskens, R. Gleiter, J.H. van Lenthe, M. Lutz and A.L. Spek, *J. Org. Chem.*, **65** (2000) 4584.

[3] C. Bulliard, M. Allan, J.M. Smith, D.A. Hrovart, W. Thatcher Borden and S. Grimme, *Chem. Phys.*, **225** (1997) 153.

[4] E. Farenhorst, *Tetrahedron Lett.*, **52** (1966) 6465.

[5] J.J.C. Mulder, *J. Am. Chem. Soc.*, **99** (1977) 5177.

[6] R.P. Johnson and K.J. Daoust, *J. Am. Chem. Soc.*, **118** (1996) 7381.

[7] E. Heilbronner, *Tetrahedron Lett.*, (1964) 1923.

[8] R.W.A. Havenith, J.H. van Lenthe and L.W. Jenneskens, *to be submitted* (2000).

[9] R.B. Woodward and R. Hoffmann, The conservation of orbital symmetry, (Verlag Chemie GmbH, Academic Press Inc., New York USA, 1971).

[10] R. Breslow, J. Napierski and A.H. Schmidt, *J. Am. Chem. Soc.*, **94** (1972) 5906.

[11] R.W.A. Havenith, J.H. van Lenthe and L.W. Jenneskens, *manuscript in preparation* (2000).

[12] R.A. King, T.D. Crawford, J.F. Stanton and H.F. Schaefer III, *J. Am. Chem. Soc.*, **121** (1999) 10788.

[13] T. Bally and G.N. Sastry, *J. Phys. Chem. A*, **101** (1997) 7923.

[14] B. Braïda and P.C. Hiberty, *J. Phys. Chem. A*, **102** (1998) 7872.

[15] C.D. Sherrill, M.S. Lee and M. Head-Gordon, *Chem. Phys. Lett.*, **302** (1999) 425.

[16] M. Sodupe, J. Bertran, L. Rodríguez-Santiago and E.J. Baerends, *J. Phys. Chem. A*, **103** (1999) 166.

[17] D.J. Tozer, R.D. Amos, N.C. Handy, B.O. Roos and L. Serrano-Andrés, *Mol. Phys.*, **97** (1999) 859.

[18] M. Hanrath and B. Engels, *Chem. Phys.*, **225** (1997) 197.

Summary

In the first chapters, the photo-physical properties of oligo(cyclohexylidenes) have been explored. The UV spectra of oligo(cyclohexylidenes) are superpositions of the UV spectra of the individual conformers. In the case of 1,1'-bicyclohexylidene, it is composed of the UV spectrum of its *anti*- and its *syn*-conformer. The calculations indicate (and this has later been verified for *anti*- and *syn*-4,4'-di-*tert*-butyl-bicyclohexylidene) that the UV spectra are markedly different for the two conformers, as a consequence of the change in point group. The first bands of the UV spectrum of *anti*-1,1'-bicyclohexylidene are assigned to $\pi\rightarrow\pi^*$ and $\pi\rightarrow\sigma^*$ transitions. The $\pi\rightarrow\sigma^*$ transition possesses charge transfer character from the olefinic carbon atoms towards the equatorial hydrogen atoms of the cyclohexyl rings. In the case of *syn*-1,1'-bicyclohexylidene, the $\pi\rightarrow\sigma^*$ transition has a vanishingly low oscillator strength.

Upon the extension of the molecular rod length, more $\pi\rightarrow\pi^*$ transitions are discernible. The $\pi\rightarrow\sigma^*$ transitions are shifted to higher energy, thus they will not be observable in solution UV spectroscopy.

The transition energies of the parent oligo(cyclohexylidenes) have been calculated using various methods, *viz.* the MRDCI, Direct-CI, MR-MP2 and MR-MP3 methods. All methods perform equally well for the assignment of the excited states. The transition energies of 1,1'-bicyclohexylidene calculated at the MR-MP3 level are close to those obtained using the Direct-CI method. However, the MR-MP2 method is unreliable for the calculation of transition energies, for states, *e.g.* the $\pi\rightarrow\pi^*$ excited states of 1,1':4',1"-tercyclohexylidene, possessing a high degree of multi-reference character. The MR-MP3 and MRDCI methods perform equally well in that case. Thus, the MRDCI and MR-MP3 methods are the methods of choice for calculating transition energies.

Ghost-centre calculations on 1,1':4',1"-tercyclohexylidene and 4,4'-bis(tetrahydro-4H-thiopyran-4-ylidene) elucidate that the non-degeneracy of the π bonds and the sulphur lone pairs is caused by through-bond interactions. NBO analyses show that the through-bond interactions are mediated by the H(*ax*)-C-C-H(*ax*) sub-units and the π bonds of the intervening cyclohexyl moieties. The splitting in energy between the

sulphur lone pairs is moderately affected by elongating the intervening spacer (**2(0)**: ΔE(LpS) 0.464 eV; *d*(S-S) = 3.49 Å; **2(4)**: ΔE(LpS) 0.224 eV; *d*(S-S) = 20.33 Å). Thus the oligo(cyclohexylidenes) possess good molecular wire characteristics.

In probing the extra stability of benzene, due to resonance/delocalised π-electrons, the problem is the determination of the energy of the reference compound. The energy of benzene, described by two Kekulé structures, should be compared to that of 1,3,5-cyclohexatriene, *i.e.* a reference compound described by only one Kekulé structure. The best approach towards these reference compounds is the application of *Ab Initio* Valence Bond (VB) theory. A comparison of the energies of two-Kekulé-structure benzene with one-Kekulé-structure 1,3,5-cyclohexatriene in the benzene geometry shows that benzene is only 9.6 kcal/mol more stable (-VRE). Geometry optimisation of one-Kekulé-structure 1,3,5-cyclohexatriene leads to a D_{3h} symmetric structure, with alternating bond lengths, located 7.4 kcal/mol above benzene (-TRE). A calculation on deformed benzene (two Kekulé structures) in the 1,3,5-cyclohexatriene optimised geometry shows that it is stabilised by resonance by 6.2 kcal/mol. This deformed benzene is located only 1.2 kcal/mol above benzene itself. Upon geometry optimisation, D_{6h} symmetric benzene results. The resonance between the two Kekulé structures is thus necessary for the D_{6h} symmetric geometry of benzene. The suitability of our *ab initio* Valence Bond approach, to probe the importance of Kekulé structures, prompted us to use this method for the study of complex (non)-alternant polycyclic aromatic hydrocarbons.

VB calculations on the cyclopentafused pyrene derivatives were performed to study the effect of cyclopentafusion on their aromatic properties. The resonance energies of all considered compounds have the same magnitude, in line with their aromatic stabilisation energies. All Kekulé resonance structures, in which the five membered rings actually participate in the electron delocalisation path, have negligible weights and contributions to the total resonance energy. The most important Kekulé resonance structures are those that contain the maximum number of aromatic sextets (benzene-like rings), in line with Clar's model of aromaticity. No support was found for Platt's ring perimeter model; the resonance between structures that lead to electron delocalisation around the ring perimeter has a negligible contribution to the resonance energy. All

resonance interactions between structures that lead to conjugated circuits with 4n π electrons have small contributions to the total resonance energy. Thus the results of the VB calculations show that the cyclopentafused five-membered rings should be seen as substituents and not as a part of the delocalised π system.

The NICS criterion for aromaticity suggests a gradual decrease of aromatic character upon cyclopentafusion, in contrast to the resonance criterion. We have shown that the NICS criterion should be used with care for comparing the aromatic properties of the individual rings of different molecules. The diamagnetic part of the chemical shielding at the ring centre can be used for this purpose, if identical gauge origins are ensured.

Furthermore, the results of the VB calculations show that no relation exists between the stability and resonance energy of the dicyclopentafused pyrene isomers. Imposed strain on the skeleton has a large effect on the relative stability. The order of magnitude of the strain energy is the same as that of the resonance energy. Thus strain energy may not be ignored when the relative stability order of isomers is estimated.

The results of the calculations on the thermal electrocyclic ring opening of Dewar benzene towards benzene show that for this reaction, two distinct pathways are available, *viz.* the symmetry allowed *con-rotatory* path and the symmetry forbidden *dis-rotatory* path. The activation energy for the *con-rotatory* reaction is 6.6 kcal/mol lower than that for the *dis-rotatory* one, in contrast to common belief. *Cis, cis, trans*-1,3,5-cyclohexatriene (*trans*-benzene) is not an intermediate on the *con-rotatory* reaction pathway.

Samenvatting

In de eerste hoofdstukken van dit proefschrift staat het onderzoek naar de optische eigenschappen van oligo(cyclohexylidenen) centraal. De UV spectra van oligo(cyclohexylidenen) bestaan uit superposities van de UV spectra van alle individuele conformeren. In het geval van 1,1'-bicyclohexylideen bestaat het UV spectrum van dat van zijn *anti*- en van zijn *syn*-conformeer. De berekeningen geven aan (en dit is later bevestigd voor *anti*- en *syn*-4,4'-di-*tert*-butyl-bicyclohexylideen) dat de UV spectra van beide conformeren verschillend zijn, als een gevolg van de puntgroeps verandering. De eerste absorpties in het UV spectrum van *anti*-1,1'-bicyclohexylideen zijn toegekend aan $\pi\rightarrow\pi^*$ en $\pi\rightarrow\sigma^*$ overgangen. De $\pi\rightarrow\sigma^*$ overgang gaat gepaard met ladingsoverdracht van de olefinische koolstofatomen naar de equatoriale waterstofatomen van de cyclohexyl-ringen. In het geval van *syn*-1,1'-bicyclohexylideen heeft deze $\pi\rightarrow\sigma^*$ overgang een verwaarloosbaar klein overgangsmoment.

Wanneer deze molekulen verlengd worden, zijn steeds meer $\pi\rightarrow\pi^*$ overgangen zichtbaar. Steeds meer energie is nodig om een $\pi\rightarrow\sigma^*$ overgang te bewerkstelligen, dus deze overgangen zijn niet meer waarneembaar bij UV spectroscopie in oplossing.

De excitatie energieën van de niet-gefunctionaliseerde oligo(cyclohexylidenen) zijn berekend met verschillende methoden, namelijk met de MRDCI, Direct-CI, MR-MP2 en MR-MP3 methoden. Alle methoden presteren even goed voor de toekenning van de aangeslagen toestanden. De excitatie energieën van 1,1'-bicyclohexylideen berekend met behulp van de MR-MP3 methode liggen in de buurt van de excitatie energieën verkregen met de Direct-CI methode. Echter, de MR-MP2 methode is onbetrouwbaar voor de berekening van excitatie energieën voor toestanden, zoals bijvoorbeeld de $\pi\rightarrow\pi^*$ aangeslagen toestanden van 1,1':4',1"-tercyclohexylideen, die niet beschreven kunnen worden met een enkele determinant golffunctie, welke bestaat uit de orbitals van de grondtoestand. De MR-MP3 en MRDCI methoden presteren in dat geval even goed. Dus de MRDCI en MR-MP3 methoden zijn de methoden die gekozen moeten worden voor de berekening van excitatie energieën.

Berekeningen waarbij de basis funkties geplaatst zijn op kernen met lading nul op plaatsen waar zich eerst de atoomkernen bevonden, aan 1,1':4',1"-tercyclohexylideen en 4,4'-bis(tetrahydro-4H-thiopyran-4-ylideen) laten zien dat de energie van de π bindingen en zwavel niet-gebonden (vrije) electronen paren niet gelijk zijn doordat zij een interactie met elkaar hebben via de bindingen van het deel van het molekuul dat tussen hen inligt (indirecte interactie). NBO analyses laten zien dat de betreffende orbitalen deze indirecte interacties met elkaar hebben, doordat zij een interactie hebben met de H(*ax*)-C-C-H(*ax*) eenheden en de tussenliggende π bindingen van de cyclohexyl ringen. De opsplitsing van de energienivo's van de vrije electronen paren van de zwavelatomen wordt maar een beetje beïnvloed door het verlengen van de lengte van de tussenliggende brug (**2(0)**: ΔE(LpS) 0.464 eV; *d*(S-S) = 3.49 Å; **2(4)**: ΔE(LpS) 0.224 eV; *d*(S-S) = 20.33 Å). Dus de oligo(cyclohexylidenen) hebben goede molekulaire draad eigenschappen.

Bij het onderzoek naar de extra stabiliteit van benzeen, als gevolg van resonantie/π electron delokalisatie, is het berekenen van de energie van het referentie molekuul een probleem. De energie van benzeen, dat beschreven wordt met twee Kekulé strukturen, zou vergeleken moeten worden met die van 1,3,5-cyclohexatrieen, dat een referentie molekuul is dat beschreven wordt met één Kekulé struktuur. Deze referentie verbindingen kunnen het best benaderd worden met de toepassing van de *ab initio* Valence Bond (VB) theorie. Een vergelijk van de energieën van benzeen (beschreven met twee Kekulé strukturen) en van 1,3,5-cyclohexatrieen (beschreven met één Kekulé struktuur) in de geometrie van benzeen laat zien dat benzeen alleen maar 9.6 kcal/mol stabieler is (-VRE). Een optimalisatie van de geometrie van het met één Kekulé struktuur beschreven 1,3,5-cyclohexatrieen geeft als resultaat een D_{3h} symmetrische struktuur, met alternerende bindingsafstanden, die 7.4 kcal/mol hoger in energie ligt dan benzeen (-TRE). Een berekening aan vervormd benzeen (beide Kekulé strukturen) in de optimale 1,3,5-cyclohexatrieen geometrie toont aan dat deze met 6.2 kcal/mol gestabiliseerd wordt door resonantie. Dit vervormde benzeen molekuul ligt alleen maar 1.2 kcal/mol hoger in energie dan benzeen zelf! Wanneer nu de geometrie wederom wordt geoptimaliseerd wordt de D_{6h} geometrie van benzeen verkregen. De resonantie tussen de beide Kekulé strukturen is dus noodzakelijk voor de D_{6h} symmetrische geometrie van benzeen. De

geschiktheid van onze *ab initio* Valence Bond methode om het belang van Kekulé strukturen te onderzoeken, hebben ons ertoe aangezet om met deze methode complexe (niet)-alternerende polycyclische aromatische koolwaterstoffen te onderzoeken.

VB berekeningen aan verbindingen waarbij vijfringen zijn aangebracht aan het pyreen skelet, werden uitgevoerd om het effect van deze vijfringen op het aromatische karakter van de verbindingen te onderzoeken. De resonantie energieën van alle verbindingen die beschouwd werden zijn van dezelfde grootte orde, wat overeenkomt met hun aromatische stabilisatie energieën. Alle Kekulé resonantie strukturen waarbij de vijfringen echt meedoen in het electron delokalisatie pad hebben verwaarloosbare gewichten en bijdragen aan de totale resonantie energie. De belangrijkste Kekulé resonantie strukturen zijn die met het grootste aantal aromatische zesringen (gelijkend op de benzeenring). Dit is in overeenstemming met Clar's model voor aromaticiteit. Geen ondersteuning werd gevonden voor Platt's ring perimeter model; de resonantie tussen de benodigde strukturen voor electron delokalisatie om de ring perimeter draagt maar beperkt bij aan de totale resonantie energie. Alle resonanties tussen strukturen die leiden tot electron delokalisatie in ringen met 4n π electronen dragen maar beperkt bij aan de totale resonantie energie. Dus de resultaten van de VB berkeningen laten zien dat vijfringen beschouwd moeten worden als substituenten en niet als een deel van het gedelokaliseerde π systeem.

Het NICS criterium voor aromaticiteit suggereert een geleidelijke afname van het aromatische karakter wanneer vijfringen aan het pyreen skelet worden gezet, wat in tegenstelling is tot het resonantie criterium. Wij hebben laten zien dat het NICS criterium niet zonder meer toepasbaar is voor het vergelijk van het aromatische karakter van verschillende ringen in verschillende molekulen. Het diamagnetische deel van de afscherming in het centrum van de ring kan voor dit doel gebruikt worden, als identieke gauge oorsprongen gegarandeerd worden.

Bovendien laten de resultaten van de VB berekeningen zien dat geen relatie bestaat tussen de stabiliteit en de resonantie energie van de di-gesubstitueerde pyreen isomeren. Opgelegde spanning op het skelet heeft een groot effect op de relatieve stabiliteit. De spannings energie is van dezelfde grootte orde als de resonantie energie.

Dus de spannings energie mag niet genegeerd worden bij het maken van een schatting van de relatieve stabiliteit van isomeren.

De berekeningen aan de thermische electrocyclische ringopenings reaktie van Dewar benzeen naar benzeen laten zien dat voor deze reaktie twee paden beschikbaar zijn, namelijk het symmetry toegestane *conrotatorische* en het symmetry verboden *disrotatorische* reaktiepad. De activeringsenergie voor de *conrotatorische* reaktie is 6,6 kcal/mol lager dan die voor de *disrotatorische* reaktie, in tegenstelling tot wat men altijd dacht. *Cis, cis, trans*-1,3,5-cyclohexatrieen (*trans*-benzeen) is geen intermediair op het *conrotatorische* reaktiepad.

Dankwoord

Hé hé, poeh, poeh, zo, nu even zitten. Het *echte* werk gaat nu pas beginnen. Maar eerst even het proefschrift afronden. Dit boekje zou niet hebben bestaan zonder de hulp van een aantal mensen. Ik wil hen bij deze hartelijk danken voor hun inzet en toewijding. Met name wil ik Leo Jenneskens en Joop van Lenthe bedanken voor hun begeleiding op zowel wetenschappelijk als persoonlijk gebied. Leo, jouw kennis van de (organische) chemie was onontbeerlijk voor de interpretatie van de theoretische data. Jij stond ook altijd open om aan iets nieuws te beginnen, gewoon even kijken of het wat zou worden. Banyak-banyak terima kasih, Leo. Joop, niet alleen op theoretisch chemisch gebied had jij een bijzondere inbreng, ook buiten het werk heb jij bijgedragen tot de vorming van mijn persoonlijkheid. Jij hebt voor mij de creatie operator weer een nieuwe betekenis gegeven en uitgelegd hoe ik misschien eens met het spelletje Risk zou kunnen winnen.

Mede dankzij de aanwezigheid van de andere leden van de secties Theoretische en Fysisch Organische Chemie heb ik de afgelopen vier jaar altijd met plezier gewerkt. De theoretici Frans, Paul, Simon, Fokke (TURTLE en VB kenner), Huub, Jan, Affen, Wim, Asger, Elly, Walter, Claire, Jeanne en Arno en natuurlijk de organici Jan (mooie film was het), Wibren (zonder de plaatjes zou hoofdstuk 6 toch minder mooi zijn geworden), Martín, Alwin, Ivo, Carola, Patrick, Ingrid, Thomas, Marijo, Wieke, Ed, Kees, Vera en Rita, allemaal bedankt voor de prettige werksfeer! Ron wil ik graag bedanken voor zijn inzet bij de synthese van de *anti*- en *syn*-conformeren van het *tert*-butyl gesubstitueerde bicyclohexylideen.

Jan den Boesterd en Ingrid van Rooijen, bedankt voor jullie inspanningen voor het maken van mooie posters op iedere keer weer het allerlaatste moment.

I would like to thank Bernd Engels and Michael Hanrath for providing us their newly developed MRDCI programs. Ulli Fleischer is gratefully acknowledged for his gift of the Direct IGLO program. Patrick Fowler, Paul von R. Schleyer and Hajun Jiao are gratefully acknowledged for their contribution to the aromatics part of this thesis.

Als laatste wil ik mijn ouders bedanken die mij altijd op ieder front hebben gesteund.

Curriculum Vitae

Remco Walter Alexander Havenith werd geboren op 24 juni 1971 te Apeldoorn. In 1989 behaalde hij het Gymnasium diploma aan het Stedelijk Gymnasium te Apeldoorn. Hierna werd begonnen met de studie Scheikunde aan de Universiteit Utrecht. Het doctoraal examen, met als hoofdvak Fysisch organische chemie, werd in juni 1994 afgelegd.

Van juli 1994 tot juni 1995 was hij werkzaam bij de Universiteit Twente. Van september 1996 tot augustus 2000 was hij als assistent in opleiding (AIO) verbonden aan de secties Fysisch Organische Chemie en Theoretische Chemie van de Universiteit Utrecht alwaar hij onder leiding van Prof. Dr. L.W. Jenneskens en Dr. J.H. van Lenthe het in dit proefschrift beschreven onderzoek uitvoerde.

List of publications

[1] R.W.A. Havenith, J.H. van Lenthe, L.W. Jenneskens and F.J. Hoogesteger, The lowest valence transitions of 1,1'-bicyclohexylidene and 1,1':4',1"-tercyclohexylidene. An ab initio MRDCI study, *Chem. Phys.*, **225** (1997) 139-152.

[2] R.W.A. Havenith, L.W. Jenneskens and J.H. van Lenthe, The effect of *syn-anti* isomerism on the lowest valence transitions of 1,1'-bicyclohexylidene. An ab initio MRDCI investigation, *Chem. Phys. Lett.*, **282** (1998) 39-48.

[3] M.J. de Groot, R.W.A. Havenith, H.M. Vinkers, R. Zwaans, N.P.E. Vermeulen, and J.H. van Lenthe, Ab initio calculations on iron-porphyrin model systems for intermediates in the oxidative cycle of cytochrome P450s, *J. Comp.-Aided Molec. Design* (1998) 183-193.

[4] M. Sarobe, H.C. Kwint, T. Fleer, R.W.A. Havenith, L.W. Jenneskens, E.J. Vlietstra, J.H. van Lenthe and J. Wesseling, Flash vacuum thermolysis of acenaphtho[1,2-*a*]acenaphthylene, fluoranthene, benzo[*k*]- and benzo[*j*]-fluoranthene - homolytic scission of carbon-carbon single bonds of internally fused cyclopenta moieties at T≥1100 °C, *Eur. J. Org. Chem.* (1999) 1191-1200.

[5] M. Sarobe, R.W.A. Havenith, L.W. Jenneskens, *Tris*cyclopenta[*cd,fg,jk*]pyrene: another congener of the externally cyclopenta-fused pyrene series, *Chem. Commun.* (1999) 1021-1022.

[6] R.W.A. Havenith, H.J.J. van Dam, J.H. van Lenthe and L.W. Jenneskens, The excitation energies of 1,1'-bicyclohexylidene and 1,1':4',1"-tercyclohexylidene. A comparison of multi-reference configuration interaction and perturbation theory approaches, *Chem. Phys.*, **246** (1999) 49-56.

[7] R.W.A. Havenith, L.W. Jenneskens and J.H. van Lenthe, Disrotatory versus conrotatory electrocyclic ring opening of dewar benzene: the conrotatory pathway is preferred and does not involve *trans*-benzene, *J. Mol. Struct. (Theochem)*, **492** (1999) 217-224.

[8] A.W. Marsman, C.A. van Walree, R.W.A. Havenith, L.W. Jenneskens, M. Lutz, A.L. Spek, E.T.G. Lutz and J.H. van der Maas, Infinite, undulating chains of intermolecularly hydrogen bonded (*E,E*-2,2-dimethylcyclohexane-1,3-dione dioximes in the solid state. A single crystal X-ray, charge density distribution and spectroscopic study, *J. Chem. Soc., Perkin Trans. 2* (2000) 501-510.

[9] A.W. Marsman, R.W.A. Havenith, S. Bethke, L.W. Jenneskens, R. Gleiter and J.H. van Lenthe, Through-bond orbital coupling in end-functionalized bicyclohexylidenes - photo-electron spectroscopy and ab initio SCF-MO calculations, *Eur. J. Org. Chem.* (2000) 2629-2641.

[10] A.W. Marsman, R.W.A. Havenith, S. Bethke, L.W. Jenneskens, R. Gleiter, J.H. van Lenthe, M. Lutz and A.L. Spek, Long-range σ-π interactions in tetrahydro-*4H*-thiopyran end-capped oligo(cyclohexylidenes). Photo-electron spectroscopy, ab initio SCF MO calculations, and natural bond orbital analyses, *J. Org. Chem.*, **65** (2000) 4584-4592.

[11] R.W.A. Havenith, J.H. van Lenthe, F. Dijkstra and L.W. Jenneskens, Aromaticity of pyrene and its cyclopentafused congeners; Resonance and NICS criteria. An *ab initio* valence bond analysis in terms of Kekulé resonance structures, *submitted to J. Phys. Chem. A.*

[12] R.W.A. Havenith, H. Jiao, L.W. Jenneskens, J.H. van Lenthe, M. Sarobe, P. von R. Schleyer, A. Necula, L.T. Scott, and M. Kataoka, Stability and aromaticity of the cyclopenta-fused pyrene congeners, *to be submitted*.

[13] R.W.A. Havenith, J.H. van Lenthe and L.W. Jenneskens, Möbius aromaticity in small [n] *trans*-annulenes?, *to be submitted*.

[14] R.W.A. Havenith, J.H. van Lenthe, L.W. Jenneskens and A.W. Marsman, Long range through-bond interactions in functionalised oligo(cyclohexylidenes) and the photo-physical properties of 4,4'-bis(tetrahydro-4H-thiopyran-4-ylidene), *to be submitted*.

[15] J.H. van Lenthe, R.W.A. Havenith, F. Dijkstra and L.W. Jenneskens, 1,3,5-Cyclohexatriene captured in computro; the concept of aromaticity, *to be submitted*.

Printed by Universal Press